Reprinted from 'Molecular Spectroscopy and Quantum Dynamics' ,
R. Marquardt and M.Quack eds. , pp.231-282, Elsevier, Amsterdam,

1st Edition, 2020, ISBN978-012-817234-6

(https://doi.org/10.1016/B978-0-12-817234-6.00012-X)

CHAPTER 7

Atomic and Molecular Tunneling Processes in Chemistry

MARTIN QUACK • GEORG SEYFANG
Laboratorium für Physikalische Chemie, ETH Zürich, CH-8093 Zürich, Switzerland, Martin@Quack.CH

Abstract

The article presents an overview of atomic and molecular tunneling processes, where tunneling of "heavy" particles (i.e., nuclei, not electrons) is important. After an introductory tour d'horizon including a brief history of the tunnel effect, we discuss some topics of current interest. These include tunneling and parity violation in chiral molecules, tunneling in weakly bound complexes, and tunneling processes in slightly asymmetric potentials with tunneling switching and the development of a molecular quantum switch. We then present a selection of recent results for isomerization reactions, bimolecular reactions, tunneling in ions, radicals and electronically excited states, and of the motions of molecules inside a cage. We conclude with some remarks on certain general problems related to tunneling.

7.1 INTRODUCTION

7.1.1 Aim and Overview of the Article

Tunneling is a fundamental quantum-mechanical phenomenon with a wide range of applications in chemistry and physics, on which numerous books have been written already. As far as atomic and molecular processes are concerned, one must distinguish phenomena where the "light" electrons are involved in tunneling (for instance, in redox reactions, tunneling ionization in strong fields, etc.) and processes, where the tunnel effect is important for the "heavy" particles, that is, the atomic nuclei, where we assign the attribute "heavy" also to "light nuclei" such as hydrogen and deuterium where tunneling processes are of particular relevance. The present review deals only with such processes involving "heavy-particle" tunneling, which is also often called "quantum atomic and molecular tunneling", which also forms the theme of a conference series (Eckert et al., 2015, 2017, 2019). The organization of the chapter is as follows: After an introductory "tour d'horizon" of the role of atomic and molecular tunneling in current chemical and molecular dynamics, we provide a brief sketch of the history of the tunnel effect, which is motivated by some interesting aspects of the early history, on the one hand, and by the frequent misrepresentations and misconceptions of that history in the literature, on the other hand. In the main part of the article we discuss in turn various topics of particular current interest, as already outlined in the abstract and table of contents, and we conclude with some remarks and an outlook. The present article is in part based on an earlier brief review (in German) (Seyfang and Quack, 2018).

7.1.2 The Quantum Mechanical Tunneling Process for "Heavy" Particles (Atoms and Molecules): a Tour d'Horizon

Tunneling processes with the motion of electrons are dominating many physical and chemical processes due to the small mass of the electron. The quantum-mechanical tunneling process was discovered, however, by Friedrich Hund (1927a; 1927c; 1927b) for the example of molecular transformations with the motion of "heavier" atomic particles, like the stereomutation of the enantiomers of chiral molecules or for the "textbook example" of the inversion motion of ammonia, NH_3. The early history is found in text- and handbooks of spectroscopy and kinetics (Herzberg, 1939, 1945; Bell, 1980), and historical articles (Quack, 2014), and also for recent developments, for example, in Quack and Merkt (2011). We shall give a brief summary below. Remarkable progress has been made recently by the development of new spectroscopic methods (Quack and Merkt, 2011), and especially by theoretical methods for the description of high-dimensional quantum mechanics of polyatomic molecules (Császár et al., 2012, 2020, Chapter 2, Carrington, 2011; Yamaguchi and Schaefer, 2011; Breidung and Thiel, 2011; Tennyson, 2011) in the framework of the equally high-dimensional underlying potential hypersurfaces (Marquardt and Quack, 2011).

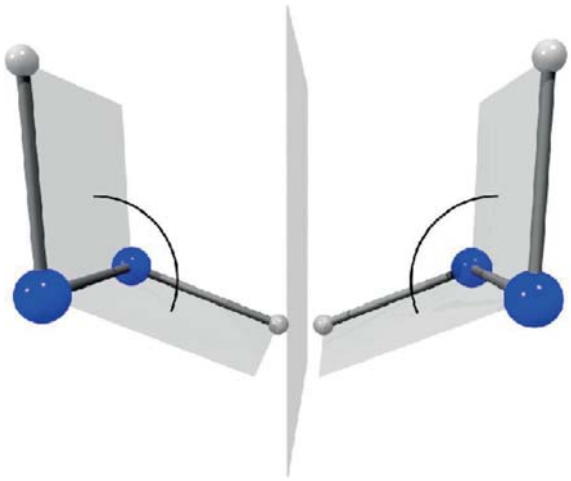

FIG. 7.1 H_2O_2 in its two enantiomeric equilibrium geometries: P-enantiomer on the left and M-enantiomer on the right connected by a fast tunneling reaction (after Quack, 1999, see also Fehrensen et al., 1999a,b, 2007).

The still today widespread classical molecular dynamics (MD) with empirical force fields (van Gunsteren et al., 2006; Riniker et al., 2012; Meier et al., 2013b; Karplus, 2014; Levitt, 2014; Warshel, 2014), as well as Car–Parrinello "ab initio" MD based on the potential hypersurfaces from density functional theory (Car and Parrinello, 1985) neglect the quantum mechanical tunnel effect which might be crucial for many processes with the motion of H-atoms and, as we know today, also for many processes with the motion of heavier atoms (like C, N, S, Cl, etc.), also in many biologically relevant reactions (Allemann and Scrutton, 2009). The development of exact procedures and "good" approximation procedures for the description of the tunneling process are therefore a field of research with vigorous development.

Thereby in the first place, Diffusion Quantum Monte Carlo (DQMC) methods have been applied for the full-dimensional description of tunneling processes in the simplest hydrogen-bond complexes like $(HF)_2$ (Quack and Suhm, 1991a, 1995; Klopper et al., 1998b), later on the more widely usable DVR-methods (discrete variable representation) (Meyer, 1970; Luckhaus and Quack, 1992; Bačić and Light, 1989; Light and Carrington, 2001; Carrington, 2011; Tennyson, 2011), which also allowed for a first full-dimensional time-independent and time-dependent description of stereomutation reaction between the two enantiomers of the hydrogen peroxide molecule HOOH (Fehrensen et al., 1999b, 2007) (see also Fig. 7.1). Today exact methods are implemented in software packages like GENIUSH (Fábri et al., 2011; Császár et al., 2012; Császár and Furtenbacher, 2016). This accurate approach has recently been combined with the accurate theoretical treatment of the interaction with coherent radiation fields (Quack, 1978) to provide a full-dimensional quantum picture of the control of the tunneling motion in ammonia isotopomers (including the chiral NHDT) (Fábri et al., 2019). Exact treatments can also be used for the validation of approximation methods like the quasiadiabatic channel RPH method (Fehrensen et al., 1999b, 2007, 1999a), (reaction path Hamiltonian, Miller et al., 1980), which also can be related to older methods such as the statistical adiabatic channel model (Quack and Troe, 1974, 1998; Merkel and Zülicke, 1987) or similar methods (Hofacker, 1963; Hougen et al., 1970), related to "adiabatic transition state theory". Approximation concepts related to semiclassical dynamics and transition state theory (Miller, 1975b) are also found in the instanton theory of the tunneling process (Benderski et al., 1994; Zimmermann and Vaníček, 2010; Richardson, 2016; Richardson et al., 2015; Kästner, 2014b,a), see also Chapter 9 (Cvitaš and Richardson, 2020). Additional newer developments are found in the RPD-method (ring polymer dynamics) (Richardson and Althorpe, 2009, 2011; Richardson, 2016). The development of the quantum mechanical path integral method for the description of tunneling processes has great potential for an extension of the program systems of the classical MD for the application to biomolecular tunneling processes (Ceriotti et al., 2011; Mátyus et al., 2016; Zimmermann and Vaníček, 2010; Buchowiecki and Vaníček, 2010; Marx, 2006; Ivanov et al., 2015, see also Marquardt and Quack, 2020, Chapter 1), where there are also a large number of experimental investigations (Roston and Kohen, 2013; Roston et al., 2014; Francis et al., 2016; Luk et al., 2013; Ruiz-Pernía et al., 2013; Chan-Huot et al., 2013; Shenderovich et al., 2015).

Another very versatile procedure for the description of the quantum dynamics of polyatomic molecules including tunneling is based on the MCTDH method (multiconfiguration time-dependent Hartee) (Meyer et al., 1990, 2009; Ansari and Meyer, 2016; Manthe, 2015). The "multimode" package has also been applied to tunneling processes, together with an RPH-like approximation (Carter et al., 2013; Wang and Bowman, 2013; Homayoon et al., 2014). An interesting theoretical development is also found in the investigation of the "electronic" and "nuclear flux" in the tunneling process (Grohmann et al., 2013; Liu et al., 2015; Bredtmann et

al., 2015; Hermann et al., 2016; Bredtmann et al., 2016; Lu et al., 2016).

We have mentioned here a selection of recent theoretical methods for the description of the tunneling process which can now be applied to interesting physical-chemical processes. We shall turn to these after providing a short survey of the history of the discovery of the tunnel effect.

7.1.3 A Brief History of the Discovery of the Tunnel Effect and Further Developments

When one discusses the history of the tunnel effect, one must distinguish between the *experimental observation of phenomena which involve the tunnel effect and the theoretical understanding of the underlying effect based on quantum mechanics and wave mechanics*. Only the latter should be counted as part of the history of the discovery of the "tunnel effect" properly speaking. Otherwise one would have to tell the history of all kinds of wave phenomena, including even macroscopic surface wave phenomena (Stocker and Johnson, 1991) (which can be related to the tunnel effect) in the long and old history of science. Also, radioactive α-decay was discovered experimentally early on by Rutherford (1900), but without any understanding of the underlying quantum mechanical phenomena. Indeed, it is the discovery and theoretical understanding of this most striking phenomenon of transgressing a potential barrier without ever having sufficient energy to overcome that barrier – completely impossible, even unthinkable of in classical mechanics – which should be qualified as the discovery of the tunnel effect. This discovery was made by Friedrich Hund (1927a; 1927c; 1927b) in a theoretical investigation of certain spectroscopic and kinetic consequences of the quantum-mechanical treatment of the vibrational (vibrational-tunneling) dynamics of molecules, in particular chiral molecules and pyramidal molecules such as ammonia. In this early work Hund provided a careful explanation of the quantum mechanical phenomena and the basic equations for the relation of the "tunneling splitting" ΔE between energy eigenstates of different parity in such molecules and their time evolution, which we quote here as the tunneling period τ,

$$\tau = h/\Delta E, \tag{7.1}$$

and the transfer time for the motion of the molecular system from one well in a double minimum potential to the other well separated by a potential barrier much exceeding the total available energy of the molecule (see also Figs. 7.2 and 7.5 further below)

$$t_{\text{transfer}} = \tau/2 = h/(2\Delta E). \tag{7.2}$$

Hund then proceeds to discuss also the dependence of the tunneling time upon shape, with height and width, of the potential barrier. With simple quantum-mechanical estimates of the Born–Oppenheimer like potential barriers for substituted chiral methane derivatives, he calculated lifetimes longer than millions of years for such chiral molecules, therefore resolving what was later often called by others "Hund's paradox": The fact that for chiral molecules one does not observe the energy eigenstates of well defined parity (assuming parity conservation to be exact as was common then) but localized time-dependent states. The predicted long lifetimes would provide a resolution of the "paradox" (see also Janoschek, 1991). We shall see in Section 7.2 that the physics of the situation is changed today fundamentally. We might also note in passing that later (Pfeiffer, 1983) and Primas (1981) have discussed another paradox: Why can one synthesize and buy the chiral enantiomers but not the achiral superpositions which might be assumed to be more "natural" by being energy eigenstates? As pointed out in Quack (1989), this latter paradox has two solutions: first, by dominant parity violation making, in fact, the chiral states to be the energy eigenstates, and second, because the phase relations necessary for the superpositions or "parity isomers" are quickly destroyed by collisions.

Returning to the history of tunneling, the next effects to be treated along these lines were electron emission (Fowler and Nordheim, 1928) and α-decay (Gamov, 1928b,a; Gurney and Condon, 1928, 1929). Indeed, Gamov's work on α-decay is frequently referred to as the discovery of the tunnel effect in the literature, frequently also without any mention of Hund. A recent example among many is the article by Reiss (2014), although historical articles and books do mention the earlier work of Hund (Bell, 1980; Devault, 1984; Merzbacher, 2002). The work of Gamov and of Gurney and Condon was actually carried out independently and essentially simultaneously (the first paper by Gurney and Condon has a submission date 30 July 1928, published September 1928, and the paper by Gamov has a submission 2 August 1928, published shortly thereafter in 1928). Both papers date from about a year after the work of Hund, thus quite long afterwards. Indeed, Gurney and Condon (1928) make explicit reference to Hund's publication, noting also the similarly striking, very strong dependence of the tunneling rate upon barrier height and width. While this work carried out in another continent across the Atlantic thereby gives explicit reference and credit to the earlier work of Hund, the paper of Gamov submitted from Göttingen in the Zeitschrift für Physik, thus from the same place and in the same journal (also

in German) just like Hund's (1927a; 1927c; 1927a) work makes no mention of Hund's publication. Gamov mentions earlier work by Oppenheimer (Oppenheimer, 1928) and Nordheim (Fowler and Nordheim, 1928) on electron emission. It seems unlikely that, while in Göttingen and being a reader of Zeitschrift für Physik, Gamov did not know about Hund's work. Thus the omission is striking. Similarly later Eckart (1930) and Bell (1933) make no mention of Hund's work in their treatment of the tunnel effect while Wigner (1932) does mention it in the very first instance as being important for chemical reaction. In these early papers the word "tunneling" is not used for the effect. Wigner (1932) calls it "non-mechanical transgression" (unmechanisches Überschreiten) and Born and Weisskopf (1931) in a treatment of adsorption use the words "breaking the energy barrier" ("Durchbrechung der Energieschwelle"). On the other hand, Cremer and Polanyi (1932) already use the expression "tunneling-theory" ("Tunneltheorie") and "tunnel-effect" ("Tunneleffekt") in their treatment of quantum effects in heterogeneous catalysis, see also Schottky (1931, writing about a "wave-mechanical tunnel effect" (einen wellenmechanischen Tunneleffekt)). Later much use is made of these expressions and also of the effect in chemical reactions, particularly in relation to non-classical "tunneling corrections" to transition state theory (Eyring, 1938a,b; Wigner, 1938; Eyring et al., 1944; Bell, 1980). We shall add just a sketch of further developments. The early work is usually restricted to one-dimensional treatments of tunneling both in terms of model problems for various processes (Heilbronner et al., 1956; Brickmann and Zimmermann, 1968, 1969; Löwdin, 1963; Zimmermann, 1964) and in applications to spectroscopic problems (Herzberg, 1939, 1945), where even the one-dimensional treatment was considered to be quite demanding numerically until about 1970, giving motivation to provide and use solutions in extended tables (see, e.g., Coon et al., 1966; Quack and Stockburger, 1972). Similarly in transition state theory, numerous one-dimensional tunneling corrections were discussed (see, e.g., the review by Truhlar et al., 1996) or mentioned in the state selective version of transition state theory in the framework of the statistical adiabatic channel model (SACM) (Quack and Troe, 1974, 1998). An important development towards multidimensional tunneling theory arose from Miller's semiclassical approach towards quantum dynamics (Miller, 1974, 1975a, 2014), which can be considered to be related to WKB theory (Wentzel, 1926; Kramers, 1926; Brillouin, 1926) which itself can be related to the "old" quantum theory of Bohr and Sommerfeld (see Merkt and Quack, 2011). Multidimensional tunneling is thus incorporated into transition state theory (Stratt et al., 1979; Hernandez and Miller, 1993; Clary, 2018; Shan et al., 2019) and in the so-called instanton theory of tunneling (Miller, 2014; Benderski et al., 1994; Goldanskii, 1976; Richardson, 2016, 2018; Richardson and Althorpe, 2011; Meisner and Kästner, 2018; Rommel et al., 2011). As mentioned, the approximate reaction-path Hamiltonian (RPH) is an alternative to multidimensional tunneling in transition state theory (Miller et al., 1980). It is essentially a version of adiabatic transition state theory, see also Hofacker (1963); Marcus (1964, 1965); Quack and Troe (1974, 1998). An extension is based on an idea of the statistical adiabatic channel model (SACM) to "diabatize" vibrationally adiabatic channels in such a way that certain channels may cross in order to allow them to maintain their physical nature, which leads to the quasiadiabatic channel RPH model (Fehrensen et al., 1999a,b, 2007; Prentner et al., 2015), which has been successfully applied to spectroscopic problems and tested against full-dimensional, "numerically exact" computations of stereomutation (Fehrensen et al., 2007; Quack et al., 2008). By now, exact quantum dynamics for tunneling has been carried out, for example, using diffusion quantum Monte Carlo (DQMC) techniques for the dimer $(HF)_2$, indeed, already some time ago (Quack and Suhm, 1991a) much extended later on, using other techniques (Vissers et al., 2003; Wu et al., 1995; Felker and Bačić, 2019). Full-dimensional vibration–rotation–tunneling, including time dependence under coherent laser excitation, was studied most recently for the prototype system of ammonia isotopomers (Fábri et al., 2019) which brings us to modern times to be discussed from here onwards.

7.2 TUNNELING AND PARITY VIOLATION IN CHIRAL MOLECULES

7.2.1 Exact and Approximate Studies of Tunneling in Prototypical Molecules: Hydrogen Peroxide and Ammonia Isotopomers

Chiral molecules have, as already mentioned, played a central role in the history of the discovery of the tunneling process (Hund, 1927a,c,b; Bell, 1980; Quack, 2014). Fig. 7.1 shows the H_2O_2 molecule with the two enantiomers in their equilibrium geometry. This was to our knowledge the first example where a reaction of stereomutation was described on a full-dimensional potential surface with all 6 internal degrees of freedom (Kuhn et al., 1998) and a quantum-mechanical treatment with exact DVR methods for the spectroscopic

TABLE 7.1
Tunneling splittings from the numerically exact solution ($\Delta\tilde{\nu}_i^{6D}$), from the quasiadiabatic channel RPH approximation ($\Delta\tilde{\nu}_i^{RPH}$) and from experiment ($\Delta\tilde{\nu}_i^{\exp}$). T^{6D} is the tunneling transfer time[a].

i	$\omega_i/\mathrm{cm}^{-1}$	$\tilde{\nu}_i^{\exp}/\mathrm{cm}^{-1}$	$\tilde{\nu}_i^{6D}/\mathrm{cm}^{-1}$	$\Delta\tilde{\nu}_i^{\exp}/\mathrm{cm}^{-1}$	$\Delta\tilde{\nu}_i^{6D}/\mathrm{cm}^{-1}$	$\Delta\tilde{\nu}_i^{RPH}/\mathrm{cm}^{-1}$	T^{6D}/ps
0	0.0	0.0	0.0	11.4	11.0	11.1	1.5
1	3778	3609.8	3617.7	8.2	7.6	8.4	2.2
2	1453	1395.9	1392.0	(2.4?)	6.1	5.0	2.7
3	889	865.9	850.5	12.0	11.1	10.8	1.5
4	392	254.6	259.3	116	118	120	0.14
5	3762	3610.7	3605.8	8.2	7.4	7.4	2.0
6	1297	1264.6	1236.5	20.5	20.8	21.8	0.8

[a] After Fehrensen et al., 1999b, 2007.

stationary states and the time-dependent wave packet dynamics of the tunneling process (Fehrensen et al., 1999b, 2007). Hydrogen peroxide is well suited as a prototype molecule for such investigations due to the large tunneling splitting of ca. 10 cm^{-1} in the ground state which leads to the result that effectively a quantum dynamics in the spirit of Hund is valid independent of the also existing, but for the dynamics negligible, parity violation (see below) (Bakasov et al., 1996, 1998; Berger and Quack, 2000a,b). In Table 7.1 the tunneling splittings from the numerically exact solution are compared to the approximate results from the quasiadiabatic channel RPH approach and to experimental results. The strongly mode selective tunneling times as a function of the excitation of the different degrees of freedom can be recognized. Thus by exciting various vibrational modes, say with a pulsed laser, one can control the stereomutation rates. For example, the excitation of the OH-stretching vibration results in a slowing down of the tunneling process even though the excitation energy is a multiple of the barrier height: it remains an effectively quasiadiabatic tunneling process with a slightly modified effective quasiadiabatic channel potential and moment of inertia ("quasi"-tunneling mass) slightly increased by the excitation of the OH-stretching vibration which explains qualitatively the slowing down of the process. Similar effects have been found for the inversion motion in the aniline isotopomers (with the chiral isotopomer C_6H_5NHD) (Hippler et al., 2011; Albert et al., 2016d), which shows such a mode selective "non-statistical" tunneling process with a slowing down after NH-stretching excitation despite the very high density of states at high excitation.

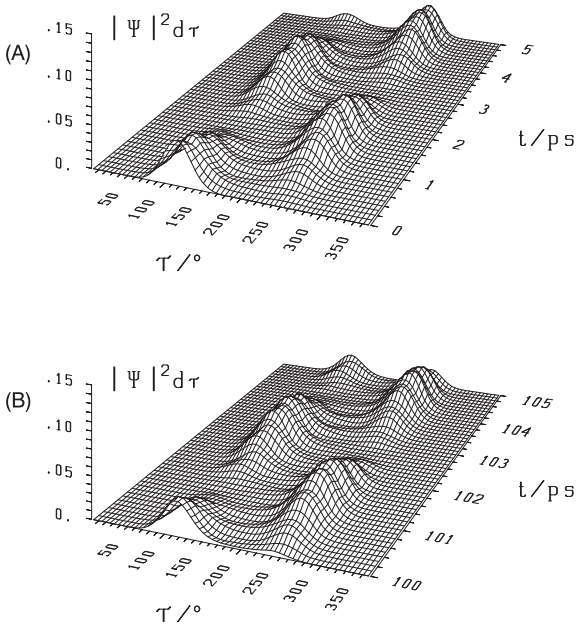

FIG. 7.2 Six-dimensional wave packet evolution for H_2O_2; $|\Psi|^2$ shows the time-dependent probability as a function of the torsional coordinate, where the probability density is integrated over all other coordinates: (A) shows the time interval 0–5 ps and (B) the time interval 100–105 ps with identical initial conditions at $t = 0$ as in (A) (Fehrensen et al., 1999b, 2007). The migration of the wave packet from the left to the right corresponds to a change from one enantiomer to the other in Fig. 7.1.

Fig. 7.2 shows as an example the "wave packet dynamics" in the ground state of the H_2O_2 molecule in terms of the 6-dimensional quantum-mechanical prob-

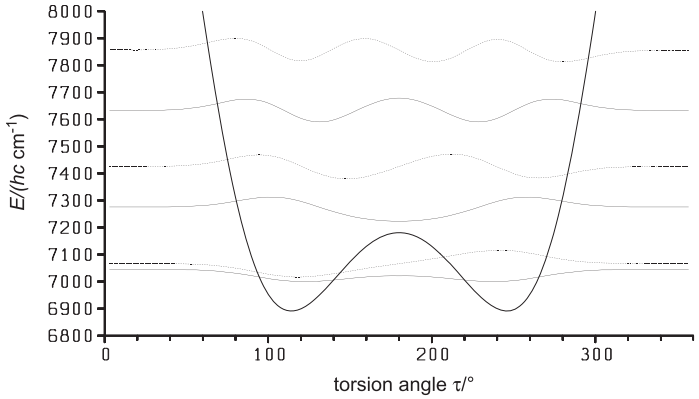

FIG. 7.3 The lowest torsional wavefunctions supported by the adiabatic channel corresponding to the antisymmetric bending fundamental ν_6 (calculated with the RPH model). (Full lines) Wavefunctions of positive parity (+); (Dotted lines) Wavefunctions of negative parity (-). The ordinate axis labels refer to the energies $E/(hc\ \mathrm{cm}^{-1})$, the wavefunctions are shown without scale for illustration, centered at the positions of the corresponding energy levels (after Fehrensen et al., 2007).

ability density as a function of the torsional angle (integrated over the other 5 degrees of freedom). One can see the initially, at time $t = 0$, "left" localized density which shows an approximately Gaussian shape around the equilibrium geometry of the "left" enantiomer and which after 1.5 ps transforms to the "right" localized wavepacket close to the equilibrium geometry of the second ("right") enantiomer.

The detailed full-dimensional analysis of the wavepacket dynamics can be used to test the validity of the quasiadiabatic channel-RPH approximation, which turns out to be a remarkably good approximation for this example. Even at high energies one finds indeed quasiadiabatic tunneling above the barrier. The different tunneling velocities for various excitations of different channels in all possible degrees of freedom can be used for a "mode selective" tunneling control of the reaction velocity, for instance, with the help of laser excitation (Prentner et al., 2015; Fábri et al., 2019).

Fig. 7.3 shows a quasiadiabatic channel potential with one quantum excitation of the antisymmetric bending fundamental ν_6 in HOOH, together with the supporting torsional wavefunctions. As seen from Table 7.1, this excitation leads to an enhancement of the tunneling rate by a factor of 2, and the quasiadiabatic channel RPH result is within 5% of the exact result. The time-dependent wavepackets from the exact and approximate results are virtually indistinguishable by eye although the small numerical differences can, of course, be established easily (Fehrensen et al., 2007).

While rotation was treated approximately by Fehrensen et al. (1999b, 2007), in the recent work on tunneling in ammonia isotopomers all degrees of freedom (vibration and rotation) were treated numerically exactly in a 9-dimensional vibration–rotation–tunneling calculation (Fábri et al., 2019). In addition to tunneling wavepackets in the isolated ammonia isotopomers, the control of tunneling rates by well-designed electromagnetic (laser) radiation fields was studied in this work. Fig. 7.4 shows the *tunneling enhancement* achieved for the chiral isotopomer NHDT, where with a suitable laser excitation a transfer time of 40 ps can be obtained compared to a transfer time of 150 ps in the isolated NHDT molecule in its ground state.

7.2.2 Tunneling in Chiral Molecules Where Parity Violation Dominates Over Tunneling

At the time of Hund's discussion of chiral molecules (1927), parity conservation was assumed to be rigorous. The discovery of parity violation in particle physics (Lee and Yang, 1956; Wu et al., 1957; Garwin et al., 1957; Friedman and Telegdi, 1957; Schopper, 1957) leads to a fundamental change also in the tunneling dynamics of chiral molecules, as a consequence in molecular physics arising from high energy physics. Such tunneling processes and their theoretical analysis have gained recently a new fundamental interest in connection with the phenomenon of parity violation in chiral molecules (Quack, 2011b; Quack et al., 2008). Indeed, parity vi-

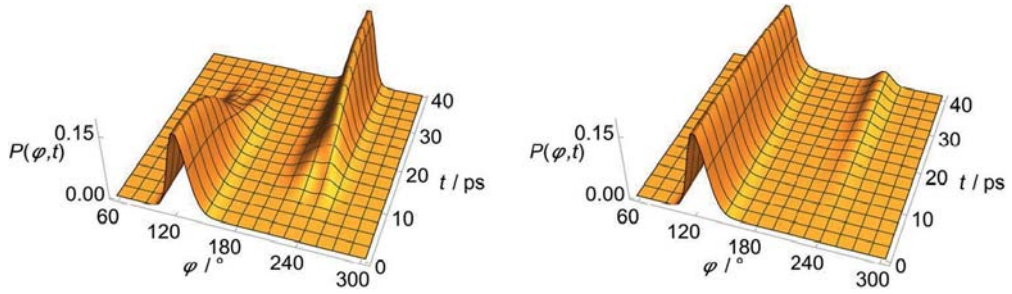

FIG. 7.4 Reduced probability density as a function of the inversion coordinate φ and time t for NHDT. The two enantiomeric structures correspond to $\varphi \simeq 120°$ and $\varphi \simeq 240°$, respectively. The left and right panels show reduced probability densities (probability densities integrated over all other coordinates) for the tunneling enhancement (left) and field-free dynamical schemes (right). The parameters of the laser pulse are $\tilde{\nu}_0 = 793.5.0\ \mathrm{cm}^{-1}$, $I_{\max} = 3.15\ \mathrm{GW\,cm}^{-2}$, and $t_p = 40$ ps (after Fábri et al., 2019).

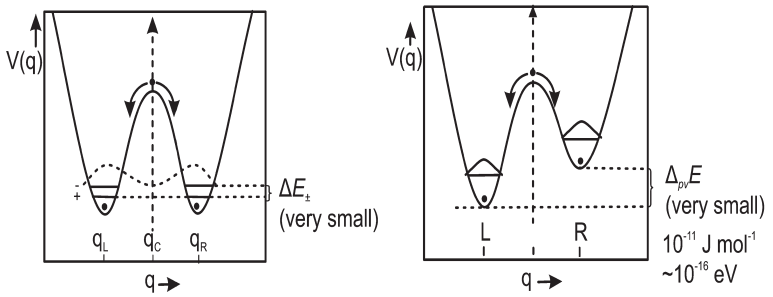

FIG. 7.5 Illustration of the symmetrical potential (left, as discussed by Hund 1927a; 1927c; 1927b) for chiral molecules and the asymmetry induced by the electroweak interaction in an originally symmetric double minimum potential (right, see Quack et al., 2008; Quack, 1986, 2015b).

olation creates an effectively asymmetric potential for tunneling as shown in Fig. 7.5, as calculated by "electroweak quantum chemistry" derived from the standard model of particle physics (SMPP) which allows one to obtain the very small extra potential showing the asymmetry (it should not be viewed as Born–Oppenheimer potential; Bakasov et al., 1996, 1998). While older theories of this effect were incorrect by one to two orders of magnitude, the new theoretical values (Bakasov et al., 1996, 1998; Berger and Quack, 2000a,b; Quack and Stohner, 2000) are now confirmed by several research groups (see reviews in Quack et al., 2008; Quack, 2011b, 2015b,a). The asymmetric potential distinguishing between the enantiomers is predicted to be in the sub-feV range (corresponding to about 100 pJ/mol); it dominates the dynamics in molecules with very small tunneling splitting (Prentner et al., 2015). Recent examples of this kind are the HOOH-analogue molecule ClOOCl (Prentner et al., 2015; Horný and Quack, 2015; Horný et al., 2016) and the 1,2-dithiine molecule (Albert et al., 2016a,b). A further example with a more complex tunneling dynamics is the HSSSH molecule, trisulfane (Fábri et al., 2015). In this molecule typical tunneling splittings $\Delta E_{\pm}$ on the order of less than $(\mathrm{hc}) \cdot 10^{-20}\ \mathrm{cm}^{-1}$ (corresponding to about 1 yeV, yoctoelectronvolt $= 10^{-24}$ eV) are calculated for the ground state, while the parity violating energy difference $\Delta_{\mathrm{PV}}\mathrm{E}$, corresponding to the effective asymmetry of the potential, is calculated in the range from $(\mathrm{hc}) \cdot 10^{-11}$ to $10^{-12}\ \mathrm{cm}^{-1}$ (corresponding to ca. 1 to 0.1 feV, see also Prentner et al., 2015; Horný and Quack, 2015; Horný et al., 2016; Albert et al., 2017, 2016a,b; Fábri et al., 2015). For these cases, as always when one has

$$\Delta_{\mathrm{PV}} E \gg \Delta E_{\pm}, \tag{7.3}$$

parity violation is dominating the quantum dynamics, as demonstrated also quantitatively for ClSSCl (Berger et al., 2001). Indeed, in the work on ClSSCl a new extrapolation method was developed based on WKB theory and exact calculations in order to estimate tunneling

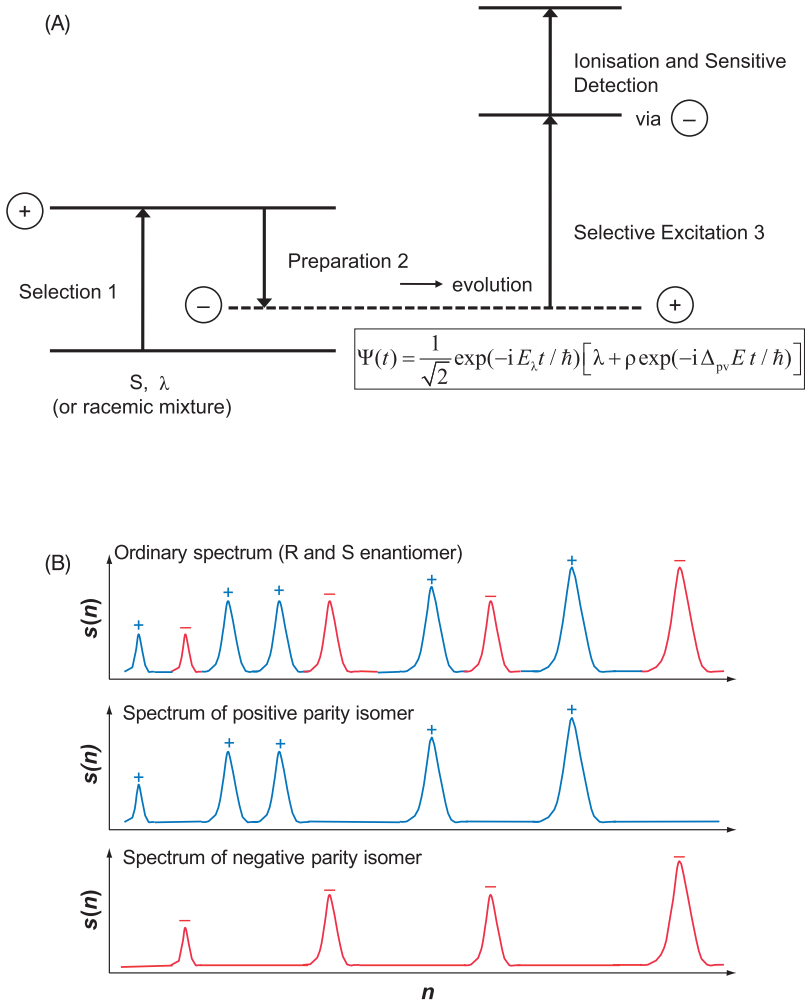

FIG. 7.6 (A) Sequence of the steps in the experiment to measure the parity violating energy difference Δ_{PV}E (Quack, 1986, 2015b). (B) Time evolution of the measured spectra under the influence of the parity violating energy difference Δ_{PV}E after preparation of a superposition state with initially negative parity (in the example, the reverse would be equivalent) (Quack et al., 2008; Quack, 2015b). ($n=(\nu-\nu_0)/\nu_0$ is a reduced frequency scale and $s(n)$ is a reduced absorbance signal.)

splittings $\Delta E_{\pm} \ll (\mathrm{hc})10^{-60}$ cm^{-1} for the hypothetical symmetrical potential while $\Delta E_{\mathrm{PV}} \simeq (\mathrm{hc})10^{-12}$ cm^{-1}.

The extremely small values of $\Delta_{\mathrm{PV}}E$ can be measured according to a scheme shown in Fig. 7.6. After the selection of a parity state, a "parity isomer" of a chiral molecule is prepared which is at the same time an R and S (or P and M) enantiomer, therefore a superposition of both enantiomers, which shows a well-defined parity (a negative parity in our example of Fig. 7.6). Due to parity violation, this state develops into a state of opposite parity which shows a different spectrum (Fig. 7.6B), where the population p_+ (t) of the new state (initially forbidden) follows the equation

$$p_+(t) = \sin^2(\pi t \Delta_{\mathrm{PV}}E/h) = 1 - p_-(t), \qquad (7.4)$$

and approximately at the beginning (for small values of t and the argument of the $\sin^2$ function)

$$p_+(t) \approx \pi^2 t^2 \Delta_{\mathrm{PV}}E^2/h^2. \qquad (7.5)$$

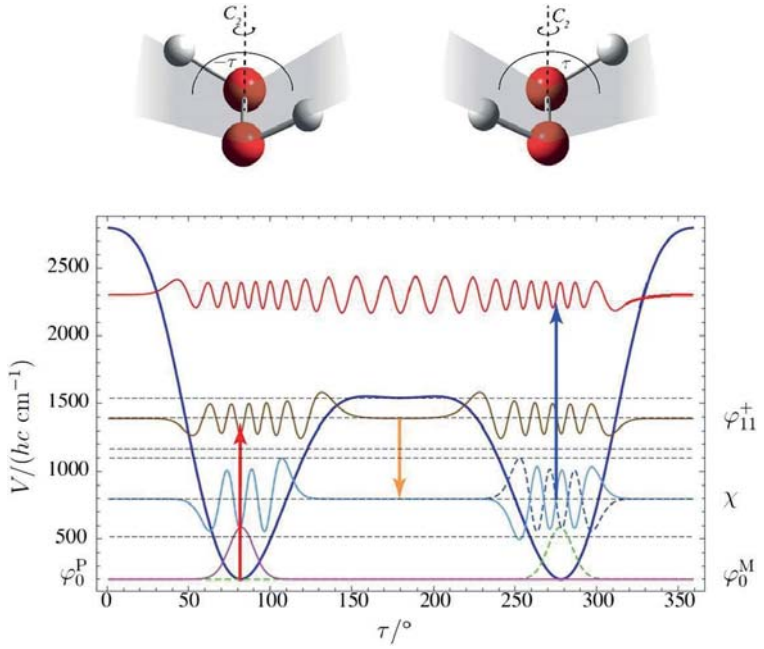

FIG. 7.7 Model calculations for the laser preparation (red) and of the laser detection (blue) for the measurement of the parity violating energy difference in an XYYX-molecule (Cl_2O_2). The wave functions of the levels populated by the laser excitation are shown (after Prentner et al., 2015).

This state of positive parity can then be detected very sensitively by multiphoton ionization as a function of time.

For the example of the achiral ammonia molecule NH_3, it could be shown recently in test experiments that a sensitivity can be reached which allows, in principle, for the measurement of values of $\Delta_{\mathrm{PV}}\mathrm{E} \simeq 100$ aeV or larger (Dietiker et al., 2015). A simulation for the realistic example of the chiral ClOOCl molecule shows that in principle for this molecule a measurement should be possible (Prentner et al., 2015) (see also Figs. 7.7 and 7.8). This simulation is a first example where tunneling processes including the weak parity violating interaction and coherent laser excitation could be addressed. In addition to the quasiadiabatic RPH approximation for the multidimensional tunneling process, also the rotational states have been considered explicitly with an approximate effective Hamilton operator. The time-dependent interaction with the coherent laser field has been calculated with and without the quasiresonant approximation (Quack, 1978; Quack and Sutcliffe, 1985, 1986; Marquardt and Quack, 1989, see also Chapter 1, Marquardt and Quack, 2020). However, there are no appropriate lasers available in the necessary frequency range for the ClOOCl molecule.

The laser sources for such a molecular beam experiment in the mid-infrared (Dietiker et al., 2015) are in principle available for molecules like 1,2-dithiine and trisulfane which should have appropriate molecular states above 2500 cm^{-1} for the parity selection. The relatively complex spectra of these molecules are currently subject of intense investigations (Albert et al., 2017, 2016b,a; Fábri et al., 2015). Fig. 7.9 shows the potential for the tunneling process and the parity violating potential in dithiine for which a very favorable, relatively high value for $\Delta_{\mathrm{PV}}E$ is predicted (approximately 1 feV or $\Delta_{\mathrm{PV}}E/hc \simeq 10^{-11}\ \mathrm{cm}^{-1}$). For the example of the trisulfane, due to the two hindered S–H-rotors, in principle, a two-dimensional tunneling problem has to be solved for which the 2-dimensional potential surface is shown in Fig. 7.10. However, trisulfane has the advantage that for such a 5-atomic molecule today, in principle an exact multidimensional calculation is feasible (9-dimensional) which will for a long time not be possible for larger molecules like 1,2-dithiine. These problems of the tunneling dynamics including parity violation are the subject of current studies at the limit of experimental and theoretical possibilities and of our knowledge of effects reaching from high energy physics to molecular quantum dynamics. Trisul-

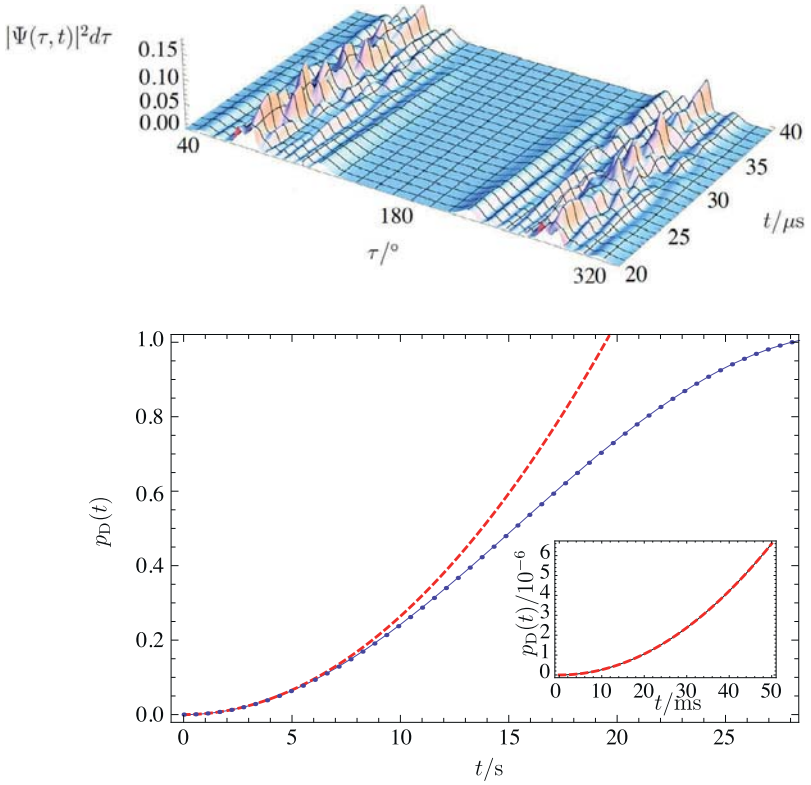

FIG. 7.8 (A) Time dependence of the wave packet for ClOOCl from Fig. 7.7 after the end of the preparation step. For $t = 40$ μs, a wave packet with well defined parity is obtained. (B) Time evolution of the level population $p_+(t)$ corresponding to $\Delta_{PV}E \gg \Delta E_\pm$ (blue) and $p_+(t) = \sin^2(\pi t \Delta_{PV} E/h) = 1 - p_-(t)$ or approximated by $p_+(t) = \pi^2 t^2 \Delta_{PV} E^2/h^2$ (red). The insert shows the evolution for the first 50 ms (after Prentner et al., 2015).

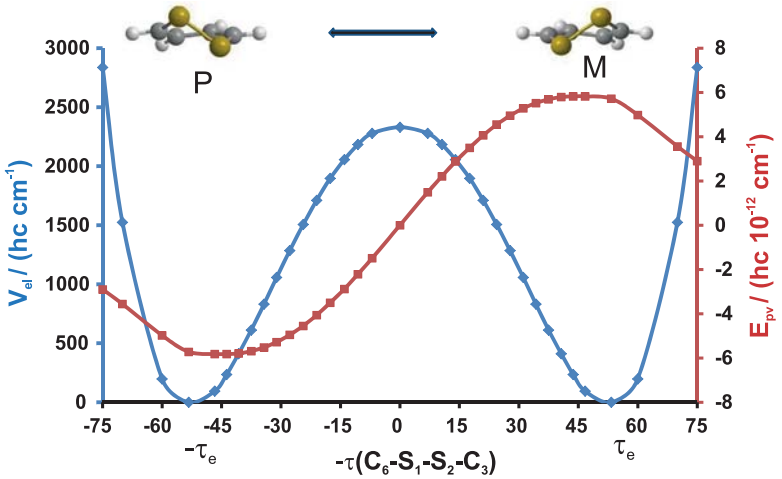

FIG. 7.9 Calculated symmetric Born–Oppenheimer potential (blue, scale to the left) and the parity violating antisymmetric potential (red, scale to the right) for 1,2-dithiine. The structure of the two enantiomers is displayed in the upper part of the figure (after Albert et al., 2016b).

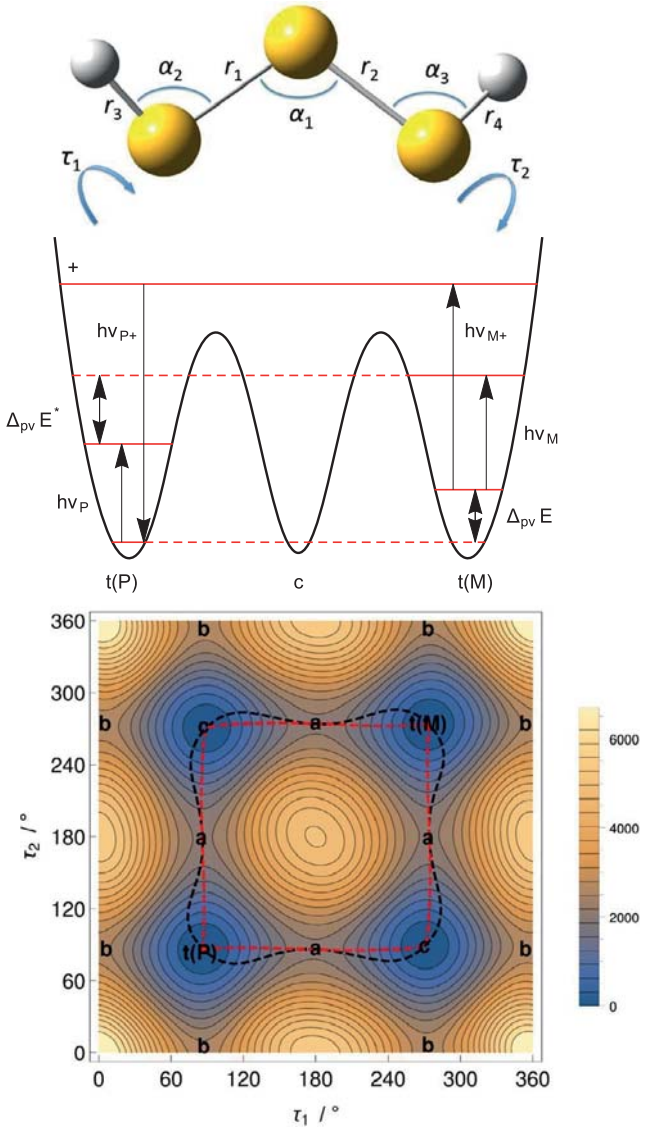

FIG. 7.10 One- (upper) and two-dimensional potential (lower part) energy surface for trisulfane, HSSSH. Also displayed are the different laser steps to measure the parity violating interaction Δ_{PV}E in trisulfane as given by the arrows in the scheme in the upper part of the figure (Fábri et al., 2015; Albert et al., 2017). For the nomenclature of P and M see Helmchen (2016); $\Delta_{PV}E$ is greatly overemphasized (not to scale) for this illustration.

fane, HSSSH, is also interesting at a more conventional level of tunneling processes, as it shows "sequential tunneling" trans(P) → cis → trans(M) with an intermediate cis structure of slightly higher energy than the two trans structures (P and M) for which the energy difference Δ_{PV}E is overemphasized (not to scale); see Fig. 7.10.

7.3 TUNNELING PROCESSES IN WEAKLY BOUND COMPLEXES

The dimer $(HF)_2$, Fig. 7.11, is prototypical for hydrogen bond complexes and is the first example where the tunneling process for the reorganization of the hydrogen bound has been investigated by high-resolution microwave (MW) spectroscopy (Dyke et al., 1972) and

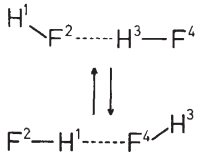

FIG. 7.11 Scheme of $(HF)_2$ conformations and inter conversions with definition of the numbering of the nuclei for the molecular symmetry group (after von Puttkamer and Quack, 1987).

later understood in detail by full-dimensional calculations (Quack and Suhm, 1991a; Klopper et al., 1998b). Here too, the mode selectivity showed pronounced non-classical and non-statistical behavior (Manca et al., 2008; Quack, 1981; von Puttkamer and Quack, 1989). Because $(HF)_2$ has been such an important prototype in our understanding of hydrogen bond tunneling dynamics, we add a little more detail here. This dimer is highly non-rigid with large amplitude motions, both by vibration and rotation, which greatly influence the tunneling rearrangement process shown in Fig. 7.11. Thus it is the permutation inversion group $S^*_{2,2} = S_2 \times S'_2 \times S^*$ and its subgroups such as M_{S4} which are relevant for analyzing the spectroscopy and quantum dynamics for the vibration–rotation–hydrogen-bond–tunneling motion. We use the notation of Quack (1977, 2011b); Merkt and Quack (2011) where S_2 is the symmetric group of the permutations of the two equivalent H atoms (or protons) 1 and 3, S'_2 corresponds to the F nuclei 2 and 4, and S^* is the inversion group. Table 7.2 provides the relevant character tables (from von Puttkamer and Quack, 1987). We note that the character table for $S^*_{2,2}$ is not given explicitly but is easily obtained, because of the direct product property $S^*_{2,2} = S_{2,2} \times S^*$, by taking the table for $S_{2,2}$ and adding E^* and all permutation inversions with a star such as $(13)^*$, etc. The symmetry species A_1, A_2, B_1, B_2 will have an exponent "+" for all characters of the starred operations being the same as the unstarred and will have an exponent "–" for all species where the characters of the starred operations have the opposite sign compared to the unstarred operation (thus + and – indicate positive and negative parity for the same species in the permutation group).

Because the barrier to exchanging protons attached to different F atoms is very high (Klopper et al., 1998a) the tunneling splitting corresponding to such exchanges is not observed and the subgroup of feasible permutation-inversion operations, according to Longuet-Higgins (1963), is the molecular symmetry group M_{S4} of order 4 given in Table 7.2 as well. This has four symmetry species A^+, A^-, B^+, B^- in the systematic notation of Quack (1977) (with an alternative notation being added in parenthesis), which assigns unique permutation species (symmetric A, antisymmetric B) and parity (positive + and negative –). This group describes the observable tunneling splittings for the rearrangement process of Fig. 7.11. It should be noted here that the concept of "feasible" symmetry operations of Longuet-Higgins (1963), which has occasionally been criticized, invokes the concept of "high barriers" in the Born–Oppenheimer approximation preventing "feasibility".

TABLE 7.2
Character tables for the symmetry groups of the dimer (HF-HF).

(a) Character table of the molecular symmetry group M_{S4} of $(HF)_2$ (after von Puttkamer and Quack, 1987)

Species	E	E^*	(ab) $(13)(24)$	$(ab)^*$ $(13)(24)^*$	$\Gamma(M_{S4}) \uparrow S^*_{2,2}$
$A^+(A_g)$	1	1	1	1	$A_1^+ + A_2^+$
$A^-(A_u)$	1	−1	1	−1	$A_1^- + A_2^-$
$B^+(B_u)$	1	1	−1	−1	$B_1^+ + B_2^+$
$B^-(B_g)$	1	−1	−1	1	$B_1^- + B_2^-$

(b) Character table for $S_{2,2}$

Species	E	(13)	(24)	(13)(34)	$(S_{2,2}) \downarrow M_{S2}$
$A \times A \equiv A_1$	1	1	1	1	A
$B \times B \equiv A_2$	1	−1	−1	1	A
$B \times A \equiv B_1$	1	−1	1	−1	B
$A \times B \equiv B_2$	1	1	−1	−1	B

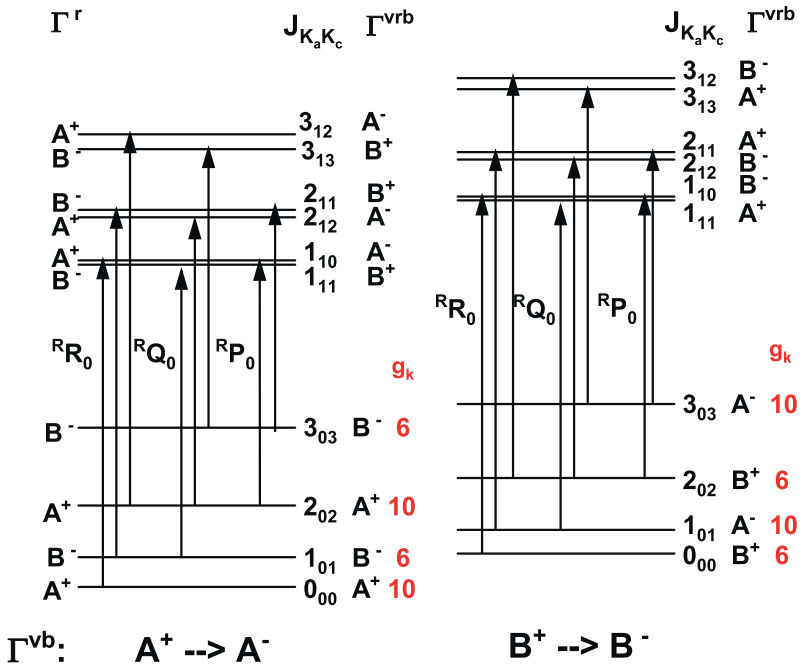

FIG. 7.12 Scheme for the observed rovibrational transitions assigned to the torsional (out of plane bending) fundamental of $(HF)_2$; $\Gamma^{vb}\Gamma^{r} = \Gamma^{vrb}$ is the vibrational, rotational symmetry species including the bending motion with the tunneling splitting; Γ^{r} is the rotational symmetry species (after von Puttkamer and Quack, 1987). The nuclear spin statistical weights g_k are given in red color and help the unique assignment of the high resolution spectra.

It can, however, be introduced much more rigorously relying only on exact theory or, in fact, directly on experiment, without invoking the Born–Oppenheimer or other related approximations (Quack, 1985, 2011b; Merkt and Quack, 2011; see also Chapters 1 and 2 and Section 7.9 of the present chapter). Fig. 7.12 shows in an exemplary way how these symmetry considerations leading to selection rules and nuclear spin statistics allow for an assignment of tunneling spectra.

In the investigations of $(HF)_2$ it turned out that tunneling depends in a highly mode-selective way on the excitation of various degrees of freedom. The "low frequency" motions such as strongly non-rigid K-rotation of the near symmetric rotor and the out of plane bending, "librational" or "torsional" mode promote tunneling appreciably (von Puttkamer and Quack, 1987; von Puttkamer et al., 1988). On the other hand, excitation of the high frequency (HF)-stretching vibration (Pine and Lafferty, 1983; Pine et al., 1984; Pine and Howard, 1986) as well as the even higher lying (HF)-stretching overtones (von Puttkamer and Quack, 1985, 1989; Hippler et al., 2007; Chuang et al., 1997; He et al., 2007; Yu et al., 2005; Manca et al., 2008) leads to a decrease of the tunneling splittings and a considerable lengthening of the tunneling times for the switching process in Fig. 7.11. This early work has revealed many interesting and fundamental facets of the hydrogen bond dynamics in such clusters, see the early review (Quack and Suhm, 1998). The possibilities for concerted proton exchange were studied systematically for the larger (cyclic) hydrogen fluoride clusters, $(HF)_n$ (with $n = 3$–6) (Klopper et al., 1998a). It was shown that pair potentials are quite insufficient to describe tunneling barriers, at least 3-body terms in the many body expansion must be included (see also Quack et al., 1993b, 2001; Quack and Suhm, 1997; Marquardt and Quack, 2011). The early results on simple prototype systems $(HF)_n$ can be seen as an introduction to much later work on more complex systems. $(H_2O)_n$ is an obvious candidate of interest, and we refer to the review by Cvitaš and Richardson in Chapter 9 (Cvitaš and Richardson, 2020). Indeed, many of the basic effects originally found in the quantum dynamics of hydrogen fluoride clusters were later also found in water clusters. These include the mode

selective enhancement or inhibition of tunneling by rotational and vibrational excitation, or the importance of three-body terms in the development of the potential hypersurfaces to give just two important effects (Quack and Suhm, 1991a,b, 1995; Quack et al., 1997; Quack and Suhm, 1998; Quack et al., 1993b, 2001; Klopper et al., 1998a,b; Keutsch et al., 2001; Mukhopadhyay et al., 2018; Barclay et al., 2019; Luzar and Chandler, 1996; Luzar, 2000; Richard et al., 2014; Leforestier, 2012; Paesani, 2016; Cole et al., 2015, 2017, 2018), and for many body effects in water clusters see (Xantheas, 1996), for example. But also other and even more complex systems have found interest recently. Indeed, since then numerous additional hydrogen-bond complexes have been investigated. Tunneling processes are generally fast here, due to the low barrier for these processes. Many experimental studies have used microwave- or IR-spectroscopy (Grabow, 2011; Shipman and Pate, 2011; Caminati, 2011; Tanaka et al., 2011; Endo and Sumiyoshi, 2011; Albert et al., 2011; Snels et al., 2011; Havenith and Birer, 2011; Potapov and Asselin, 2014). Three relatively complex recent examples concern the structure and tunneling in methylsalicylate-monohydrate (Ghosh et al., 2015), benzoic-acid monhydrate (Schnitzler and Jäger, 2014), and the trimer of fluoroethanol (Thomas et al., 2015) and the H_2O_2 - formic acid complex (Li et al., 2018). Further complex tunneling systems have been investigated by low temperature UV–VIS and NMR spectroscopy with the aim to understand the influence of the polarity on the isomerization of carboxylate and similar phenomena (Koeppe et al., 2013; Pylaeva et al., 2015). Among the prototypical larger complexes recent studies of the trimer $(HF)_3$ could be mentioned (Asselin et al., 2014) where already earlier a full dimensional potential with a many body potential expansion has been formulated (Marquardt and Quack, 2011; Quack et al., 1993a,b, 1997, 2001). $(HF)_n$ clusters up to $n = 6$ have been studied by supersonic jet spectroscopy (Quack et al., 1993a; Luckhaus et al., 1995), see also Nesbitt (1994) and this species has also led to the first IR-spectroscopic observation of nanoclusters (Quack and Suhm, 1997; Quack et al., 1997; Maerker et al., 1997). Much effort has been devoted to understand the far infrared and microwave spectra of water clusters of different size theoretically (Richardson et al., 2011, 2013, 2016, see also Cvitaš and Richardson, 2020, Chapter 9 in the current volume). Quantum effects and tunneling processes in supercooled water have been investigated by neutron scattering and relaxation spectroscopy (Agapov et al., 2015). The GENUISH program was used to understand the spectra and tunneling processes in ionic complexes F^- (H_2O)) and F^- (D_2O)) (Sarka et al., 2016b) and for the important prototypical complex (CH_4–H_2O) (Sarka et al., 2016a), the prototype of the methane-hydrates (see also the review by (Tanaka et al., 2011) for spectroscopic studies of complexes). Tunneling phenomena may even be of relevance in every day phenomena such as the slipperiness of ice. It was already established that this effect is related to the surface mobility of H_2O molecules by a rolling motion, so far studied with a classical molecular dynamics simulation in relation to experiments (Weber et al., 2018). However, since such a motion involves rearrangement of hydrogen bonding, tunneling may be important.

The double proton (or H-atom) transfer by tunneling in the dimer $(HCOOH)_2$ of formic acid has a long history as a simple straightforward example of this kind of processes (Ortlieb and Havenith, 2007; Havenith and Birer, 2011; Luckhaus, 2006; Zielke and Suhm, 2007; Xue and Suhm, 2009, see also Quack and Jans-Bürli, 1986; Blumberger et al., 2000). Recently an attempt was made to describe the process on a full dimensional potential hypersurface (Qu and Bowman, 2016). Also tunneling processes in the prototype system malonaldehyde still find much interest (Tautermann et al., 2002; Hargis et al., 2008; Lüttschwager et al., 2013; Vaillant et al., 2018, and references cited therein).

7.4 TUNNELING PROCESSES IN SLIGHTLY ASYMMETRIC POTENTIALS, TUNNELING SWITCHING, AND THE MOLECULAR QUANTUM SWITCH

The very weakly asymmetric potentials of chiral molecules under the influence of parity violation are an extreme case which is still today only proven by theory (Quack, 2011a,b). Somewhat larger asymmetries, but often still rather small ones, are found for isomerization reactions of isotopically substituted molecules. For such reactions the electronic Born–Oppenheimer potential for the tunneling process is symmetric, see also Chapters 1 and 2 (Marquardt and Quack, 2020; Császár et al., 2020). Through an appropriate substitution with isotopes the effective potential becomes asymmetric due to zero point energy effects. A straightforward example is the rearrangement of the hydrogen bonding in the dimer $(HF)_2$ (Dyke et al., 1972; Quack and Suhm, 1991a,b; Klopper et al., 1998a,b). As discussed in Section 7.3 this process exchanges the positions of the symmetrically equivalent (by the generalized Pauli principle identical) H-atoms in the dimer. The tunneling splitting ($\Delta E_T/hc$) is approximately 0.7 cm^{-1} in the ground

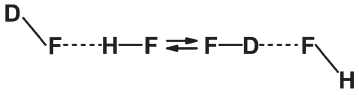

FIG. 7.13 If in the HF-Dimer one H is replaced by a D, then the structures are distinguishable and the zero point energy is different for the two structures.

state. If one H-atom is substituted by D the two structures become distinguishable (Fig. 7.13).

Even though the potential minima have the same energy within the Born–Oppenheimer approximation the zero point energy of the two structures is different which results in an energy difference of the ground states of $(\Delta E_{\text{eff}}/\text{hc}) \approx 70\ \text{cm}^{-1}$ (Klopper et al., 1998b). As there is

$$\Delta E_{\text{eff}} \gg \Delta E_T, \tag{7.6}$$

the energy levels of the corresponding isomers are localized in the ground state. For more highly excited levels one finds

$$\Delta E_{\text{eff}} \ll \Delta E_T \tag{7.7}$$

with delocalized eigenstates. This transition is called "tunneling switching" (Quack and Willeke, 2006; Albert et al., 2013). Another example is found in the mixed H/D isotopomers of the CH_4^+-cations (Signorell et al., 1999; Signorell and Merkt, 2000; Wörner et al., 2007; Wörner and Merkt, 2009). The high resolution analyses of tunneling processes of this kind in more complex and larger molecules are rare. It was predicted (Albert et al., 2013) that for phenol, marked with deuterium in the ortho or meta position, an energy difference on the order of $(\Delta E_{\text{eff}}/\text{hc}) \simeq 1\ \text{cm}^{-1}$ is to be expected, orders of magnitude larger than ΔE_T in symmetric phenol C_6H_5OH. This prediction and also the phenomena of tunneling switching after excitation could be confirmed recently in the high resolution analysis of the GHz- (mm wave) and THz (FTIR)-spectra with synchrotron radiation of meta-D-phenol (Albert et al., 2016c).

Fig. 7.14 shows a summary of the results for transitions between syn- and anti-isomers. For the ground state and the transition to the first excited state of the torsional vibration of the OH-group relative to the rigid aromatic ring structure, an effectively localized structure is found which could be proven by the different rotational constants of the two isomers in the rotational spectra and also of the corresponding rotational-vibrational spectra in comparison with the theory (Albert et al., 2016c). One finds separate transitions for both isomers, without transitions between the isomers. Above the torsional state excited with 2 quanta, one finds delocalized structures with correspondingly allowed transitions between the syn- and anti-structures, as is shown in the corresponding diagram of Fig. 7.14. The transitions considered are slightly weaker than the "main" transitions in the center of the spectrum, but the rotational fine structure could be precisely simulated and the corresponding spectroscopic parameters could be ascertained. A similar picture is obtained in ab initio predictions with the quasiadiabatic channel RPH model where the agreement with experiment (without any adjustment) is excellent within the uncertainty of the quantum chemical electronic structure methods for problems of this size. This first spectroscopic proof of such a tunneling switching is on the one hand of importance for the corresponding analysis of molecules like 1,2-diithine showing tunneling switching with parity violating potentials which then requires most highly resolved, currently available laser spectroscopy. On the other hand, tunneling switching in molecules like m-D-phenol can be used for quantum mechanical molecular switches and a possible quantum technology and quantum mechanical machine of this kind (Albert et al., 2016c; Fábri et al., 2018). Indeed, based on the accurate spectroscopic data and the analysis for m-D-phenol, a true molecular quantum switch could be recently demonstrated. Fig. 7.15 shows the wavepacket for the quantum switch transfer from a syn- to an anti-structure, which behaves quasiclassically. On the other hand, Fig. 7.16 shows the preparation of a "bistructural state" at the end of the laser pulse sequences, which is a superposition of syn- and anti-structures and shows time independent probability distributions, but time dependent spectra. This type of quantum switch may offer realistic opportunities for quantum machines and quantum computing in the future (Fábri et al., 2018).

Here we should point out also a fundamentally new isotope effect which is introduced by the parity violating interaction in "isotopically chiral" molecules (Quack, 1989). This effect has been calculated quantitatively for the first time (for $PF^{35}Cl^{37}Cl$) in Berger et al. (2005). It arises from the differences in the electroweak charges Q_W of the nuclei as available from the standard model of particle physics (SMPP) see Quack (2006) and Marquardt and Quack (2020), Chapter 1. A requirement for this effect and for stable isotopic chirality is a sufficiently small tunneling splitting (e.g., not fulfilled in the case of NHDT or hydrogen peroxide) for the stereomutation. The small effects of isotopic chirality have been discussed recently in connection with asymmet-

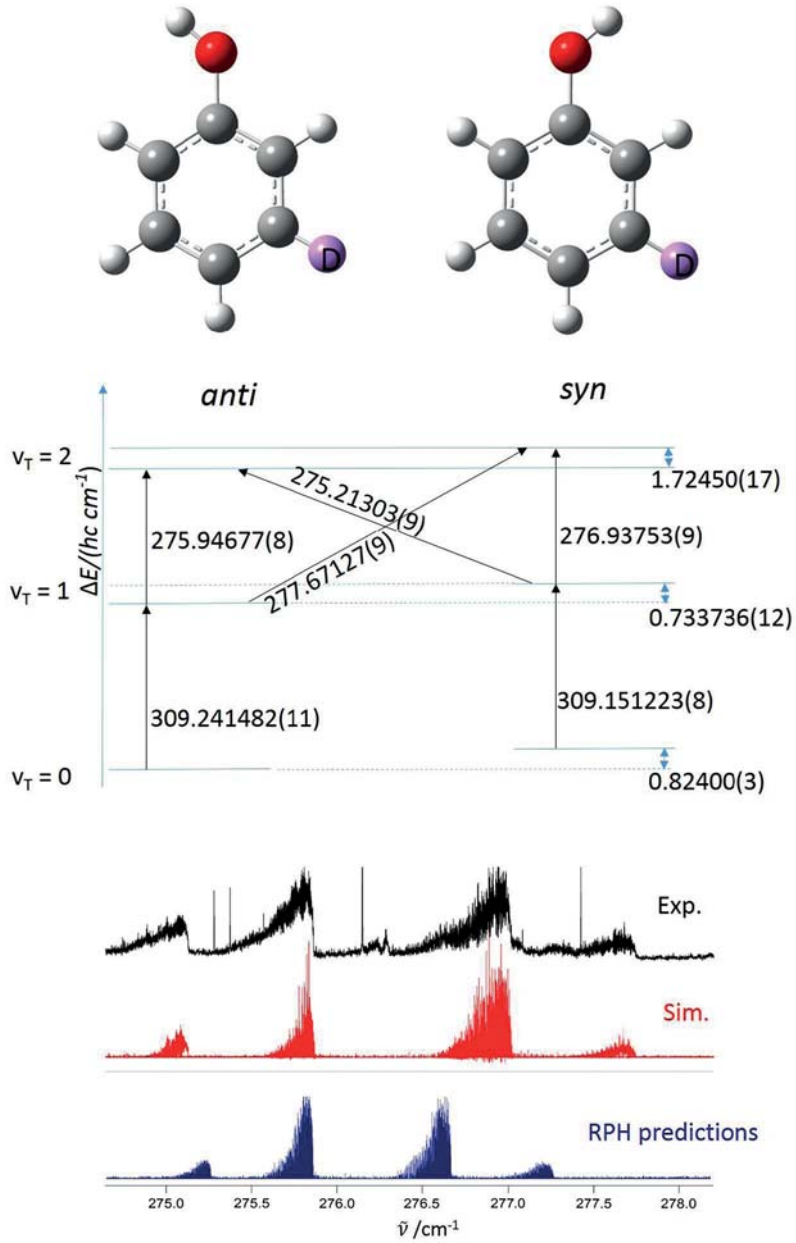

FIG. 7.14 (Top) Conformers of the meta-D-phenol. (Middle) Scheme of the energy levels with respect to the tunneling coordinate up to $v_T = 2$. (Bottom) Measured spectrum for the transition from $v_T = 1$ to $v_T = 2$, compared to a simulation with the fitted parameter of an effective Hamiltonian and with the parameters of the RPH-prediction. The transitions, which are crossing over between left and right in the level scheme, correspond to the weaker transitions becoming allowed by the tunneling switching (after Albert et al., 2016c).

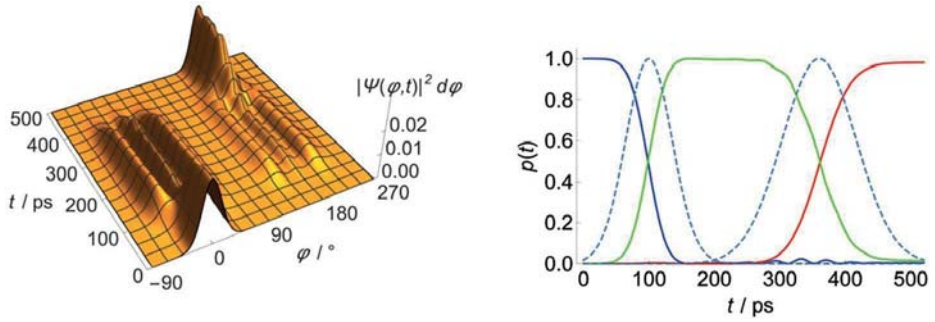

FIG. 7.15 Time-dependent wavepacket for meta-D-phenol (reduced probability density as a function of the torsional angle φ and time t) and populations ($|0_{\text{anti}}\rangle$, blue; $|0_{\text{syn}}\rangle$, red; $|2_{\text{lower}}\rangle$, green) for the two-pulse excitation scheme $|0_{\text{anti}}\rangle \rightarrow |2_{\text{lower}}\rangle \rightarrow |0_{\text{syn}}\rangle$. The parameters of the two laser pulses are $\tau_P = 50$ ps, $t_0 = 100$ ps, $I_{\max} = 150$ MW cm^{-2} and $\tilde{\nu}_0 = 582.82$ cm^{-1} (first pulse, resonant with the $|0_{\text{anti}}\rangle \rightarrow |2_{\text{lower}}\rangle$ transition), and $\tau_P = 80$ ps, $t_0 = 360$ ps, $I_{\max} = 150$ MW cm^{-2} and $\tilde{\nu}_0 = 582.00$ cm^{-1} (second pulse, resonant with the $|0_{\text{syn}}\rangle \rightarrow |2_{\text{lower}}\rangle$ transition). The Gaussian envelope functions (normalized to maximum intensity) of the two sequential laser pulses are shown by the dashed lines (after Fábri et al., 2018, where detailed definitions and conditions are given).

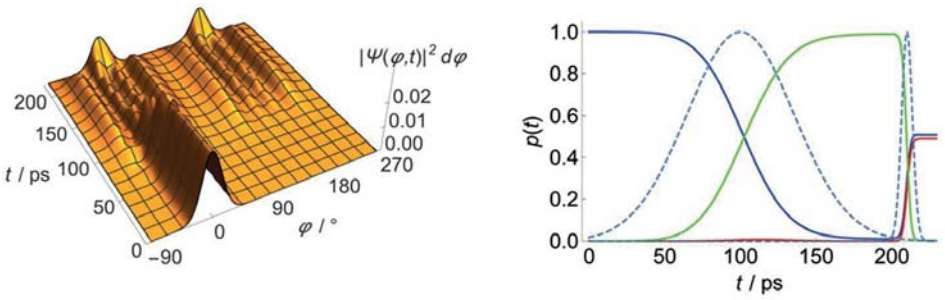

FIG. 7.16 Time-dependent wavepacket and populations for meta-D-phenol ($|0_{\text{anti}}\rangle$, blue; $|0_{\text{syn}}\rangle$, red; $|3_{\text{lower}}\rangle$, green) for the two-pulse excitation scheme $|0_{\text{anti}}\rangle \rightarrow |3_{\text{lower}}\rangle \rightarrow |0_{\text{anti}}\rangle + |0_{\text{syn}}\rangle$. The parameters of the two laser pulses are $\tau_P = 50$ ps, $t_0 = 100$ ps, $I_{\max} = 1$ GW cm^{-2} and $\tilde{\nu}_0 = 813.72$ cm^{-1} (first pulse, resonant with the $|0_{\text{anti}}\rangle \rightarrow |3_{\text{lower}}\rangle$ transition), and $\tau_P = 5$ ps, $t_0 = 210$ ps, $I_{\max} = 60$ GW cm^{-2} and $\tilde{\nu}_0 = 813.10$ cm^{-1} (second pulse). The Gaussian envelope functions (normalized to maximum intensity) of the two sequential laser pulses are shown by the dashed lines (after Fábri et al., 2018, where detailed definitions and conditions are given).

ric induction by the Soai mechanism (Soai et al., 1995; Kawasaki et al., 2009; Sato et al., 2003; Matsumoto et al., 2016) which is of interest in the context of the evolution of biological homochirality (Quack, 2002, 2015b; Blackmond, 2004; Al-Shamery, 2011; Luisi, 2006; Lehn, 2002; Hawbaker and Blackmond, 2019). If asymmetric induction is possible by labeling with "heavy" atoms (like ^{14}N/^{15}N) this might be an indication for a possible asymmetric induction by the very small effects arising from the parity violating interaction (see also the recent report on the history of the nomenclature of chiral molecules Helmchen, 2016, and a more general overview in Jortner, 2006; Meierhenrich, 2008; Quack, 1989, 1999, 2015b,a).

7.5 ISOMERIZATION REACTIONS WHICH ARE SUBSTANTIALLY INFLUENCED BY TUNNELING

7.5.1 A Brief Overview Over Some Recent Studies

We provide here a brief review of examples for such reactions. Isomerization reactions with a reaction barrier between 30 and 60 kJmol^{-1} are ideally suited for investigations by infrared spectroscopy in a low temperature matrix (Schreiner et al., 2011; Schreiner, 2017). There the reaction can be initiated through the absorption of a photon in the infrared or visible spectral region. Examples for such isomerization reactions with significant contributions from tunneling are: 2,4-pentanedione

(Lozada-Garcia et al., 2012), tetrazol-5-yl-acetic acid (TAA) (Araujo-Andrade et al., 2014), glyoxalic acid (Gerbig and Schreiner, 2015), pyruvic acid (Reva et al., 2015), oxalic acid (Schreiner et al., 2015), carbonic acid (Wagner et al., 2016), trifluoromethyl-hydroxycarbene (Mardyukov et al., 2016). For the interpretation of the data often ab initio calculations are used in combination with the WKB (Wentzel–Kramers–Brillouin) theory of tunneling. The case of methyl-hydroxy-carbene is of interest as it shows two competing reactions: on the one hand, to vinyl alcohol through a [1,2] hydrogen shift along the C–C bond and, on the other hand, to acetaldehyde through a [1,2] hydrogen shift along the C–O bond. At low temperatures below 250 K, the reaction channel to the aldehyde is preferred with a higher but narrower barrier than for the competing channel to the alcohol which can be explained easily by theory (Kästner, 2013). An even more complex tunneling reaction is the proton transfer in triplet 2-formyl phenylazide which is produced by UV-photolysis. It reacts in the dark on a time scale of 7 hours to 6-imino-2,4-cyclohexadiene-1-ketene. The [1,4] H-atom migration from the nitrene to the imino ketene proceeds on the triplet surface before the molecule is transferred to the ground state (Nunes et al., 2016).

The tautomerism of porphycene has been studied by femtosecond pump–probe experiments in a molecular beam (Ciaćka et al., 2016). The rate of isomerization is an order of magnitude faster in the S_0-state compared to the S_1-state with a strong isotope effect upon N-deuteration. This study was extended to 19 differently substituted porphycenes (Ciaćka et al., 2015), as well as to experiments in He-droplets in a molecular beam (Mengesha et al., 2015) and on a metal surface Cu(111) (Böckmann et al., 2016) and to investigations of single molecules using an STM (Scanning Tunneling Microscope) (Ladenthin et al., 2016). Details on this interesting type of reactions have been summarized in a recent review article (Waluk, 2017).

The one-dimensional rotational motion of CH_2Cl about the C–Cl axis was investigated by infrared spectroscopy after photolysis of CH_2ClI in solid parahydrogen at 3.7 K. It was found that the nuclear spin conversion between the ortho and para nuclear spin species of the radical occurred on a time scale of a few hours (Miyamoto et al., 2013). The conformational composition and the change in conformational ratio induced by UV irradiation of β-alanine have been investigated in solid parahydrogen using FTIR spectroscopy. It could be shown that the conformational changes are significantly faster in p-H_2 in an Ar-matrix (Wong et al., 2015). Benzvalene, fulvene and Dewar benzene were obtained by exposing benzene to UV-radiation at 193 or 253.7 nm in solid parahydrogen. Neither tunneling reaction for any isomerization nor reaction with a hydrogen molecule from the matrix could be detected on the time scale of days (Toh et al., 2015).

Heavy atom tunneling is the dominant mechanism in ring-expansion and ring-opening reactions at cryogenic temperatures after activation by a visible or UV-photon. Photon activated 1H-bicyclo[3.1.0]-hexa-3,5-diene-2-one rearranges to 4-oxacyclo-hexa-2,5-dienylidene. The rate of rearrangement was found to be temperature independent for temperatures smaller than 20 K and was interpreted as a tunneling process (Ertelt et al., 2014). Through experiments in H_2, HD, and D_2 at cryogenic temperatures, is has been shown that tunneling governs the insertion of 1-azulenylcarbene into H_2 and D_2 (Henkel and Sander, 2015). Benzazirines were identified by IR-spectroscopy after photolysis of 4-methoxyphenyl azide and 4-methylthiophenyl azide. Despite a calculated barrier of 14 kJ mol^{-1}, the benzazirines rearranged to ketenimines at 10 K by a tunneling process (Inui et al., 2013). By a similar tunneling process the triplet 2-formyl phenylnitrene, obtained from the photolysis of 2-formyl phenylazide, is reacting to singlet 6-imino-2,4-cyclohexadiene-1-ketene (Nunes et al., 2016). The ring expansion of noradamantylmethylcarbene could either proceed to 2-methyladamantene or to 3-vinylnoradamantane. It could be shown by DFT calculations that at 10 K the formation reaction of 3-vinylnoradamantane is by 8 orders of magnitude faster than the one to 2-methyladamantene (Kozuch et al., 2013). The SCI (small-curvature tunneling) approximation has been applied to estimate tunneling corrections to classically calculated rate constants for the ring expansions of noradamantyl-carbenes to form adamantenes. The calculation showed that below temperatures of 30–50 K the rearrangement is dominated by heavy atom tunneling (Kozuch, 2014b). Another system which can be treated as heavy atom tunneling is the isomerization of substituted pentalenes, heptalenes, and acepentalenes (Kozuch, 2014a). Particularly noteworthy are also the studies of Limbach and coworkers on proton tunneling in organic model systems (Limbach, 2007). Tunneling by the puckering motion in ring compounds has been studied extensively (Laane, 1999), and we refer here to the prototypical study of the cyclobutane as an example (Blake and Xantheas, 2006; Frey et al., 2011).

For the prototypical reaction of the degenerate isomerization of semibullvalene there is a prediction that at low temperatures a temperature independent rate constant of $2 \cdot 10^{-3}$ s^{-1} should be found (Zhang et

al., 2010). This prediction has been tested by studies of the rate of equilibration after the synthesis of a mixture of 1,5-dimethyl-semibullvalene-2-D_1 and 4-D_1 (Ertelt et al., 2015). Another prototypical isomerization is the proton transfer in tropolone (Tanaka et al., 1999). This has been recently studied by making the effective potential for tunneling slightly asymmetric with various ^{13}C substitutions (Tanaka et al., 2019), similar to our study of phenols, discussed in Section 7.4 (Fábri et al., 2018; Albert et al., 2013).

Tunneling is not only relevant for conversion processes but may also influence the molecular structure, if the atomic wave function penetrates deeply into the classically forbidden region of the potential function. An extreme example is the very weakly bound He_2 molecule (Zeller et al., 2016). Here, it was shown in recent experiments that 80 % of the probability density in the ground state of the molecule is found within the classically forbidden region. This results in an extremely large "bond length", which, however, is not to be understood as a sharply defined quantity.

7.5.2 Ammonia as a Prototype for the Inversion at Nitrogen and Mode Selective Control of Tunneling Processes

Ammonia has for a long time been a fundamental molecule of physics and chemistry (Townes, 1964, 1965; Townes and Schawlow, 1975; Ertl, 2008) In addition to complex isomerization reactions in organic prototype molecules, the simplest tunneling processes in the ammonia molecule have further attracted interest with new results. For the ammonia molecule a number of full-dimensional potential energy surfaces were formulated in the last decade. A global potential hypersurface not only took into account the tunneling process of the inversion at low excitation energies, but also all possible dissociation reactions at higher energies (Marquardt et al., 2005; Marquardt and Quack, 2011; Marquardt et al., 2013). The inversion potential for NH_3 has been prototypical for this type of inversion at the nitrogen atom (Hund, 1927a,c,b; Fermi, 1932; Prelog and Wieland, 1944; Laane, 1999). Mode selective tunneling has been repeatedly discussed in the past for the ammonia molecule and its isotopomers, for example, in Herzberg (1945); Marquardt et al. (2003a,b, 2005); Snels et al. (2000, 2003, 2006b,a, 2011). Tunneling splittings have been discussed and analyzed in different recent publications (Marquardt et al., 2013, 2003a; Al Derzi et al., 2015; Fábri et al., 2014). The time dependent dynamics has also been discussed (Marquardt et al., 2003a; Sala et al., 2012) and was extended in most recent times to the complete series of isotopomers NH_3, NH_2D, NHD_2, ND_3, NHDT, NH_2Mu, ND_2Mu, and NHDMu, where the stereomutation of the chiral isotopomers is of special importance (Fábri et al., 2015; Fábri et al., 2019). Very highly resolved measurements of infrared spectra using a special OPO laser system resulted in hyperfine structure resolved spectra of the excited NH-stretching vibrations and have also been used as a test system for the preparation of an experiment to measure the parity violating energy difference in chiral molecules (Dietiker et al., 2015).

Because ammonia has been a prototypical system for tunneling by inversion, somewhat related to our discussion of $(HF)_2$ being prototypical for tunneling in hydrogen bonded systems, we shall discuss here also in some more detail the developments in our understanding of spectroscopy and tunneling dynamics in the NH_3 molecule. Indeed, after the early discussion of Hund (1927a,c,b) there was an analysis of the vibrational spectrum and potential by Fermi (1932) and at almost that same time as well a quantitative analysis of the tunneling dynamics in the framework of WKB theory (Dennison and Uhlenbeck, 1932). The early work typically dealt with the ground state tunneling – including notably the ammonia Maser (Gordon et al., 1955) – and used one-dimensional models for the tunneling process (Morse and Stückelberg, 1931; Manning, 1935; Wall and Glockler, 1937; Newton and Thomas, 1948; Costain and Sutherland, 1952; Swalen and Ibers, 1962). Much of the early history can be found in Herzberg (1939, 1945, 1966). Ammonia tunneling by inversion has been reviewed on the broader context of potential barriers for inversion at the nitrogen atom by Lehn (1970) and in relation to one dimensional potential functions for tunneling by Laane (1999). Strongly hindered inversion at nitrogen has been discussed in the context of molecular chirality (Prelog and Wieland, 1944; Felix and Eschenmoser, 1968), see also the review by Quack (1989). Ammonia has also been used as a testing ground for developing quantum chemical methods to compute barriers for isomerization (see Veillard et al., 1968; Császár et al., 1998; Klopper et al., 2001; Marquardt et al., 2005, 2013, and references therein). Finally, tunneling is also important in prototypical studies of the photoionization of ammonia isotopomers (Hollenstein et al., 2007; Merkt et al., 2011) and ammonia has been used as a test case for nuclear spin symmetry conservation (Wichmann et al., 2020). Here we shall discuss in some detail a recent extended investigation of spectroscopy and quantum dynamics of ammonia and its isotopomers in view of an understanding of its multidimensional tunneling and mode selective reaction

TABLE 7.3
Character table of the symmetry group S_3^* for NH_3 (ND_3) isotopomers (compared to D_{3h}). The first three columns provide species following three different notations: 1, [partition]^{parity}; 2, [S_3 species]^{parity}; and 3, D_{3h} point group species (see text).

	D_{3h} (class):	E	$2C_3$	$3C_2$	σ_h	$2S_3$	$3\sigma_v$		
	S_3^* (class):	E	2(123)	3(12)	E*	2(123)*	3(12)*		
	species								
$\Gamma[S_3^*]$		$\Gamma[D_{3h}]$						$\Gamma(S_3^*)\downarrow S_2^*$	$\Gamma(S_3^*)\downarrow M_{S6}(C_{3v})$
$[3]^+$	A_1^+	A_1'	1	1	1	1	1	1	A^+	A_1
$[1^3]^+$	A_2^+	A_2'	1	1	−1	1	1	−1	B^+	A_2
$[2,1]^+$	E^+	E'	2	−1	0	2	−1	0	$A^+ + B^+$	E
$[3]^-$	A_1^-	A_1''	1	1	1	−1	−1	−1	A^-	A_2
$[1^3]^-$	A_2^-	A_2''	1	1	−1	−1	−1	1	B^-	A_1
$[2,1]^-$	E^-	E''	2	−1	0	−2	1	0	$A^- + B^-$	E

TABLE 7.4
Character table of the symmetry groups S_2^* for NH_2D and NHD_2 compared to C_{2v} (transition state structure group).

	C_{2v} (class):	E	C_2	σ_{yz}	σ_{xz}			
	S_2^* (class):	E	(12)	E*	(12)*	$\Gamma(S_2^*)\uparrow S_3^*$	$\Gamma(S_2^*)\downarrow M_{S2}(C_S)$	$\Gamma(S_2^*)\downarrow S^*$
species	$\Gamma(S_2^*)$	$\Gamma(C_{2v})$						
$[2]^+$	A^+	A_1	1	1	1	1	$A_1^+ + E^+$	A	A^+
$[2]^-$	A^-	A_2	1	1	−1	−1	$A_1^- + E^-$	B	A^-
$[1^2]^-$	B^-	B_1	1	−1	−1	1	$A_2^- + E^-$	A	A^-
$[1^2]^+$	B^+	B_2	1	−1	1	−1	$A_2^+ + E^+$	B	A^+

control of the corresponding isomerization by inversion at the nitrogen atom. As far as tunneling in vibrationally excited states is concerned, an extensive MARVEL analysis has reviewed the available data for the isotopomer $^{14}NH_3$ (Al Derzi et al., 2015).

Much less work is available on the deuterated isotopomers. However, in an extended spectroscopic project directed specifically also at the understanding of vibrationally mode-selective effects and control of tunneling rates the deuterated isotopomers ND_3, NHD_2, and NH_2D were investigated in some detail (Snels et al., 2000, 2003, 2006b,a) and combined with quantum-dynamical wavepacket calculations under coherent excitation including global potential and electric dipole hypersurfaces (Marquardt et al., 2003b,a; Fábri et al., 2019). Here we highlight some of the aspects with respect to mode selective tunneling dynamics as derived from the high resolution spectra. One important aspect concerns the symmetry of the rotation–vibration–tunneling levels, which can be understood in relation to the character tables (Tables 7.3, 7.4, 7.5, and 7.6) relevant for the different isotopomers. For ammonia and its isotopomers one has the special situation that one can use equivalently the point group of the planar transition structure (D_{3h} for NH_3, ND_3, C_{2v} for NH_2 D and NHD_2 and also C_s for NHDT, for which, however, no high resolution spectroscopic data seem to be available (Snels et al., 2006a; Quack, 2002)) or the corresponding isomorphous permutation inversion groups S_3^*, S_2^* and S^* with a one-to-one relation between group elements and irreducible representations (symmetry species). This procedure is not generally possible, for instance, for methane and other molecules this would not be possible (Quack, 2011b). However, for ammonia we can give the corresponding notations in Tables 7.3, 7.4, 7.5, and 7.6. The tables include also relevant induced and subduced

TABLE 7.5
Character table molecular symmetry group M_{S2} and point group C_s for NH_2D and NHD_2.

	C_S (class)		E	σ	
	M_{S2} (class)		E	$(12)^*$	
species	Γ (C_S)	Γ (M_{S2})			Γ (M_{S2})$\uparrow S_2^*$
	A'	A	1	1	$A^+ + B^-$
	A"	B	1	−1	$B^+ + A^-$

TABLE 7.6
Character table of the subgroup M_{S6} of the molecular symmetry group M_{S12} (S_3^*) and induced representation Γ (M_{S6}) $\uparrow S_3^*$; M_{S6} is isomorphous to C_{3v}[a].

C_{3v}	E	$2C_3$	$3\sigma_v$	
M_{S6}	E	2(123)	$3(12)^*$	$\Gamma(M_{S6}) \uparrow S_3^*$
A_1	1	1	1	$A_1^+ + A_2^-$
A_2	1	1	−1	$A_2^+ + A_1^-$
E	1	−1	0	$E^+ + E^-$

[a] After Dietiker et al., 2015.

representations. Table 7.6 gives also the character table for C_{3v}, isomorphous to the molecular symmetry group M_{S6}. The induced representation Γ (M_{S6}) $\uparrow S_3^*$ gives the symmetry structure of the tunneling sublevels in NH_3 and ND_3. We note furthermore that for NH_3 the Pauli principle excludes the A_1^+ and A_1^- levels in the corresponding tunneling doublets (thus hypothetical, but not real) whereas E^+ and E^- doublets exist and are observable by spectroscopy. On the other hand, all the rovibrational symmetry species $A_1^\pm$, $A_2^\pm$ and $E^\pm$ are Pauli allowed for ND_3 with appropriate nuclear spin functions and therefore all the tunneling doublets exist as observable levels. Fig. 7.17 summarizes one main result from the analysis of the tunneling spectra in ND_3 (Snels et al., 2000).

The ground state tunneling splitting in ND_3 is 0.053 cm^{-1}, as expected much smaller than in NH_3 (0.7 cm^{-1}). Thus the tunneling transfer time is rather long in the vibrational ground state (314 ps). However, exciting the symmetric ND_3 stretching fundamental at 2420.1 cm^{-1} one finds an increase of the tunneling splitting to 0.541 cm^{-1} corresponding to a "promotion" or enhancement of the tunneling rate by a factor of 10, with a shorter tunneling transfer time of 31 ps.

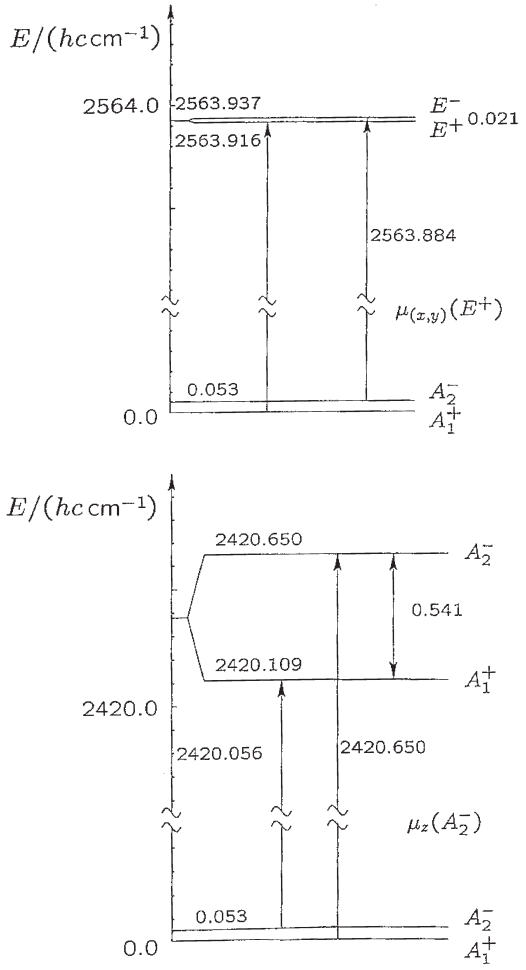

FIG. 7.17 Schematic drawing of observed transitions and vibrational tunneling levels in ND_3. The tunneling splittings are about to scale: the vibrational wavenumber scale is interrupted (after Snels et al., 2000). See also text.

While such an enhancement of tunneling with vibrational excitation might seem natural, one finds the reverse effect at even higher excitation with the degenerate ND_3 stretching fundamental centered at 2563.9 cm^{-1}, where the tunneling splitting is reduced to 0.021 cm^{-1}, by more than a factor of 2 compared to the ground state splitting and correspondingly an inhibition of the tunneling rate with an excitation well above the "tunneling barrier" and a very long tunneling transfer time of more than 600 ps. Of course, a very comparable situation has been found for H_2O_2 (see Table 7.1) and this is a further illustration of "quasiadiabatic above barrier tunneling". Indeed, a very rich variety of such en-

TABLE 7.7
Summary of tunneling times $\tau_{L\to R}$ (in ps) for NH_2D and NHD_2 ground states and fundamentals[a].

	NH_2D		NHD_2	
	$\tilde{\nu}$ (cm^{-1})	$\tau_{L\to R}$ (ps)	$\tilde{\nu}$ (cm^{-1})	$\tau_{L\to R}$ (ps)
ν_0	0	41	0	98
ν_1	2506	27	3404	214
ν_2	886	0.83	815	1.8
ν_{3a}	3366	7.1	2433	4.4
ν_{3b}	3439	99	2560	107
ν_{4a}	1598	1.1	1235	6.6
ν_{4b}	1390	28	1462	84

[a] After Snels et al., 2006a.

hancements and inhibitions of tunneling is also found in the extensive analysis on the NH_2D and NHD_2 isotopomers as summarized in Table 7.7. There the overall ranges of enhancements and inhibitions with various excitation of fundamental vibrations cover a factor of more than 100 with a shortest tunneling transfer time of about 1 ps and a longest tunneling transfer time of 214 ps. These experimental results can be compared to recent full-dimensional theoretical calculations (Fábri et al., 2015, 2019).

7.5.3 Methyl Group Internal Rotation as a Prototype for Tunneling

The methyl group ($-CH_3$) is a ubiquitous building block of organic molecules and biomolecular systems. Its torsional motion, a hindered internal rotation, shows a great variety of tunneling effects, which range from slightly anharmonic torsional vibration with only very small tunneling splittings to essentially free internal rotation, depending upon the molecular environment. The quantum dynamics of methyl group tunneling has been extensively studied in the solid, liquid and gas phases by NMR spectroscopy, neutron diffraction and optical spectroscopy, including high resolution studies from the microwave to the UV regions. It is a "classic" among the tunneling systems and has been extensively reviewed (Press, 1981; Heidemann et al., 1987; Prager and Heidemann, 1997; Horsewill, 1999; Bauder, 2011; Pratt, 2011). A great variety of systems has been studied in detail (Tan et al., 1989, 1991; de Haag et al., 1990; Barlow et al., 1992; Piecha-Bisiorek et al., 2014), including also $-CD_3$ group dynamics (Lalowicz et al., 1988; Börner et al., 1991). A particularly noteworthy aspect is the coupling of the tunneling motion with nuclear spin symmetry and the studies of the kinetics of the nuclear spin symmetry conversion (Haupt, 1972; Beckmann et al., 1977; Vandemaele et al., 1986; Buekenhoudt et al., 1990; Häusler, 1990; Würger, 1990; Hartmann et al., 1992; Plazanet et al., 2000). Due to the generalized Pauli principle (Quack, 2011b) the symmetries of the lowest tunneling levels for the hindered rotation are (in C_3) A combining with a total nuclear spin of the three protons $I_{3H} = 3/2$ in the ground state and E with $I_{3H} = 1/2$ in the first excited state, with only weak couplings between levels of different nuclear spin symmetry and correspondingly slow interconversion kinetics, depending also on the environment. The quantum dynamics of the methyl group tunneling in 4-methyl pyridine (γ-picoline, CH_3–C_5H_5N), for example, generates a tunneling splitting of about 130 GHz (4 cm^{-1}) resulting in long lived nuclear spin states (up to hours and more) and the so-called Haupt effect (Haupt, 1972). This effect has notably been used for a development of Haupt magnetic double resonance (Tomaselli et al., 2003, 2004) in view of sensitivity enhancements in NMR spectroscopy, see also Ludwig et al. (2010); Icker and Berger (2012); Ernst et al. (1987) and the theoretical treatment in Meier et al. (2013a); Dumez et al. (2015). We should mention here also the close relation of the symmetry effects in the long lived nuclear spin symmetry states in the methyl group tunneling with the effect of nuclear spin symmetry conservation observed by high resolution infrared spectroscopy of supersonic jet expansions of CH_3X molecules (Horká-Zelenková et al., 2019) and of NH_3 (Wichmann et al., 2020).

We shall discuss here as an example in some detail methanol (CH_3OH), which is among the simplest examples for the tunneling motion by hindered internal rotation of the methyl group, or strictly speaking the relative internal rotation of the methyl- and OH-fragments with respect to each other and with the corresponding reduced moment of inertia. The spectroscopy and quantum dynamics of methanol have been extensively studied and reviewed (Moruzzi et al., 2018). It shows many of the essential features of methyl group tunneling and also some interesting special effects. For this molecule a full-dimensional ab initio potential hypersurface has been developed by Qu and Bowman (2013), which includes the dissociation into $CH_3 + OH$ at high energies but also the low energy hindered internal rotation barriers. The mode selective multidimensional tunneling dynamics has been studied by Fehrensen et al. (2003) using the approximate quasiadiabatic channel reaction path Hamiltonian approach. Fig. 7.18 shows the molecular structure and coordinate definitions including the torsional angle τ defining in essence the tunneling reac-

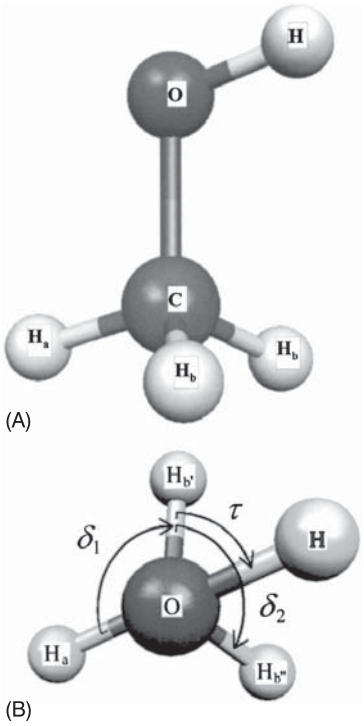

FIG. 7.18 (A) Equilibrium r_e structure of CH_3OH calculated with a basis of triple ζ quality on the MP2 level of theory (Fehrensen et al., 2003) The corresponding structure parameters are $r_{CO} = 142.3$ pm, $r_{OH} = 95.8$ pm, $r_{CHb} = 108.8$ pm, $r_{CHa} = 108.1$ pm, $\theta(HOC) = 107.9°$, $\theta(OCH_a) = 112.0°$, $\theta(OCH_b)) = 106.6°$, and $\delta(HOCH_b) = 61.5°$ (r = bond lengths, θ = bond angles, δ = dihedral angle). (B) Newman projection of methanol indicating the torsional angle τ, which is defined as the dihedral angle between the HOC plane and the $H_{b'}CO$ plane; τ closely follows the reaction coordinate, but relaxation of the CH_3 group bond angles and lengths slightly breaks the C_3 symmetry along τ. A more accurate (but still approximate) representation of the reaction coordinate is the symmetry adapted combination $\tau + (\delta_1 - \delta_2)/3$; δ_1 is defined as dihedral angle between the planes spanned by $H_{b'}$, C, O and by C, O, H_a, δ_2 is the corresponding dihedral angle between the planes spanned by $H_{b'}$, C, O and by C, O, $H_{b''}$; τ, δ_1 and δ_2 have a clockwise orientation (after Fehrensen et al., 2003).

tion path coordinate, and Fig. 7.19 shows the effective tunneling potential with the lowest energy levels of A and E symmetry (Fehrensen et al., 2003).

The ground state splitting between the lowest levels is $\Delta\tilde{\nu}_{EA} = \tilde{\nu}_E - \tilde{\nu}_A = 9.12$ cm^{-1} from experiment, in good agreement with the ab initio predictions from the anharmonic quasiadiabatic channel RPH model (7.9 cm^{-1}). It is thus about twice as large as for the 4-methylpyiridine mentioned above. The first excited torsional state is located essentially at the top of the barrier with inverted order for symmetry reasons and has a $\Delta\tilde{\nu}_{EA}(1) = \tilde{\nu}_E(1) - \tilde{\nu}_A(1) = -85.5$ cm^{-1} from experiment (Moruzzi et al., 2018) and -81.1 cm^{-1} from the prediction, expressed here as a negative quantity in order to retain the definition of $\Delta\tilde{\nu}_{EA}$ and showing the inversion. Given the position at the barrier it is obviously a "borderline tunneling" problem at this level. At higher energies the levels approach the energy level patterns of free internal rotation in a well known manner, see, for example, the correlation scheme given in Bauder (2011). An interesting result concerns the interaction of the tunneling motion with the OH stretching vibration ν_1, which in fact acts as an inhibiting mode, slowing down the tunneling motion. For the first excited OH stretching state $v_1 = 1$ one finds $\Delta\tilde{\nu}_{EA}(v_1 = 1) = 6.3$ cm^{-1} (6.2 cm^{-1} from the prediction) and this trend continuous smoothly up to $\Delta\tilde{\nu}_{EA}(v_1 = 6) = 1.5$ cm^{-1} (1.5 cm^{-1} from the prediction). The agreement between the experimental result by Boyarkin et al. (1999) and the ab initio prediction from the quasiadiabatic channel RPH model is very good. Fig. 7.20 summarizes the trend for the tunneling splittings in conjunction with the trend for the quasiadiabatic channel potential barriers, which smoothly increase from less than 400 cm^{-1} at $v_1 = 0$ to more than 600 cm^{-1} at $v_1 = 6$. This increase of the effective barriers explains in part the decrease in tunneling splitting. An about equally important contribution to the decrease in tunneling splittings arises from the lengthening of the effective O–H bond length $\langle r_{OH} \rangle$ with excitation of the strongly anharmonic O–H stretching vibration. This lengthening of $\langle r_{OH} \rangle$ results in an increase of the effective moment of inertia which acts in a similar way as an effective "tunneling mass" (Fehrensen et al., 2003).

Another interesting effect was observed in experiments of the tunneling splittings of the asymmetric CH stretching fundamentals ν_2 and ν_9, where the tunneling doublets are inverted $\Delta\tilde{\nu}_{EA}(v_2 = 1) = -3.26$ cm^{-1} and $\Delta\tilde{\nu}_{EA}(v_9 = 1) = -5.48$ cm^{-1} (Xu et al., 1997; Wang and Perry, 1998). This effect is explained within the quasiadiabatic channel RPH model as arising from a Herzberg–Longuet-Higgins–Berry type phase from a conical intersection of the vibrationally adiabatic potential surface in the collinear C–OH structure where the modes ν_2 and ν_9 correlate with a degenerate mode of symmetry E in C_{3v}. The theoretical results give then correspondingly $\Delta\tilde{\nu}_{EA}(v_2 = 1) = -3.6$ cm^{-1} and $\Delta\tilde{\nu}_{EA}(v_9 = 1) = -3.2$ cm^{-1} in reasonable agreement with experiment (Fehrensen et al., 2003). This type of

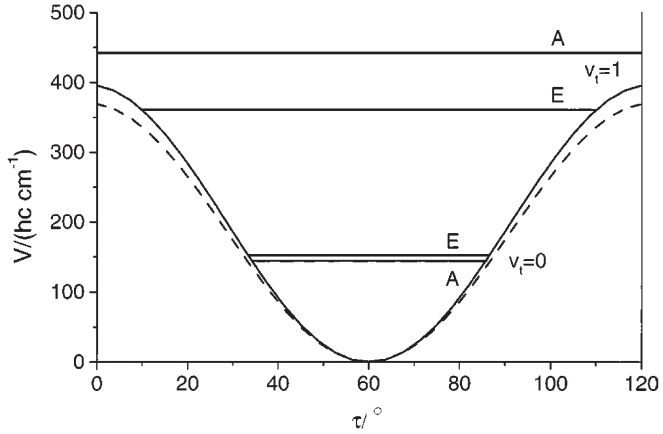

FIG. 7.19 Quasiadiabatic channel potential (full line) for the zero point level of $^{12}CH_3OH$ including the ground state doublet and the first excited torsional state doublet. For comparison the pure electronic potential $V_e(\tau)$ relative to its minimum energy is shown with a dashed line. The maximum of the adiabatic channel potential corresponds to 406.4 cm^{-1} and for the pure electronic potential V_e to 369.0 cm^{-1}, in each case relative to the corresponding minimum energy. The potential is periodic with period 120° (after Fehrensen et al., 2003).

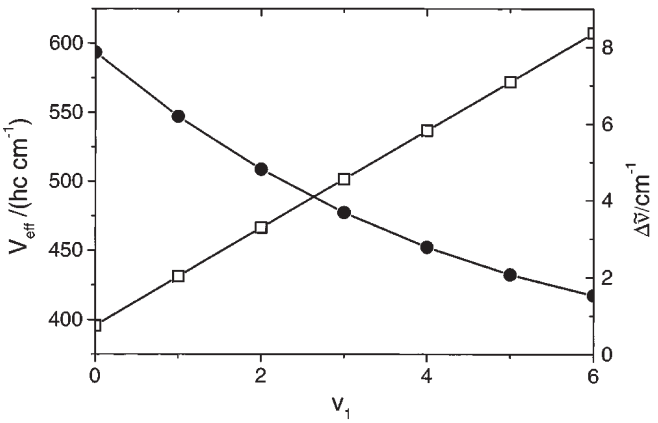

FIG. 7.20 Effective quasiadiabatic channel barrier height V_{eff} as a function of the OH stretching excitation v_1 (open squares) and the corresponding tunneling splittings $\Delta\tilde{\nu}_{EA} = \tilde{\nu}_E - \tilde{\nu}_A$ (filled circles, after Fehrensen et al., 2003).

symmetry effect arising from vibrational conical intersections has notably been further pursued by Perry and coworkers (Perry, 2008, 2009; Dawadi and Perry, 2014) and by Li Hong Xu and coworkers (Xu et al., 2010, 2011, 2014) using various models and perspectives and we shall not enter here the intricate discussions of the many detailed effects arising in the different model treatments (see also Fehrensen et al., 2003; Hänninen et al., 1999).

We should point out, however, a general aspect both of the "conical intersections" and the relative phases associated with them. Similar to the case of conical intersections of electronic potential energy hypersurfaces arising from the Born–Oppenheimer approximation (Yarkony, 1996; Domcke and Yarkony, 2012), these effects are always model dependent. If one omits the Born–Oppenheimer approximation and treats the electrons and nuclei "exactly" on a similar footing in a treatment, which has been called "pre-Born–Oppenheimer theory" (Simmen et al., 2013; see also Marquardt and Quack, 2020, Chapter 1, and Császár et al., 2020,

Chapter 2) there are no Born–Oppenheimer potential hypersurfaces, and thus no conical intersections and associated "Berry phases". This holds true in an analogous fashion for the vibrational-rotational problem in CH_3OH: If that is treated without making the vibrationally adiabatic approximations, say in a 12-dimensional (or 15-dimensional vibration-rotation) computation, no reference needs to be made to vibrational conical intersections and the associated phases. While such an "exact" treatment (similar to that quoted above for NH_3) would give numerically accurate results, there is still merit in the simpler models beyond just the enormous reduction in computational costs: The simple models such as the quasiadiabatic channel RPH model allow for an interpretation and deeper understanding of the plain numerical results (Quack, 2014). An example for such an understanding can be seen from Fig. 7.19 and Fig. 7.20 and, of course, there are many such cases.

We may mention here the discussion of the role of vibrational conical intersections in water dimers (Hamm and Stock, 2013) in relation to intramolecular vibrational redistribution (IVR) also in the chiral conformers for methanol isotopomers (Quack and Willeke, 1999) as intrinsically vibrationally non-adiabatic effects (Beil et al., 1997; Kushnarenko et al., 2018). In a more general context we may mention also the role of parity violation in the isotopomer CHD_2OH with transient chirality due to tunneling and CHDTOH with persistent chirality (Arigoni and Eliel, 1969; Lüthy et al., 1969; Berger et al., 2003). We conclude by mentioning also the methyl rotor tunneling studied also in the relatively complex molecules formic-acetic-acid anhydride (Bauder, 2013) and in para-halotoluenes (Shubert et al., 2013) showing most interesting dynamical effects. M. Schnell provided a detailed discussion of some complex cases with several methyl rotors (Schnell, 2011).

7.6 TUNNELING IN BIMOLECULAR REACTIONS

7.6.1 Direct Bimolecular Reactions

The prototype for tunneling in direct bimolecular reaction is certainly

$$H + H_2 \rightarrow H_2 + H \tag{7.8}$$

with its various isotopic variants. It has been in the focus of interest from the start of reaction dynamics, when it also was used for designing potential hypersurfaces for reaction dynamics and for experiments on the ortho–para conversion in H_2 (Eyring et al., 1944). Just as H_2, as a molecule, has been the prototype for fundamental tests of theory until today (Sprecher et al., 2013; Hölsch et al., 2019 and references therein), the $H + H_2$ reaction system continues to be of interest in the study of the tunnel effect in direct bimolecular reactions, as is also the H_3^+ system for complex forming reactions to be studied in the later Section 7.6.2.

A comprehensive review of the $H + H_2$ system would be far beyond our scope. We shall mention here a few highlights. Early studies started with classical trajectory calculations on ab initio potential hypersurfaces and simple tunneling corrections, if any; see Karplus (2014) for a review. The reaction may have been the first, where instanton theory was used to study tunneling in a bimolecular reaction (Chapman et al., 1975). It was the reaction where the so-called Marcus Coltrin path was discussed with "corner cutting" (Marcus and Coltrin, 1977). Among early experiments providing absolute cross-sections, we may mention the work of Wolfrum and coworkers (Buchenau et al., 1990; Wolfrum, 2001; Kneba and Wolfrum, 1980) and notably the recent work of Zare and coworkers on $H + D_2$ and $D + H_2$ and other isotopic variants (Jankunas et al., 2012, 2013a,b; Jambrina et al., 2016; Mukherjee et al., 2017; Aoiz and Zare, 2018; Althorpe et al., 2002; Aoiz et al., 2002; Ayers et al., 2003; Pomerantz et al., 2004; Ausfelder et al., 2004; Koszinowski et al., 2005 and references therein).

The reaction of muonium, the "lightest isotope of the H atom" (with a mass of 0.114 Da), with H_2 has recently received attention due to its large inverse kinetic isotope effect and the extremely large enhancement of the rate when H_2 is in its first excited vibrational state. The reaction rate constant for 300 K has been determined experimentally and by converged quantum dynamics calculations using a Born–Huang (BH) definition for the potential surface (Bakule et al., 2012). The importance of zero-point energy, tunneling and adiabaticity of the vibrational state for the understanding of this reaction has been summarized in a recent review article (Mielke et al., 2015). Different theoretical methods to consider the zero-point energy and tunneling effects within a classical or semiclassical framework were compared to accurate quantum calculations for the reaction $D + HMu \rightarrow DMu + H$. It was found that RPMD (ring polymer molecular dynamics) calculations provide overall a better result than methods based on transition state theory (TST) like canonical variational theory (CVT) or semiclassical instanton theory (SCI) (de Tudela et al., 2013). In time independent quantum calculations and quasi classical trajectory calculations the rate constants for H-atom abstraction and Mu-transfer were calculated for the temperature range from 100 to 1000 K. The calculations showed that for

the complete temperature range the rate constant for the Mu-transfer is found 1 to 2.5 orders of magnitude above the rate constant for H-atom abstraction (Aoiz et al., 2014).

The reaction of myonic helium with H_2 has been investigated experimentally and by accurate quantum dynamics calculations on a Born–Huang potential energy surface and compared to the reaction of myonium with H_2 in the temperature range from 300 to 500 K. For the higher temperatures the calculated rate constant agreed with experiment. However, for the lower temperatures the theoretical value was found to be substantially smaller than for the experiment (Fleming et al., 2011b,a).

The importance of tunneling in bimolecular reactions has been extensively studied in the past for the reaction $F + H_2$ and its deuterated modifications, where quantum effects are important already at room temperature (Lee, 1987). To model the temperature dependence of the rate constant for the temperature range from 10 to 350 K, a model function for the temperature dependence of the Arrhenius activation energy was derived by comparison with exact quantum calculations. It was found that the temperature dependence of the activation energy can be characterized by a "sub-Arrhenius" behavior (Aquilanti et al., 2012; Cavalli et al., 2014). Instanton and canonical variational transition state theories with optimized multidimensional tunneling were applied to calculate the reaction rates and kinetic isotope effects for the reaction $H_2 + OH \rightarrow H_2O + H$ and all its possible isotopic combinations down to temperatures of 50 K. It was found that atom tunneling is becoming important for temperatures below 250 K for proton transfer and below 200 K for deuterium transfer (Meisner and Kästner, 2016). In recent experiments He-droplets have been found to be an ideal environment for heavy atom tunneling. In a He-droplet the heliophilic Xe resides inside the droplet, while the heliophobic Rb stays outside at the surface of the droplet. The dissociation of this XeRb-complex could be described by a tunneling process (Poms et al., 2012).

Parahydrogen, forming quantum crystals at low temperatures, is a new matrix to study the physical and chemical processes of molecules at low temperatures. The large lattice constant and the large zero-point amplitude of the lattice vibrations in solid hydrogen provide more free space for the guest molecules than other matrices and the interactions with the surrounding host molecules become weak compared with those in noble gas matrices. An early experiment is the reaction of H_2 with differently deuterated methyl radicals at 5 K. For the deuterated modifications a rate constant around 10^{-6} s^{-1} was found which is increasing with the number of D atoms. For the reaction with CH_3 an upper limit for the rate constant of $8 \cdot 10^{-8}$ s^{-1} could be determined (Hoshina et al., 2004).

Bimolecular reactions on dust grains play an important role in interstellar chemistry (Bromley et al., 2014). An experimental investigation of O-atom diffusion and reactivity on water ice in the temperature range of 6–25 K showed that tunneling processes are important for O-atom diffusion at 6 K (Minissale et al., 2013; Congiu et al., 2014). The formation of O_2 and O_3 at low temperatures on an amorphous silicate surface is determined by the mobility and reactivity of the adsorbed O-atoms. The diffusion of O-atoms in the temperature range from 6.5 to 30 K could be explained by a Langmuir–Hinshelwood mechanism taking into account a non-negligible tunneling process (Minissale et al., 2014). A hybrid model of quantum and molecular mechanics has been combined with instanton theory to investigate the reaction H + HNCO on an amorphous solid water surface. Including contributions from tunneling the rate constant was calculated for temperatures down to 103 K and compared with results for the gas phase. The kinetic isotope effect (KIE) increased from 146 for the gas phase to 231 for the reaction on the cold surface (Song and Kästner, 2016). In a recent publication the reaction rate for the reaction $H + H_2O_2$ has been calculated for temperatures down to 50 K using the instanton theory based on electronic potentials from DFT calculations of different complexity. The calculations showed that at 114 K the reaction to H_2O + OH is preferred by 2 orders of magnitude as compared to the reaction to $H_2 + HO_2$. Including the Eley–Rideal reaction mechanism it could be shown that the second reaction is at low temperature on surfaces of similar order of magnitude (Lamberts et al., 2016). The MCTDH (Multiconfiguration Time-Dependent Hartree) method was used to calculate the relaxation rates of the vibrational states for H-atoms adsorbed on a Pd(111) surface. The calculation showed that even at room temperature quantum effects cannot be neglected to describe the diffusion of H-atoms on a Pd(111) surface (Firmino et al., 2014). An interesting discussion of the importance of tunneling in interstellar chemistry and applications of "harmonic quantum transition state theory" as a reformulation of instanton theory can be found in (Bromley et al., 2014).

7.6.2 Bimolecular Reactions With Intermediate Complex Formation

Numerous bimolecular reactions do not occur by direct collision mechanisms but rather pass in a two step pro-

cess from reactants to products via a more or less long lived and possibly strongly bound intermediate complex according to the general scheme

$$A + BC \rightleftharpoons ABC^* \rightleftharpoons AB + C. \qquad (7.9)$$

One thus has in a first step a (re)combination or capture and in the second step a (re)dissociation, which is a unimolecular reaction. Indeed, by microscopic reversibility all these processes can be understood as unimolecular reaction dynamics of the intermediate complex ABC^*. The reactions are frequently very fast, occurring without barriers (or very small ones), when they involve free radicals such as the reaction (Farrar and Lee, 1974), Fig. 7.21

$$F + C_6H_5Cl \rightarrow C_6H_5FCl^* \rightarrow C_6H_5F + Cl, \qquad (7.10)$$

or (Quack and Troe, 1974, 1975a,b, 1976, 1977a,b,c; Glänzer et al., 1976, 1977; Quack, 1979)

$$H + CH_3 \rightarrow CH_4^* \rightarrow CH_3 + H, \qquad (7.11)$$

or when they involve ions such as the prototypical ion molecule reaction (and its isotopic variants)

$$H^+ + H_2 \rightarrow H_3^+ \rightarrow H_2 + H^+, \qquad (7.12)$$

which has no barrier for the "capture" process forming the strongly bound molecular ion H_3^+ with a deep minimum in the electronic potential, quite in contrast to the direct reaction (7.8) involving neutral H_3 which has a pronounced barrier. When two ions of opposite charge are concerned one has charge recombination quite specifically. Numerous reactions of this general type have been studied, both for radical and ion molecule collisions and we provide just a small selection of some early references (Herschbach, 1973; Farrar and Lee, 1974; Schultz et al., 1972; Rice, 1975; Chesnavich and Bowers, 1979; Herschbach, 1987; Lee, 1987; Polanyi, 1987). Fig. 7.21 shows a schematic energy diagram for an example of such reactions (Quack, 1980).

For barrierless reactions one might assume that tunnel effects are unimportant, except for a small quantum effect with a threshold law that slightly reduces the cross-section compared to the classical reaction cross-section (Quack and Troe, 1974, 1975a,b, 1981, 1998). However, in such reactions there are important effects from angular momentum conservation (Zare, 1988; Quack and Troe, 1975a, 1998). Thus in collisions with capture one has to take into account effective potentials, which have "centrifugal barriers" due to extra rotational energy to be added to the purely attractive electronic

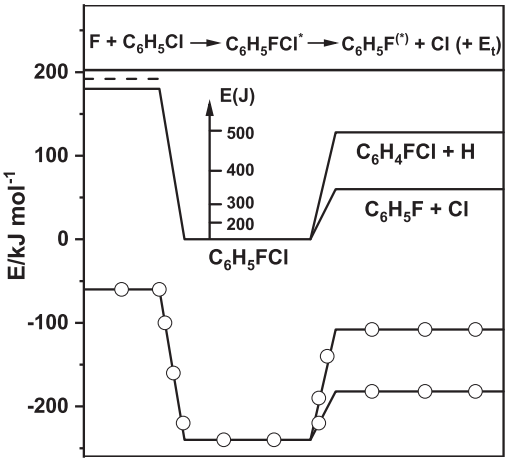

FIG. 7.21 Schematic energy diagram for a typical complex forming reaction. $E(J)$ gives the minimum rotational energy for a total angular momentum J of C_6H_5FCl as indicated by the numbers. The open circles represent the electronic energy without the zero point energy (after Quack, 1980).

potential. Tunneling through these effective potential barriers then becomes important at threshold as shown in Fig. 7.22.

These effective barriers for tunneling have been widely calculated using treatments where the relative rotation of the collision partners is considered to be free, with a quasidiatomic quasiclassical treatment for the centrifugal barriers, such as in phase space theory (Pechukas and Light, 1965; Nikitin, 1965), Gorin type models for radical recombinations (Gorin, 1938), or Langevin models for ion–molecule reactions (Gioumousis and Stevenson, 1958; Levine and Bernstein, 1989; Levine, 2005). We shall address here an important aspect for such effective tunneling potentials, which can be understood in the framework of the quasiadiabatic channel model (Quack and Troe, 1998). There the effective tunneling potential includes effects from the quantized energy of hindered relative rotation of the diatomic or polyatomic collision partners as illustrated with the potential labeled $V_{acm}(J, a)$ in Fig. 7.22. These zero point energy effects are quite important and have been calculated quantitatively in a numerically exact way by the quasiadiabatic channel Diffusion Quantum Monte Carlo (DQMC) method of Quack and Suhm (1991a) for the collisions

$$2HF \rightarrow (HF)_2 \qquad (7.13)$$

forming the hydrogen bonded complex $(HF)_2$. Fig. 7.23 shows such results for the lowest quasiadiabatic channel potentials with $J = 0$, where the effective barriers

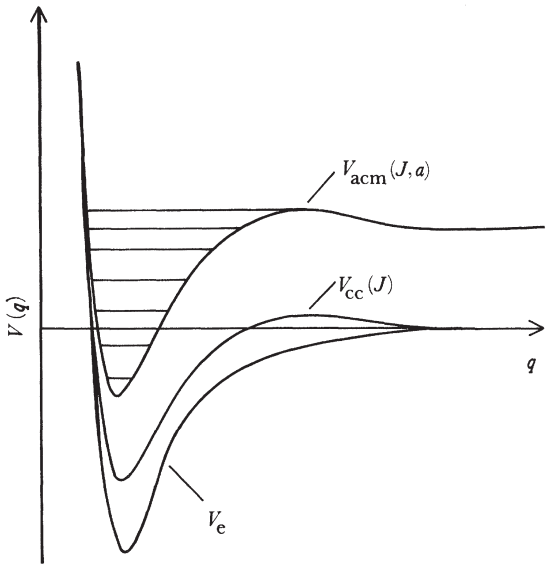

FIG. 7.22 Effect of zero point energy and angular momentum on polyatomic reaction dynamics as illustrated by the adiabatic channel model. V_e is the electronic (Born–Oppenheimer) potential in the reaction coordinate q, $V_{cc}(J)$ the effective, classical centrifugal potential (for a total angular momentum quantum number J, and $V_{acm}(J,a)$ the effective adiabatic channel potential including zero point energy for J and channel a (after Quack, 1990).

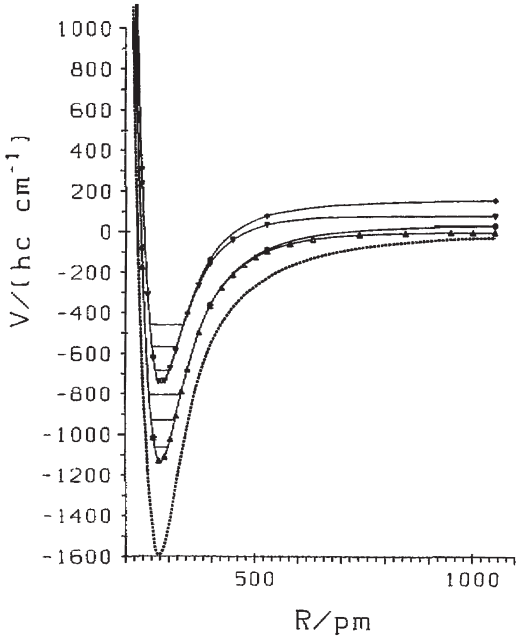

FIG. 7.23 Lowest quasiadiabatic DQMC dissociation channels of A^+ (△), A^- (▽), B^+ (◯), B^- (◇) symmetry and 1D stretching levels for $(HF)_2$. Note that for the A^- and B^- channels, the symbol is about the size of the error bar, while it is twice the error bar for B^+ and 5–20 times the error bar for A^+, depending on $R_{ab'}$. The channel potentials V_a (R_{ab}) are referred to V_0 ($R_{ab} \to \infty$) ≡ 0. The electronic potential is shown as a dotted line, defining V_{el} ($R_{ab} \to \infty$) ≡ 0 in this case (after Quack and Suhm, 1991a).

are not visible, and Fig. 7.24 shows the lowest channels for higher total angular momenta ($J = 10, 30, 60$), where they are easily visible. These full-dimensional quasiadiabatic channel Quantum Monte Carlo calculations carried out on the full-dimensional SQSBDE potential hypersurface have demonstrated the great quantitative importance of the zero point energy effects. For instance, in the $J = 60$ channel the effective pure rotational energy barrier for capture occurs at $R'_{ab} = 15a_0$ with an energy $E'_B = (hc)33.6\ cm^{-1}$, whereas with inclusion of the correct quantum zero point energy by DQMC it occurs at $R'_{ab} = 11a_0$ with a much higher energy $E'_B = (hc)123\ cm^{-1}$. This demonstrates that clearly the full quantum dynamical treatment of the effective potentials must be carried out before doing calculations for capture in such systems with or without tunneling.

Notably, Troe and coworkers have applied the SACM (statistical adiabatic channel model), sometimes including further approximations to a variety of capture processes (Auzinsh et al., 2013; Troe, 1987, 1992, 1996; Nikitin and Troe, 2010a,b; Dashevskaya et al., 2003, 2010, 2011).

The fast reaction with intermediate complex formation have received further recent attention due to developments in studying reactions at very low temperatures (Smith, 2006; Hoshina et al., 2004; Ospelkaus et al., 2010; Perreault et al., 2017; Kilaj et al., 2018; Hall et al., 2013), see also Bergmann et al. (2019) for state selective preparation by STIRAP, and references therein. Besides the possible role of tunneling through small centrifugal barriers in such reactions, there are also interesting threshold effects due to symmetry, which we can illustrate again with the $(HF)_2$ system. Fig. 7.25 illustrates the symmetry correlations for the lowest quasiadiabatic channels (Quack and Suhm, 1991a). We can use again the group $S^*_{2,2}$ as discussed in Section 7.3 or the smaller group M_{S4} if the HF monomer units remain intact, because the barrier for exchanging protons between the different F-atom partners in the HF units is very high. One sees in Fig. 7.25 that the ground state tunneling doublet correlates with the ground state products A^+ and an excited vibrational state with B^+-symmetry and

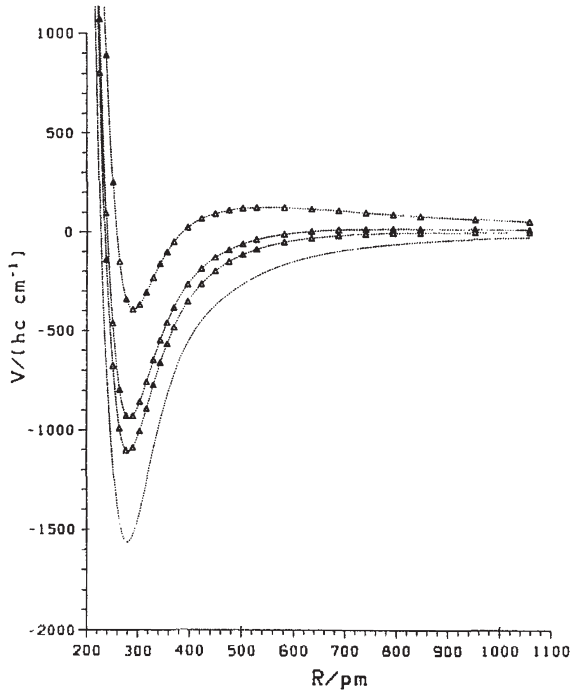

FIG. 7.24 Lowest quasiadiabatic DQMC dissociation channels for $J = 10, 30, 60$ together with the minimum energy path potential of dissociation (after Quack and Suhm, 1991a).

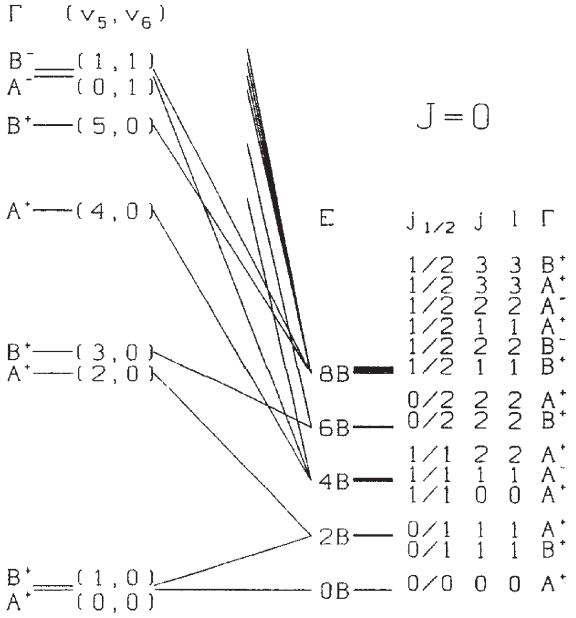

FIG. 7.25 Correlation diagram for the lowest rotationless states of $(HF)_2$ and the corresponding monomer fragments; $v_3 > v_6$ is assumed (after Quack and Suhm, 1991a).

an energy corresponding to 2B (with B being the rotational constant of HF). The lowest A^- channel involves excitation of the out of plane bending (vibrational, torsional) mode v_6 neat 400 cm^{-1} in $(HF)_2$ and correlates at the product side with the lowest possible A^- state with energy corresponding to $4B$. This implies, for instance, that the excited levels of $(HF)_2$ with A^- symmetry and $J = 0$ cannot predissociate even if their energy is above the lowest threshold (energy = 0 in Fig. 7.25) but below $(hc * 4B)$, unless one invokes parity violation (Quack, 2011b). These excited states would therefore be extremely long lived. The upper tunneling level of $v_6 = 1$ has B^- symmetry and correlates with a product B^- channel of energy $(hc * 8B)$. Thus B^- excited levels (with $J = 0$) cannot predissociate above threshold unless they reach an energy $(hc * 8B)$ or more. In the energy range between $hc * 4B$ to $hc * 8B$ they could predissociate with violation of nuclear spin symmetry and below $hc * 4B$ again only with parity violation, thus being extremely long lived. Of course, these correlations also appear in the effective channel potentials in Fig. 7.24.

As a fully state selective version of transition state theory the statistical adiabatic channel model (SACM) allowed for proper explicit inclusion of all conserved quantum numbers, such as angular momentum, parity and nuclear spin symmetry, as also of other approximately conserved quantum numbers. At the same time it allowed for a consistent treatment of barrierless reactions by a kind of transition state approximation, a unique property at the time of its development, as the usual versions of transition state theory relied on a well defined transition structures at a saddle point (in the multidimensional hypersurface), which is absent in barrierless reactions. The latter feature was later included in the so-called "variational transition state theory" (Truhlar and Garrett, 1984; Truhlar et al., 1996), but which has been shown to be only an approximation to the full SACM (Quack and Troe, 1977c,a,b). Variational transition state theory generally gives somewhat too high values for the rate constant of barrierless reactions, although the results are much better than in the older versions of transition state theory or RRKM (Rice–Ramsperger–Kassel–Marcus) theory. As a early crucial experimental test we may mention the prediction of an increase of the barrierless methyl radical recombination rate by a factor of 20 by the then available RRKM calculations

$$CH_3 + CH_3 \rightarrow C_2H_6, \qquad (7.14)$$

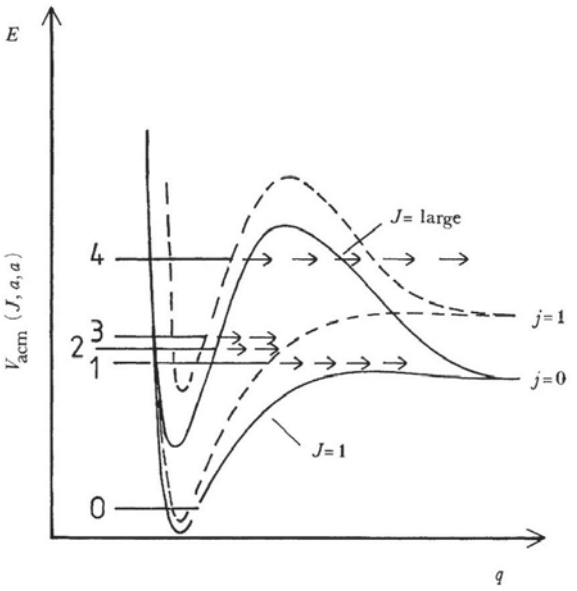

FIG. 7.26 Schematic drawing of adiabatic channel potentials for the predissociation of H_3^+ (see detailed discussion in the text, the electronic potential is omitted) (after Quack, 1990).

whereas the SACM predicts a constant or slightly decreasing rate coefficient over the range 300 to 1300 K. The SACM prediction (Quack and Troe, 1974) was confirmed by experiment (Glänzer et al., 1976, 1977).

7.7 TUNNELING IN IONS AND IN ELECTRONICALLY EXCITED STATES

We have already mentioned the prototypical ion H_3^+ in the context of barrierless recombination reactions. It can also be used as a prototype for studying tunneling and symmetry in unimolecular dissociation of ions. Indeed, its high resolution infrared predissociation spectrum has remained for decades without assignment and analysis (Carrington et al., 1982; Carrington and Kennedy, 1984). Symmetry and tunneling in this predissociation can be analyzed as illustrated in Fig. 7.26 (Quack, 1990).

For the symmetry analysis one can in practise use the group $S_3^* = S_3 \otimes S^*$ as the direct product of the symmetric group S_3 of the three protons and the inversion group S^*. We consider here the case of the totally symmetric electronic ground state. The $j = 1$ and $j = 0$ product rotational channels in

$$H_3^+ + h\nu \rightarrow (H_3^+)^* \rightarrow H_2(j) + H^+ \qquad (7.15)$$

are separated by about 120 cm^{-1} (1.4 kJ mol^{-1}) for a low total angular momentum channel with J = 1 with no or with nearly zero barrier, or a high angular momentum channel with large J and a large centrifugal barrier as indicated in Fig. 7.26.

Let us consider a predissociating state labeled (1) in Fig. 7.26. It may dissociate to give $j = 0$ product with an "orbital" angular momentum quantum number $l = 1$ for the relative motion of the fragments ($l = J = 1$ in this case with $j = 0$, i.e., para-H_2). This channel has negative parity and E^- symmetry with total nuclear spin I = 1/2, as A_1^- is Pauli forbidden. Thus if $|1\rangle$ is of A_2^+ symmetry, it can only predissociate by parity violation not by tunneling, thus it will be extremely long lived. The same conclusion is true for an E^+ level of H_3^+ at an energy of $|1\rangle$. On the other hand, an E^- state at that energy can predissociate by tunneling, the lifetime will then only depend on the tunneling probability and may be short enough to be found in predissociation. An A_2^- level at the energy of $|1\rangle$ could only predissociate by nuclear spin symmetry change, thus it would be long lived (but not as long lived as an A_2^+ level). More conclusions can be obtained in a similar way, see Quack (1990). One can reverse this reasoning: When detecting the product state of H_2 in reaction (7.15) (ortho or para) in conjunction with the predissociation spectral line, one can assign the symmetry of the predissociating state of H_3^+ observed through that line. We may note here that for the reaction

$$H_2^+ + H_2 \rightarrow H_3^+ + H, \qquad (7.16)$$

which proceeds without barrier through a very short lived H_4^+, the symmetry selection rules (Quack, 1977) were experimentally confirmed by Uy et al. (1997).

Tunneling processes are also of relevance in other positively charged ions where H_5^+ is an important example. The GENUISH program has been used to calculate the rotational-vibrational energy levels for H_5^+ and its deuterated modifications for a reduced and full dimensional model (Sarka and Császár, 2016). The "astructural" highly non-rigid ion CH_5^+ has found much interest as well (Fábri et al., 2017 and references therein). The calculations showed that energy separations of the rotational and vibrational levels are in each case on the same order of magnitude, reflecting the flatness of the potential hypersurface and therefore there is no good way to separate "rotational" from "vibrational" spectral structures, while, however, symmetries can be properly included following (Fábri et al., 2017).

Tunneling processes in the ground state of the ion had to be included to explain the ZEKE (zero-kinetic energy) spectra of propen-H_6 and -D_6 (Vasilatou et al.,

2010). A modified Hamiltonian for the Jahn–Teller effect has been derived to enable a joint treatment of the Jahn–Teller effect and the internal hindered rotation to explain the zero-kinetic energy photoelectron spectrum of C_2H_4 and C_2D_4 (Schulenburg and Merkt, 2010). Threshold photoelectron–photonion coincidence spectra on the two isotopic modifications of dimethyl ether, $(CH_3OCH_3$, DME-$H_6)_n$ and $(CD_3OCD_3$, DME-$D_6)_n$, $n = 1$ and 2 did not show any isotope effect. The assumption of a barrierless proton transfer across weak CH···O hydrogen bonds was supported by DFT calculations (Yoder et al., 2015). The tunneling process of the pseudo rotation in the $1^2E'$ ground state of Na_3, a classical example for the Jahn–Teller effect, has been revisited in a recent publication (Hauser et al., 2015). The ground state of Na_3 is defined by the interplay of Jahn–Teller-, spin-orbit-, rovibrational and hyperfine interactions. In the investigation the rovibrational levels, theoretically obtained from an effective Hamiltonian have been compared to the results from highly resolved microwave spectra (Hauser et al., 2015).

Rotational and vibrational predissociation is a prominent tunneling process in the electronically excited states of small molecules and ions (Herzberg, 1966; Merkt and Quack, 2011; Merkt et al., 2011; Wörner and Merkt, 2011; Amano, 2011; Pratt, 2011; Schmitt and Meerts, 2011; Guennoun and Maier, 2011). In the vacuum ultraviolet spectrum of the $C_1 \leftarrow X_0^+$ and $D_0^+ \leftarrow X_0^+$ band system of ArXe a second state of $\Omega = 1$ symmetry was assumed to explain several tunneling/predissociation resonances found $\sim$200 cm^{-1} above the C_1-state (Pittico et al., 2012). For the benzoic acid dimer a tunneling time of 111 ps is found experimentally for the double proton exchange in the electronic ground state and of 666 ps in the electronically excited state. In the electronically exited state the predicted excitonic splitting of the S_1- and S_2-state is of the same order of magnitude. For the electronically excited states an exciton splitting between the S_1- and S_2-state is predicted theoretically. However, an exciton splitting of 0.94 cm^{-1} is found experimentally, significantly smaller than predicted (Ottinger and Leutwyler, 2012; Ottinger et al., 2012), see also the reviews of Willitsch (2011) and Müller-Dethlefs and Riese (2011) for further experimental studies of ions and predissociation by tunneling.

At this point we should also mention an alternative theoretical approach for treating proton dynamics in polyatomic ions, not together with the other nuclei on a Born–Oppenheimer potential hypersurface but rather together with the electrons as "light" particles. This interesting approach was named nuclear-electron orbital (NEO) approach by Sharon Hammes-Schiffer and developed for a number of applications which automatically should include "quantum tunneling" of the protons implicitly as also other quantum effects related to proton motion, see Yang et al. (2017); Brorsen et al. (2017).

7.8 TUNNELING OF MOLECULES INSIDE A CAGE

The quantum dynamics of molecules in cages have found much recent interest in the context of metal organic frameworks (MOFs) (Yaghi, 2016; Yaghi et al., 2019; Yaghi, 2019; Zhou et al., 2016; Schoedel et al., 2016; Rungtaweevoranit et al., 2016; Nguyen et al., 2014; Kundu et al., 2016) and Zeolites, for example, (Sauer, 2016; Tuma and Sauer, 2015; Piccini et al., 2018), which are important examples for heterogeneous catalysis often involving presumably tunneling reactions (Sauer and Freund, 2015).

The inside volumes of C_{60} and other fullerenes provide an ideal environment for the quantum dynamics of coupled translational and rotational motions of H_2 and similar molecules which are accessible to inelastic neutron scattering. Using a 5D translational-rotational Hamiltonian, the eigenstates could be obtained to enable the assignment of the INS (inelastic neutron scattering) spectrum for different temperatures. From the assigned INS spectra a special selection rule could be derived for INS spectra of the motion of H_2 in a near-spherical potential (Xu et al., 2013, 2019; Felker et al., 2019; Lauvergnat et al., 2019). The new selection rule is also found for HF in C_{60} (Xu et al., 2019). With the same theoretical approach the 6D translational-rotational (TR) eigenstates of para- and ortho-H_2O inside C_{60} could be calculated (Felker and Bačić, 2016). The nuclear spin symmetry conversion between the ortho and para species of the endohedral H_2O inside C_{60} was studied in the solid phase by low temperature NMR. The experimental data are consistent with a second-order kinetics, indicating a bimolecular spin conversion process. Numerical simulations showed a spin diffusion process allowing neighboring ortho and para molecules to exchange their angular momenta (Mamone et al., 2014). This should be compared to nuclear spin symmetry conservation in H_2O in supersonic jet expansions (Manca Tanner et al., 2013, 2018), where nuclear spin symmetry conversion may occur with cluster formation.

Hydrogen clathrate hydrates are inclusion compounds where hydrogen molecules are trapped inside closely packed polyhedral cavities within the ice-like lattice of hydrogen-bonded water molecules. The

translational-rotational eigenstates and INS spectra were calculated by a quantum-mechanical method for H_2 inside spherical clathrate domains of gradually increasing radius and increasing number of water molecules (Powers et al., 2016). In an additional study the diffusion of H_2 and D_2 through clathrate hydrates was investigated. Path integral based molecular dynamics simulations were used to calculate the free-energy profiles for the H_2 and D_2 diffusion rates as a function of temperature. For temperatures above 25 K, zero point energies of vibrations perpendicular to the reaction path lead to a decrease of the quantum mechanical (calculated) rates compared to classically calculated rates. For low temperatures, tunneling becomes dominant (Cendagorta et al., 2016). Using neutron scattering and ab initio calculations a new "quantum tunneling state" of the water molecule confined in 500 pm wide channels in the mineral beryl has been discovered, which is characterized by extended proton and electron delocalization. The maxima in the neutron scattering data could be uniquely assigned to a new tunneling state of water (Kolesnikov et al., 2016).

Metal–organic frameworks (MOFs) represent a class of porous materials that have been considered to be promising for applications in H_2 storage. The inelastic scattering of neutrons from adsorbed H_2 is an ideal method for obtaining information on the type and nature of H_2 binding sites in porous materials. Energy levels and transition energies may be obtained from quantum dynamics calculations with an accuracy limited by the quality of the potential energy surface and can be directly compared to the experiment. In a recent review the results from some quantum and classical mechanical calculations have been summarized (Pham et al., 2016b). An example for such a porous material is $[Mg_3(O_2CH)_6]$, a metal–organic framework (MOF) that consists of a network of Mg_2^+-ions coordinated to formate ligands. In simulations and two-dimensional quantum calculations of the rotational levels it was found that different groups of maxima in the inelastic neutron scattering experiments correspond to particular adsorption sites in the material. In addition, 8 different rotational tunneling transitions could be identified experimentally and theoretically as well and their barrier height could be determined (Pham et al., 2016a).

7.9 CONCLUDING REMARKS ON TUNNELING

In many theories and mechanistic discussions in chemistry atomic and molecular tunneling processes are neglected even though chemical examples had been known from the beginning of the discovery of the tunnel effect in the early times of quantum mechanics (Hund, 1927a; Herzberg, 1939, 1945; Bell, 1980; Quack and Merkt, 2011). The present survey shows that just now in recent years a large number of phenomena in chemistry based on the tunnel effect with contributions from atoms or atomic groups in molecules and not only from electrons have been discovered and understood in detail. Here, for the future still important applications have to be expected, and we can highlight as just one example the possible use of tunneling in the design of molecular quantum switches and quantum machines (Fábri et al., 2018), discussed here in Sect 7.4. Numerous further examples of quantum atomic and molecular tunneling systems in molecular kinetics and spectroscopy have been illustrated in the present review. These provide a view of "molecules in motion" (Quack, 2001) from the true quantum perspective of the tunnel effect. By necessity a review of such a vast field cannot provide a comprehensive coverage of the literature, and we extend our apologies to those authors whose work may have been less than adequately covered in our selection of examples of recent interest and developments in the field.

To conclude we shall address a few conceptual points, which we have until now omitted but which are of some current relevance. The first concerns a remark on nomenclature for "tunneling sublevels". These are often labeled as 0^+, 0^-, 1^+, 1^-, v_n^+, v_n^-, where the number v_n give some vibrational (e.g., torsional, inversional, etc.) quantum number in the "high barrier" limit whereas the exponent "+" indicates the lower and "–" the upper tunneling sublevel. This widely used nomenclature is related to the intuitive notion that the lower sublevel is often symmetric and the upper sublevel antisymmetric with respect to some symmetry operation. This type of symmetry assignment is, however, not generally true and it obviously fails in slightly asymmetric potentials where at low energies the wavefunctions may be localized, whereas at higher energies one may have, indeed, delocalized "tunneling sublevels". A more general useful label would be simply "l" for the "lower" and "u" for the "upper" sublevel, which is a neutral nomenclature leaving the question of symmetry and localization and delocalization open and perhaps to be specified by some further nomenclature. Indeed, when the tunneling sublevels arise from a process related to the concept of "feasibility" according to Longuet-Higgins (1963), one can then use a symmetry label from the appropriate symmetry group. There has been a somewhat unfortunate multitude of conventions and nomenclatures in this field and we should strongly ad-

vocate the use of symmetry labels which give a unique symbol for symmetries in the restricted permutation group (A for symmetric, B for antisymmetric with indices A_i, B_i as may be needed, E for doubly degenerate, F for triply degenerate species, and then with increasing degeneracy systematically G, H, etc.) or else the partition in the full permutation group S_n as is conventional in mathematics. The parity of the species can be indicated by an exponent "+" for positive parity and "−" for negative parity. This notation was systematically introduced in Quack (1977) and has been recommended in Cohen et al. (2011) and Stohner and Quack (2011) for example. It differs sometimes from the various less systematic conventions used also in Bunker and Jensen (1998), which is among the frequently used sources for conventions, but there are also quite a few further ones (for instance, Oka, 2011, similar but not identical to our recommended one). A critical discussion and summary has been given in Quack (2011b), to which we refer for further details, and which also leads to the recommendation we give here (see also for some of the history and further references Mills and Quack, 2002). Obviously all this is a matter of convention and not fundamental. In principle any convention and nomenclature can be used, if it is well defined. Nevertheless, a good systematic nomenclature can be helpful in scientific work.

There is a second point of current interest, which, in fact, has led to some debate: The notion of the "tunneling time". This particular time is sometimes (not always) defined as the "time the particle spends in the classically forbidden region under the barrier during the tunneling process". We shall not enter here the details of the debate around the question of the "tunneling time", but we refer to some of the key references from which the reader can obtain a perspective on this debate (MacColl, 1932; Hauge and Stoevneng, 1989; Landauer and Martin, 1994; Lépine et al., 2014; Dahlström et al., 2012; Telle et al., 1999; Gallmann and Keller, 2011; Gallmann et al., 2012; Landsman et al., 2014; Landsman and Keller, 2014, 2015; Cattaneo et al., 2016; Hofmann et al., 2019; Pollak, 2017; Petersen and Pollak, 2017, 2018; Wörner and Corkum, 2011). The discussions have sometimes led to considerations of fundamental physics extending into cosmology (Nimtz and Haibel, 2004; Hawking, 1975; Vilenkin, 1988; Low, 1998; Nimtz, 2011). We shall not dig deeply into these considerations here but conclude with the following remark relevant to "heavy particle" tunneling in molecules in the framework of potential barriers arising in the framework of Born–Oppenheimer or related potential hypersurfaces. In the limit where the non-relativistic dynamics as described by the time-dependent Schrödinger equation can be used ($\mathrm{i} = \sqrt{-1}$),

$$\mathrm{i}\frac{h}{2\pi}\frac{\partial \Psi(\vec{q},t)}{\partial t} = \hat{H}\,\Psi(\vec{q},t), \tag{7.17}$$

one can certainly state that experimentally observable quantities can be calculated for any tunneling process, and thus if one can define some kind of "tunneling time" which can be measured experimentally, then one can also compute it by solving the Schrödinger equation and thereby "understand" it, in that sense there is no real enigma. Similar statements hold true if we use the Heisenberg picture with the Heisenberg equations of motion or considering the time evolution of the density operator according to the Liouville–von Neumann equation (Merkt and Quack, 2011; Marquardt and Quack, 2020, Chapter 1).

Finally, we shall address a fundamental aspect related to the concept of the "potential function", which appears in the usual discussions of tunneling. Indeed, at first sight it may seem that the concept of "tunneling" necessarily involves the existence of such a potential function. A closer look shows, however, that things are not quite as simple. We shall start here by considering tunneling within the quasiadiabatic channel reaction path Hamiltonian and "quasiadiabatic above barrier tunneling". The lowest levels and wavefunctions shown in Fig. 7.3 show a tunneling sublevel structure and tunneling wavepacket dynamics as given by the effective one-dimensional quasiadiabatic channel potential, although their energy is high above the barrier in the multidimensional Born–Oppenheimer surface. One might then be tempted to say that it is not a "true" tunneling process, as it results from an approximate model. However, the "exact" 6-dimensional vibration-tunneling calculation on the complete hypersurface shows about the same level structure and wavepacket dynamics as the approximate calculations, and therefore one must conclude that the full quantum dynamics shows "tunneling behavior" even above the barrier. It is furthermore true that also the tunneling sublevel structure and dynamics at energies below the 6-dimensional saddle point result from an approximation. Without the Born–Oppenheimer approximation (see also Marquardt and Quack, 2020; Császár et al., 2020, Chapters 1 and 2) the "Born–Oppenheimer potential barriers and saddle points" disappear. If one treats hydrogenperoxide or other molecules with Born–Oppenheimer barriers "exactly" by means of quantum dynamics of a collection of the electrons and nuclei in the molecule, the "true" potential arises in essence

from the Coulomb-interaction of these particles in a very high dimensional space. But even then without any Born–Oppenheimer barriers to tunnel through, the "exact" quantum dynamics will show very much the same sublevel structure and tunneling dynamics as it is described by the approximate theory and confirmed by experiment. This suggests a new definition of quantum tunneling dynamics that does not depend on the concept of potential barriers, as we have pointed out already in the context of the definition of the "molecular symmetry group" of non-rigid molecules. While Longuet-Higgins has, indeed, motivated this group by the existence of high Born–Oppenheimer potential barriers separating symmetrically equivalent isomers and thereby generating systematically degenerate level structures, we pointed out that in a rigorous discussion the symmetry groups should not be defined by an approximation but rather by the induced representation corresponding to the degenerate sublevels, which one can define from an exact theory without any approximation and also by experiment (Quack, 1977, 1985, 2011b). When the perfect degeneracy is lifted by tunneling leading to observable tunneling splittings, one can consider this effect then as the breaking of an approximate symmetry without having to refer to tunneling through potential barriers from the Born–Oppenheimer approximation. Thus the tunnel effect can be understood as a quantum dynamical phenomenon without making reference to approximate concepts such as Born–Oppenheimer potential hypersurfaces. One can say, however, that the Born–Oppenheimer approximation and also the quasiadiabatic channel reaction path Hamiltonian with their effective potentials provide us with simple models (Quack, 2014), which allow us in the first place to qualitatively understand the phenomena and in the second place also compute the phenomena approximately without too much effort (see also the general discussion by Roald Hoffmann (1998) on qualitative understanding versus computation).

The discussion can be continued similarly at an even deeper level: From the standard model of particle physics we understand even the Coulomb potential as not being a "fundamental preexisting" potential but rather as arising from photons as field particles mediating the electromagnetic interaction (Quack, 2006; Marquardt and Quack, 2020, Chapter 1). Similarly the parity violating interaction leading to the slight asymmetry effect in the effective potential as illustrated in Fig. 7.5 arises from the Z-bosons as field particles mediating the weak interaction between electrons and nuclei (or protons, neutrons, quarks, etc.). The small effective "parity violating potential" (really an extra effective potential hypersurface which is antisymmetric with respect to inversion and should not at all be interpreted as a "Born–Oppenheimer hypersurface") arises from an approximation in carrying out the computation in electroweak quantum chemistry (Bakasov et al., 1998; Berger and Quack, 2000a,b; Quack and Stohner, 2000; Quack, 2006, 2011b). While there would be no need to make the approximation, it nevertheless corresponds to a useful model which allows us to understand the small symmetry violation and to practically compute it with feasible effort. Conceptually, however, exact tunneling dynamics in this effective asymmetric potential should be understood on the basis of the quantum sublevel structure arising from the symmetry breaking removal of a degeneracy, which can be observed by experiment or could also be derived from an exact theory without making any reference to the parity violating potential hypersurface.

A brief note is also useful concerning the role of relativistic effects. As is well known, these are important for the dynamics of electron motion, whenever the heavier elements are involved in the molecules considered. These effects can be calculated by relativistic quantum chemistry (Reiher and Wolf, 2009) and can lead, indeed, to dramatic changes in the effective Born–Oppenheimer potential barriers for tunneling. Once these effects are included, the tunneling motion of atoms and molecules can be computed and understood in very much the same way using the Schrödinger equation as discussed for non-relativistic potentials. If the molecules move at relativistic speeds, one has to consider the changes in the definition of time which is then to be measured by an atomic clock moving at relativistic speed. Indeed, molecular tunneling systems such as ammonia can be and have been used as molecular clocks, and one has the well understood (and, in fact, experimentally observed) relativistic effects, such as an atomic and molecular "twin paradox" (Einstein, 1922). Further considerations arise when considering violations of time reversal symmetry and possibly a hypothetical violation of CPT symmetry and we refer to Quack (1999, 2003, 2004, 2006, 2011b,a) where one can also find a discussion of the "42 open problems", some of which are related to tunneling.

ACKNOWLEDGMENTS

We gratefully acknowledge support, help from and discussions with Ziqiŭ Chen, Csaba Fábri, Roberto Marquardt, Frédéric Merkt, Eduard Miloglyadov, Robert Prentner, Jürgen Stohner, Martin Willeke, and Gunther Wichmann as well as financial support from ETH

Zürich, the laboratory of Physical Chemistry and an Advanced Grant of the European Research Council ERC as well as the COST Project MOLIM. Many further coworkers have contributed to our work (see the lists in Quack, 2003; Ernst et al., 2013).

REFERENCES

Agapov, A.L., Kolesnikov, A.I., Novikov, V.N., Richert, R., Sokolov, A.P., 2015. Quantum effects in the dynamics of deeply supercooled water. Phys. Rev. E 91, 022312.

Al Derzi, A.R., Furtenbacher, T., Tennyson, J., Yurchenko, S.N., Császár, A.G., 2015. MARVEL analysis of the measured high-resolutions spectra of $^{14}NH_3$. J. Quant. Sepctrosc. Rad. Transf. 161, 117–130.

Al-Shamery, K., 2011. Moleküle aus dem All? Wiley-VCH, Weinheim.

Albert, S., Arn, F., Bolotova, I., Chen, Z., Fábri, C., Lerch, P., Quack, M., Seyfang, G., Wokaun, A., Zindel, D., 2016a. Synchrotron-based highest resolution terahertz spectroscopy of the ν_{24} band system of 1, 2-Dithiine ($C_4H_4S_2$): a candidate for measuring the parity violating energy difference between enantiomers of chiral molecules. J. Phys. Chem. Lett. 7, 3847–3853.

Albert, S., Bolotova, I., Chen, Z., Fábri, C., Horný, L., Quack, M., Seyfang, G., Zindel, D., 2016b. High resolution GHz and THz (FTIR) spectroscopy and theory of parity violation and tunneling for 1, 2-Dithiine ($C_4H_4S_2$) as a candidate for measuring the parity violating energy difference between enantiomers of chiral molecules. Phys. Chem. Chem. Phys. 18, 21976–21993.

Albert, S., Bolotova, I., Chen, Z., Fábri, C., Quack, M., Seyfang, G., Zindel, D., 2017. High-resolution FTIR spectroscopy of trisulfane HSSSH: a candidate for detecting parity violation in chiral molecules. Phys. Chem. Chem. Phys. 19 (19), 11738–11743.

Albert, S., Chen, Z., Fábri, C., Lerch, P., Prentner, R., Quack, M., 2016c. A combined Gigahertz and Terahertz (FTIR) spectroscopic investigation of meta-D-phenol: observation of tunnelling switching. Mol. Phys. 19, 2751–2768.

Albert, S., Keppler Albert, K., Quack, M., 2011. High resolution Fourier transform infrared spectroscopy. In: Quack, M., Merkt, F. (Eds.), Handbook of High Resolution Spectroscopy, Vol. 2. Wiley, Chichester, New York, pp. 965–1019 (Chapter 26).

Albert, S., Lerch, P., Prentner, R., Quack, M., 2013. Tunneling and tunneling switching dynamics in phenol and its isotopomers from high-resolution FTIR spectroscopy with synchrotron radiation. Angew. Chem., Int. Ed. 52 (1), 346–349.

Albert, S., Lerch, P., Quack, M., 2016d. Tunneling dynamics of aniline. In: Stohner, J., Yeretzian, C. (Eds.), Proceedings of the 19th Symposium on Atomic, Cluster and Surface Physics 2016 (SASP 2014). Davos, Switzerland. Innsbruck University Press (IUP), Innsbruck, pp. 169–177.

Allemann, R.K., Scrutton, N.S., 2009. Quantum Tunnelling in Enzyme-Catalysed Reactions. RSC Publishing, Cambridge.

Althorpe, S.C., Fernández-Alonso, F., Bean, B.D., Ayers, J.D., Pomerantz, A.E., Zare, R.N., Wrede, E., 2002. Observation and interpretation of a time-delayed mechanism in the hydrogen exchange reaction. Nature 410, 67–70.

Amano, T., 2011. High-resolution microwave and infrared spectroscopy of molecular cations. In: Quack, M., Merkt, F. (Eds.), Handbook of High-Resolution Spectroscopy, Vol. 2. Wiley, Chichester, New York, pp. 1267–1290 (Chapter 33).

Ansari, N., Meyer, H.-D., 2016. Isotope effects of ground and lowest lying vibrational states of $H_{3-x}D_xO_2^-$ complexes. J. Chem. Phys. 144, 054308.

Aoiz, F.J., Aldegunde, J., Herrero, V.J., Sáez-Rábanos, V., 2014. Comparative dynamics of the two channels of the reaction of D + MuH. Phys. Chem. Chem. Phys. 16, 9808–9818.

Aoiz, F.J., Banares, L., Castillo, J.F., Sokolovski, D., Fernández-Alonso, F., Bean, B.D., Ayers, J.D., Pomerantz, A.E., Zare, R.N., 2002. Observation of scattering resonances in the H + D_2 reaction: direct probe of the HD_2 transition-state geometry. In: Douhal, A., Santamaria, J. (Eds.), Femtochemistry and Femtobiology – Ultrafast Dynamics in Molecular Science. World Scientific, Singapore, pp. 61–72.

Aoiz, F.J., Zare, R.N., 2018. Quantum interference in chemical reactions. Phys. Today 71 (2), 70–71.

Aquilanti, V., Mundim, K.C., Cavalli, S., De Fazio, D., Aguilar, A., Lucas, J.M., 2012. Exact activation energies and phenomenological description of quantum tunneling for model potential energy surfaces. The F + H_2 reaction at low temperature. Chem. Phys. 398, 186–191.

Araujo-Andrade, C., Reva, I., Fausto, R., 2014. Tetrazole acetic acid: tautomers, conformers, and isomerization. J. Chem. Phys. 140, 064306.

Arigoni, D., Eliel, E.L., 1969. Chirality due to the presence of hydrogen isotopes at noncyclic positions. In: Allinger, N.L., Eliel, E.L. (Eds.), Topics in Stereochemistry, Vol. 4. John Wiley, Chichester, New York, pp. 127–243.

Asselin, P., Soulard, P., Madebène, B., Goubet, M., Huet, T.R., Georges, R., Pirali, O., Roye, P., 2014. The cyclic ground state structure of the HF trimer revealed by far infrared jet-cooled Fourier transform spectroscopy. Phys. Chem. Chem. Phys. 16, 4797–4806.

Ausfelder, F., Pomerantz, A.E., Zare, R.N., Althorpe, S.C., Aoiz, F.J., Banares, L., Castillo, J.F., 2004. Collision energy dependence of the HD(v = 2) product rotational distribution of the H + D_2 reaction in the range 1.30–1.89 eV. J. Chem. Phys. 120, 3255–3264.

Auzinsh, M., Dashevskaya, E.I., Nikitin, E.E., Troe, J., 2013. Quantum capture of charged particles by rapidly rotating symmetric top molecules with small dipole moments: analytical comparison of the flywheel and adiabatic channel limits. Mol. Phys. 111, 2003–2011.

Ayers, J.D., Pomerantz, A.E., Fernández-Alonso, F., Ausfelder, F., Bean, B.D., Zare, R.N., 2003. Measurement of the cross section for H + D_2 → HD(v′=3, J′=0) + D as a function of angle and energy. J. Chem. Phys. 119, 4662–4670.

Bačić, Z., Light, J.C., 1989. Theoretical methods for rovibrational states of floppy molecules. Annu. Rev. Phys. Chem. 40, 469–498.

Bakasov, A., Ha, T.K., Quack, M., 1996. Ab initio calculation of molecular energies including parity violating interactions. In: Chela-Flores, J., Raulin, F. (Eds.), Chemical Evolution, Physics of the Origin and Evolution of Life. Proc. of the 4th Trieste Conference (1995). Kluwer Academic Publishers, Dordrecht, pp. 287–296.

Bakasov, A., Ha, T.K., Quack, M., 1998. Ab initio calculation of molecular energies including parity violating interactions. J. Chem. Phys. 109 (17), 7263–7285.

Bakule, P., Fleming, D.G., Sukhorukov, O., Ishida, K., Pratt, F., Momose, T., Torikai, E., Mielke, S.L., Garrett, B.C., Peterson, K.A., Schatz, G.C., Truhlar, D.G., 2012. State-selected reaction of muonium with vibrationally excited H_2. J. Phys. Chem. Lett. 3, 2755–2760.

Barclay, A.J., McKellar, A.R.W., Moazzen-Ahmadi, N., 2019. Spectra of the D_2O dimer in the O-D fundamental stretch region: vibrational dependence of tunneling splittings and lifetimes. J. Chem. Phys. 150, 164307.

Barlow, M.J., Clough, S., Horsewill, A.J., Mohammed, M.A., 1992. Rotational frequencies of methyl group tunneling. Solid State Nucl. Magn. Reson. 1, 197–204.

Bauder, A., 2011. Fundamentals of rotational spectroscopy. In: Quack, M., Merkt, F. (Eds.), Handbook of High-Resolution Spectroscopy, Vol. 1. Wiley, Chichester, New York, pp. 57–116 (Chapter 2).

Bauder, A., 2013. Microwave spectrum of formic acetic anhydride. Mol. Phys. 111, 1999–2002.

Beckmann, P., Clough, S., Hennelf, J.W., Hill, J.R., 1977. The Haupt effect: coupled rotational and dipolar relaxation of methyl groups. J. Phys. C, Solid State Phys. 10, 729–742.

Beil, A., Luckhaus, D., Quack, M., Stohner, J., 1997. Intramolecular vibrational redistribution and unimolecular reaction: concepts and new results on the femtosecond dynamics and statistics in CHBrClF. Ber. Bunsenges. Phys. Chem. 101 (3), 311–328.

Bell, R.P., 1933. The application of quantum mechanics to chemical kinetics. Proc. Roy. Soc. A 139, 466–474.

Bell, R.P., 1980. The Tunnel Effect in Chemistry. Chapman and Hall, London.

Benderski, V.A., Makarov, D.E., Wight, C., 1994. Chemical dynamics at low temperatures. Adv. Chem. Phys. 88, 1–385.

Berger, R., Gottselig, M., Quack, M., Willeke, M., 2001. Parity violation dominates the dynamics of chirality in dichlorodisulfane. Angew. Chem., Int. Ed. 40 (22), 4195–4198; Angew. Chem. 113, 2001 4342–4345.

Berger, R., Laubender, G., Quack, M., Sieben, A., Stohner, J., Willeke, M., 2005. Isotopic chirality and molecular parity violation. Angew. Chem., Int. Ed. 44 (23), 3623–3626; Angew. Chem. 117, 2005 3689–3693.

Berger, R., Quack, M., 2000a. Multi-configuration linear response approach to the calculation of parity violating potentials in polyatomic molecules. J. Chem. Phys. 112, 3148–3158.

Berger, R., Quack, M., 2000b. Electroweak quantum chemistry of alanine: parity violation in gas and condensed phases. Chem. Phys. Chem. 1 (1), 57–60.

Berger, R., Quack, M., Sieben, A., Willeke, M., 2003. Parity-violating potentials for the torsional motion of methanol (CH_3OH) and its isotopomers CD_3OH, $^{13}CH_3OH$, CH_3OD, CH_3OT, CHD_2OH, and CHDTOH. Helv. Chim. Acta 86 (12), 4048–4060.

Bergmann, K., Nägerl, H.C., Panda, C., Gabrielse, G., Miloglyadov, E., Quack, M., Seyfang, G., Wichmann, G., Ospelkaus, S., Kuhn, A., Longhi, S., Szameit, A., Pirro, P., Hillebrands, B., Zhu, X.F., Zhu, J., Drewsen, M., Hensinger, W.K., Weidt, S., Halfmann, T., Wang, H.L., Paraoanu, G.S., Vitanov, N.V., Mompart, J., Busch, T., Barnum, T.J., Grimes, D.D., Field, R.W., Raizen, M.G., Narevicius, E., Auzinsh, M., Budker, D., Pálffy, A., Keitel, C.H., 2019. Roadmap on STIRAP applications. J. Phys. B: At. Mol. Phys. 52, 202001.

Blackmond, D.G., 2004. Asymmetric autocatalysis and its implications for the origin of homochirality. Proc. Nat. Acad. Sci. 101, 5732–5736.

Blake, T.A., Xantheas, S.S., 2006. Structure, vibrational spectrum, and ring puckering barrier of cyclobutane. J. Phys. Chem. A 110, 10487–10494.

Blumberger, J., Ha, T.K., Paff, J., Quack, M., Seyfang, G., 2000. In: Proceedings 12th SASP. Folgaria, Trento 2000, pp. PB-2, 1-4.

Böckmann, H., Liu, S., Mielke, J., Gawinkowski, S., Waluk, J., Grill, L., Wolf, M., Kumagai, T., 2016. Direct observation of photoinduced tautomerization in single molecules at a metal surface. Nano Lett. 16, 1034–1041.

Born, M., Weisskopf, V., 1931. Quantenmechanik der Adsorptionskatalyse. Z. Phys. Chem. B 12, 206–227.

Börner, K., Diezemann, G., Rössler, E., Vieth, H.M., 1991. Low-temperature methyl group dynamics of hexamethylbenzene in crystalline and glassy matrices as studied by ^2H NMR. Chem. Phys. Lett. 181, 563–568.

Boyarkin, O.V., Rizzo, T.R., Perry, D.S., 1999. Intramolecular energy transfer in highly vibrationally excited methanol. III. Rotational and torsional analysis. J. Chem. Phys. 110, 11359–11367.

Bredtmann, T., Diestler, D.J., Li, S.-D., Manz, J., Pérez-Torres, J.F., Tian, W.-J., Wu, Y.-B., Yangaf, Y., Zhaie, H.-J., 2015. Quantum theory of concerted electronic and nuclear fluxes associated with adiabatic intramolecular processes. Phys. Chem. Chem. Phys. 17, 29421–29464.

Bredtmann, T., Manz, J., Zhao, J.-M., 2016. Concerted electronic and nuclear fluxes during coherent tunneling in asymmetric double-well potentials. J. Phys. Chem. A 120, 3142–3154.

Breidung, J., Thiel, W., 2011. Prediction of vibrational spectra from ab initio theory. In: Quack, M., Merkt, F. (Eds.), Handbook of High-Resolution Spectroscopy, Vol. 1. Wiley, Chichester, New York, pp. 389–404 (Chapter 8).

Brickmann, J., Zimmermann, H., 1968. Zur Theorie des Tunneleffekts eines Teilchens im Doppelminimumpotential. Z. Naturforsch. A 23, 11–18.

Brickmann, J., Zimmermann, H., 1969. Lingering time of the proton in the wells of the double-minimum potential of hydrogen bonds. J. Chem. Phys. 50, 1608–1618.

Brillouin, M.L., 1926. Remarques sur la mécanique ondulatoire. J. Phys. Radium 7, 353–368.

Bromley, S.T., Goumans, T.P.M., Herbst, E., Jonese, A.P., Slater, B., 2014. Challenges in modelling the reaction chemistry of interstellar dust. Phys. Chem. Chem. Phys. 16, 18623–18643.

Brorsen, K.R., Yang, Y., Hammes-Schiffer, S., 2017. Multicomponent density functional theory: impact of nuclear quantum effects on proton affinities and geometries. J. Phys. Chem. Lett. 8, 3488–3493.

Buchenau, H., Toennies, J.P., Arnold, J., Wolfrum, J., 1990. H + H_2: the current status. Ber. Bunsenges. Phys. Chem. 94, 1231–1248.

Buchowiecki, M., Vaníček, J., 2010. Direct evaluation of the temperature dependence of the rate constant based on the quantum instanton approximation. J. Mol. Model. 16, 1779–1787.

Buekenhoudt, A., Vandemaele, G., Van Gerven, L., 1990. Spin conversion of tunneling CH_3 rotors in copper acetate. Phys. Rev. B 41, 9038–9044.

Bunker, P.R., Jensen, P., 1998. Molecular Symmetry and Spectroscopy. NRC Press, Ottawa.

Caminati, W., 2011. Microwave spectroscopy of large molecules and molecular complexes. In: Quack, M., Merkt, F. (Eds.), Handbook of High-Resolution Spectroscopy, Vol. 2. Wiley, Chichester, New York, pp. 829–852 (Chapter 21).

Car, R., Parrinello, M., 1985. Unified approach for molecular dynamics and density-functional theory. Phys. Rev. Lett. 55, 2471–2474.

Carrington Jr., T., 2011. Using iterative methods to compute vibrational spectra. In: Quack, M., Merkt, F. (Eds.), Handbook of High-Resolution Spectroscopy, Vol. 1. Wiley, Chichester, New York, pp. 573–586 (Chapter 14).

Carrington, A., Buttenshaw, J., Kennedy, R.A., 1982. Observation of the infrared spectrum of H_3^+ at its dissociation limit. Mol. Phys. 45, 735–758.

Carrington, A., Kennedy, R.A., 1984. Infrared predissociation spectrum of the H_3^+ ion. J. Chem. Phys. 81, 91–112.

Carter, S., Sharma, A.R., Bowman, J.M., 2013. Multimode calculations of rovibrational energies and dipole transition intensities for polyatomic molecules with torsional motion: application to H_2O_2. J. Chem. Phys. 135, 014308.

Cattaneo, L., Vos, J., Lucchini, M., Gallmann, L., Cirelli, C., Keller, U., 2016. Comparison of attosecond streaking and RABBITT. Opt. Express 24, 29060–29076.

Cavalli, S., Aquilanti, V., Mundim, K.C., De Fazio, D., 2014. Theoretical reaction kinetics astride the transition between moderate and deep tunneling regimes: the F + HD case. J. Phys. Chem. A 118, 6632–6641.

Cendagorta, J.R., Powers, A., Hele, T.J.H., Marsalek, O., Bačić, Z., Tuckerman, M.E., 2016. Competing quantum effects in the free energy profiles and diffusion rates of hydrogen and deuterium molecules through clathrate hydrates. Phys. Chem. Chem. Phys. 18, 32169–32176.

Ceriotti, M., Manolopoulos, D.E., Parrinello, M., 2011. Accelerating the convergence of path integral dynamics with a generalized Langevin equation. J. Chem. Phys. 134, 084104.

Chan-Huot, M., Dos, A., Zander, R., Sharif, S., Tolstoy, P.M., Compton, S., Fogle, E., Toney, M.E., Shenderovich, I., Gleb, S., Denisov, G.S., Limbach, H.-H., 2013. NMR studies of protonation and hydrogen bond states of internal aldimines of pyridoxal 5′-phosphate acidbase in alanine racemase, aspartate aminotransferase, and poly-L-lysine. J. Am. Chem. Soc. 135, 18160–18175.

Chapman, S., Garrett, B.C., Miller, W.H., 1975. Semiclassical transition state theory for nonseparable systems: application to the collinear H + H_2 reaction. J. Chem. Phys. 63, 2710–2716.

Chuang, C.C., Tsang, S.N., Klemperer, W., Chang, H.C., 1997. Reassignment of the 11537 cm^{-1} band of hydrogen fluoride dimer and observation of the intermolecular combination mode $3\nu_1 + \nu_4$. J. Phys. Chem. A 101, 6702–6708.

Chesnavich, W.J., Bowers, M.T., 1979. Statistical methods in reaction dynamics. In: Bowers, M.T. (Ed.), Gas Phase Ion Chemistry, Vol. 1. Elsevier Inc., Amsterdam, pp. 119–151.

Ciaćka, P., Fita, P., Listkowski, A., Kijak, M., Nonell, S., Kuzuhara, D., Yamada, H., Radzewicz, C., Waluk, J., 2015. Tautomerism in porphycenes: analysis of rate-affecting factors. J. Phys. Chem. B 119, 2292–2301.

Ciaćka, P., Fita, P., Listkowski, A., Radzewicz, C., Waluk, J., 2016. Evidence for dominant role of tunneling in condensed phases and at high temperatures: double hydrogen transfer in porphycenes. J. Phys. Chem. Lett. 7, 283–288.

Clary, D., 2018. Spiers memorial lecture: quantum dynamics of chemical reactions. Faraday Discuss. Chem. Soc. 212, 9–32.

Cohen, E.R., Cvitaš, T., Frey, J.G., Holmström, B., Kuchitsu, K., Marquardt, R., Mills, I., Pavese, F., Quack, M., Stohner, J., Strauss, H.L., Takami, M., Thor, A., 2011. Quantities, Units and Symbols in Physical Chemistry, third reviewed printing 3rd ed. Royal Soc. Chem., London.

Cole, W.T.S., Farrell, J.D., Sheikh, A.A., Yönder, O., Fellers, R.S., Viant, M.R., Wales, D.J., Saykally, R.J., 2018. Terahertz VRT spectroscopy of the water hexamer-D_{12} prism: dramatic enhancement of bifurcation tunneling upon librational excitation. J. Chem. Phys. 148, 094301.

Cole, W.T.S., Fellers, R.S., Viant, M.R., Leforestier, C., Saykally, R.J., 2015. Far-infrared VRT spectroscopy of the water dimer: characterization of the 20 μm out-of-plane librational vibration. J. Chem. Phys. 143, 154306.

Cole, W.T.S., Fellers, R.S., Viant, M.R., Saykally, R.J., 2017. Hydrogen bond breaking dynamics in the water pentamer: terahertz VRT spectroscopy of a 20 μm libration. J. Chem. Phys. 146, 014306.

Congiu, E., Minissale, M., Baouche, S., Chaabouni, H., Moudens, A., Cazaux, S., Manicó, G., Pirronello, V., Dulieu, F., 2014. Efficient diffusive mechanisms of O atoms at very low temperatures on surfaces of astrophysical interest. Faraday Discuss. Chem. Soc. 168, 151–166.

Coon, J.B., Naugle, N.W., McKenzie, R.D., 1966. The investigation of double-minimum potentials in molecules. J. Mol. Spectrosc. 20, 107–129.

Costain, C.C., Sutherland, G.B.B.M., 1952. A method of determining the potential barriers restricting inversion in ammonia, phosphine and arsine from vibrational force constants. J. Phys. Chem. 56, 321–324.

Cremer, E., Polanyi, M., 1932. Eine Prüfung der "Tunneltheorie" der heterogenenen Katalyse am Beispiel der Hydrierung von Styrol. Z. Phys. Chem. B 19, 443–450.

Császár, A.G., Allen, W.D., Schaefer III, H.F., 1998. In pursuit of the ab initio limit for conformational energy prototypes. J. Chem. Phys. 108, 9751–9764.

Császár, A.G., Fábri, C., Szidarovszky, T., Mátyus, E., Furtenbacher, T., Czakó, G., 2012. The fourth age of quantum chemistry: molecules in motion. Phys. Chem. Chem. Phys. 14, 1085–1114.

Császár, A.G., Furtenbacher, T., 2016. Promoting and inhibiting tunneling via nuclear motions. Phys. Chem. Chem. Phys. 18, 1092–1104.

Császár, A.G., Fábri, C., Szidarovszky, T., 2020. Exact numerical methods for stationary-state-based quantum dynamics of complex polyatomic molecules. In: Marquardt, R., Quack, M. (Eds.), Molecular Spectroscopy and Quantum Dynamics. Elsevier, Amsterdam. Chapter 2 (this book).

Cvitaš, M., Richardson, J., 2020. Quantum dynamics of water clusters. In: Marquardt, R., Quack, M. (Eds.), Molecular Spectroscopy and Quantum Dynamics. Elsevier, Amsterdam. Chapter 9 (this book).

Dahlström, J.M., L'Huillier, A., Maquet, A., 2012. Introduction to attosecond delays in photoionization. J. Phys. B: At. Mol. Phys. 45, 183001.

Dashevskaya, E.I., Litvin, I., Nikitin, E.E., Troe, J., 2010. Locking of the intrinsic angular momentum in the capture of quadrupole diatoms by ions. Mol. Phys. 108, 873–882.

Dashevskaya, E.I., Litvin, I., Nikitin, E.E., Troe, J., 2011. Electron capture by polarizable dipolar targets: numerical and analytically approximated capture probabilities. J. Phys. Chem. A 115, 6825–6830.

Dashevskaya, E.I., Maergoiz, A.I., Troe, J., Litvin, I., Nikitin, E.E., 2003. Low-temperature behavior of capture rate constants for inverse power potentials. J. Chem. Phys. 118, 7313–7320.

Dawadi, M.H., Perry, D.S., 2014. Conical intersections between vibrationally adiabatic surfaces in methanol. J. Chem. Phys. 140, 161101.

de Haag, P.U., Spooren, R., Ebben, M., Meerts, L., Hougen, J.T., 1990. Internal rotation in 1, 4-dimethylnaphthalene studied by high resolution laser spectroscopy. Mol. Phys. 69, 265–280.

de Tudela, R.P., Suleimanov, Y.V., Richardson, J.O., Sáez Rábanos, V., Green, W.H., Aoiz, F.J., 2013. Stress test for quantum dynamics approximations: deep tunneling in the muonium exchange reaction D + HMu → DMu + H. J. Phys. Chem. Lett. 5, 4219–4224.

Dennison, D.M., Uhlenbeck, G.E., 1932. The two-minima problem and the ammonia molecule. Phys. Rev. 41, 313–321.

Devault, D., 1984. Quantum-Mechanical Tunnelling in Biological Systems. Cambridge Univ. Press, Cambridge.

Dietiker, P., Miloglyadov, E., Quack, M., Schneider, A., Seyfang, G., 2015. Infrared laser induced population transfer and parity selection in $^{14}NH_3$: a proof of principle experiment towards detecting parity violation in chiral molecules. J. Chem. Phys. 143, 244305.

Domcke, W., Yarkony, D.R., 2012. Role of conical intersections in molecular spectroscopy and photoinduced chemical dynamics. Annu. Rev. Phys. Chem. 63, 325–352.

Dumez, J.N., Hakansson, P., Mamone, S., Meier, B., Stevanato, G., Hill-Cousins, J.T., Roy, S.S., Brown, R.C.D., Pileio, G., Levitt, M.H., 2015. Theory of long-lived nuclear spin states in methyl groups and quantum-rotor induced polarisation. J. Chem. Phys. 142, 044506.

Dyke, T.R., Howard, B.J., Klemperer, W., 1972. Radio frequency and microwave spectrum of the hydrogen fluoride dimer, a nonrigid molecule. J. Chem. Phys. 56, 2442–2454.

Eckart, C., 1930. The penetration of a potential barrier by an electron. Phys. Rev. 35, 1303–1309.

Eckert, J., Kohen, A., McMahon, R., 2017. In: Proceedings 18th International Workshop on Quantum Atomic and Molecular Tunneling in Solids and Other Phases (QAMTS). Madison/Wisconsin, 20–24 May, 2017.

Eckert, J., Meier, B.H., Merkt, F., Quack, M., 2015. In: Proceedings 17th International Workshop on Quantum Atomic and Molecular Tunneling in Solids and Other Phases (QAMTS). Beatenberg/Interlaken Switzerland, 31 May – 3 June, 2015.

Eckert, J., Georgiev, P., Quack, M., Doslic, N., Stare, J., 2019. In: Proc. 19th Int. Workshop on Quantum Atomic and Molecular Tunneling Systems (QAMTS). Borovets, Bulgaria, 16–20 June, 2019.

Einstein, A., 1922. Grundzüge der Relativitätstheorie. Vieweg, Braunschweig.

Endo, Y., Sumiyoshi, Y., 2011. Rotational spectroscopy of complexes containing free radicals. In: Quack, M., Merkt, F. (Eds.), Handbook of High-Resolution Spectroscopy, Vol. 2. Wiley, Chichester, New York, pp. 897–916 (Chapter 23).

Ernst, R.R., Carrington, T., Seyfang, G., Merkt, F., 2013. Editorial Special Issue. Mol. Phys. 111, 1939–1963.

Ernst, R.R., Bodenhausen, G., Wokaun, A., 1987. Principles of Nuclear Magnetic Resonance in One and Two Dimensions. Clarendon Press, Oxford.

Ertelt, M., Henkel, S., Zhang, W.T.X., Hrovat, D.A., Borden, W.T., 2015. Tunneling in the degenerate rearrengment of semibullvalene at cryogenic temperatures L28. In: Eckert, J., Merkt, F., Meier, B.H., Quack, M. (Eds.), Proc. 17th QAMTS. Beatenberg, Switzerland.

Ertelt, M., Hrovat, D.A., Borden, W.T., Sander, W., 2014. Heavy-atom tunneling in the ring opening of a strained cyclopropene at very low temperatures. Chem. Eur. J. 20, 4713–4720.

Ertl, G., 2008. Reactions at surfaces: from atoms to complexity (Nobel lecture). Angew. Chem., Int. Ed. 47, 3524–3535.

Eyring, H., 1938a. The calculation of activation energies. Trans. Faraday Soc. 34, 3–11.

Eyring, H., 1938b. The theory of absolute reaction rates. Trans. Faraday Soc. 34, 41–48.

Eyring, H., Walter, J., Kimball, G., 1944. Quantum Chemistry. John Wiley, New York.

Fábri, C., Albert, S., Chen, Z., Prentner, R., Quack, M., 2018. A molecular quantum switch based on tunneling in meta-d-phenol C_6H_4DOH. Phys. Chem. Chem. Phys. 20, 7387–7394.

Fábri, C., Horný, L., Quack, M., 2015. Tunneling and parity violation in trisulfane (HSSSH): an almost ideal molecule for detecting parity violation in chiral molecules. ChemPhysChem 16, 3584–3589.

Fábri, C., Marquardt, R., Császár, A., Quack, M., 2019. Controlling tunneling in ammonia isotopomers. J. Chem. Phys. 150, 014102 (and to be published).

Fábri, C., Marquardt, R., Quack, M., 2015. Full-dimensional dynamics and spectroscopy of ammonia isotopomers. In: Eckert, J., Merkt, F., Meier, B.H., Quack, M. (Eds.), Proceedings of XVIIth International Workshop on Quantum Atomic and Molecular Tunneling in Solids and Other Phases. Beatenberg, Switzerland. pp. L-42 (and to be published 2020).

Fábri, C., Mátyus, E., Császár, A.G., 2011. Rotating full- and reduced-dimensional quantum chemical models of molecules. J. Chem. Phys. 130, 074105.

Fábri, C., Mátyus, E., Császár, A.G., 2014. Numerically constructed internal-coordinate Hamiltonian with Eckart embedding and its application for the inversion tunneling of ammonia. Spectrochim. Acta A 119, 84–89.

Fábri, C., Quack, M., Császár, A.G., 2017. On the use of nonrigid-molecular symmetry in nuclear motion computations employing a discrete variable representation: a case study of the bending energy levels of CH_5^+. J. Chem. Phys. 147 (13), 134101.

Farrar, J.M., Lee, Y.T., 1974. Chemical dynamics. Annu. Rev. Phys. Chem. 25, 357–386.

Fehrensen, B., Luckhaus, D., Quack, M., 1999a. Inversion tunneling in aniline from high resolution infrared spectroscopy and an adiabatic reaction path Hamiltonian approach. Z. Phys. Chem. 209, 1–19.

Fehrensen, B., Luckhaus, D., Quack, M., 1999b. Mode selective stereomutation tunnelling in hydrogen peroxide isotopomers. Chem. Phys. Lett. 300 (3–4), 312–320.

Fehrensen, B., Luckhaus, D., Quack, M., 2007. Stereomutation dynamics in hydrogen peroxide. Chem. Phys. 338 (2–3), 90–105.

Fehrensen, B., Luckhaus, D., Quack, M., Willeke, M., Rizzo, T.R., 2003. Ab initio calculations of mode selective tunneling dynamics in $^{12}CH_3OH$ and $^{13}CH_3OH$. J. Chem. Phys. 119 (11), 5534–5544.

Felix, D., Eschenmoser, A., 1968. Slow inversion at pyramidal nitrogen: isolation of diastereomeric 4-chloro-7-azabicyclo-(4.1.0) heptanes at room temperature. Angew. Chem., Int. Ed. 7, 224–225.

Felker, P.M., Bačić, Z., 2016. Communication: quantum six-dimensional calculations of the coupled translation rotation eigenstates of $H_2O@C_{60}$. J. Chem. Phys. 144, 201101.

Felker, P.M., Bačić, Z., 2019. Weakly bound molecular dimers: intramolecular vibrational fundamentals, overtones, and tunneling splittings from full-dimensional quantum calculations using compact contracted bases of intramolecular and low-energy rigid-monomer intermolecular eigenstates. J. Chem. Phys. 153, 024305.

Felker, P., Lauvergnat, D., Scribano, Y., Benoit, D.M., Bačić, Z., 2019. Intramolecular stretching vibrational states and frequency shifts of $(H_2)_2$ confined inside the large cage of clathrate hydrate from an eight-dimensional quantum treatment using small basis sets. J. Chem. Phys. 151, 124311.

Fermi, E., 1932. Sulle bande di oscillazione et rotazione dell'ammoniaca. Nuovo Cimento 9, 277–283.

Firmino, T., Marquardt, R., Gatti, F., Dong, W., 2014. Diffusion rates for hydrogen on Pd(111) from molecular quantum dynamics calculations. J. Phys. Chem. Lett. 5, 4270–4274.

Fleming, D.G., Arseneau, D.J., Sukhorukov, O., Brewer, J.H., Mielke, S.L., Schatz, G.C., Garrett, B.C., Peterson, K.A., Truhlar, D.G., 2011a. Kinetic isotope effects for the reactions of muonic helium and muonium with H_2. Science 331, 448–451.

Fleming, D.G., Arseneau, D.J., Sukhorukov, O., Brewer, J.H., Mielke, S.L., Truhlar, D.G., Schatz, G.C., Garrett, B.C., Peterson, K.A., 2011b. Kinetics of the reaction of the heaviest hydrogen atom with H_2, the $^4He\mu + H_2 \rightarrow {}^4He\mu H + H$ reaction: Experiments, accurate quantal calculations, and variational transition state theory, including kinetic isotope effects for a factor of 36.1 in isotopic mass. J. Chem. Phys. 135, 184310.

Fowler, R.H., Nordheim, L., 1928. Electron emission in intense electric fields. Proc. Roy. Soc. A 119, 173–181.

Francis, K., Sapienza, P.J., Lee, A.L., Kohen, A., 2016. The effect of protein mass modulation on human dihydrofolate reductase. Biochemistry 55, 1100–1106.

Frey, H.M., Kummli, D., Lobsiger, S., Leutwyler, S., 2011. High-resolution rotational Raman coherence spectroscopy with femtosecond pulses. In: Quack, M., Merkt, F. (Eds.), Handbook of High-Resolution Spectroscopy, Vol. 2. Wiley, Chichester, New York, pp. 1237–1266 (Chapter 32).

Friedman, J.I., Telegdi, V., 1957. Nuclear emulsion evidence for parity nonconservation in the decay chain $\pi^+ - \pi^- - \varepsilon^+$. Phys. Rev. 105, 1681–1682.

Gallmann, L., Cirelli, C., Keller, U., 2012. Attosecond science: recent highlights and future trends. Annu. Rev. Phys. Chem. 63, 447–469.

Gallmann, L., Keller, U., 2011. Femtosecond and attosecond light sources and techniques for spectroscopy. In: Quack, M., Merkt, F. (Eds.), Handbook of High-Resolution Spectroscopy, Vol. 3. Wiley, Chichester, New York, pp. 1805–1836 (Chapter 50).

Gamov, G., 1928a. The quantum theory of nuclear disintegration. Nature 122, 805–806.

Gamov, G., 1928b. Zur Quantentheorie des Atomkernes. Z. Phys. 51, 204–212.

Garwin, R.L., Lederman, L.M., Weinrich, M., 1957. Observation of the failure of conservation of parity an charge conjugation in meson decays - magnetic moment of the free muon. Phys. Rev. 105, 1415–1417.

Gerbig, D., Schreiner, P.R., 2015. Hydrogen-tunneling in biologically relevant small molecules: the rotamerizations of α-ketocarboxylic acids. J. Phys. Chem. B 119, 693–703.

Ghosh, S., Thomas, J., Huang, W., Xu, Y., Jäger, W., 2015. Rotational spectra of two hydrogen-bonded methyl salicylate monohydrates: relative stability and tunneling motions. J. Phys. Chem. Lett. 6, 3126–3131.

Gioumousis, G., Stevenson, D.P., 1958. Reactions of gaseous molecule ions with gaseous molecules. V. Theory. J. Chem. Phys. 29, 294–299.

Glänzer, K., Quack, M., Troe, J., 1976. A spectroscopic determination of the methyl radical recombination rate constant in shock waves. Chem. Phys. Lett. 39 (2), 304–309.

Glänzer, K., Quack, M., Troe, J., 1977. High temperature UV absorption and recombination of methyl radicals in shock waves. In: 16th International Symposium on Combustion. The Combustion Institute, Pittsburgh, pp. 949–960.

Goldanskii, V.I., 1976. Chemical reactions at very low temperatures. Annu. Rev. Phys. Chem. 27, 85–126.

Gordon, J.P., Zeiger, H.J., Townes, C.H., 1955. The maser – new type of microwave amplifier, frequency standard, and spectrometer. Phys. Rev. 99, 1264–1274.

Gorin, E., 1938. Loose complex model. Acta Phys. Chim. URSS 9, 691.

Grabow, J.-U., 2011. Fourier transform microwave spectroscopy measurement and instrumentation. In: Quack, M., Merkt, F. (Eds.), Handbook of High-Resolution Spectroscopy, Vol. 2. Wiley, Chichester, New York, pp. 723–799 (Chapter 19).

Grohmann, T., Manz, J., Schild, A., 2013. Effects of molecular symmetry on the directions of nuclear flux densities during tunnelling in double well potentials. Mol. Phys. 111, 2251–2262.

Guennoun, Z., Maier, J.P., 2011. Electronic spectroscopy of transient molecules. In: Quack, M., Merkt, F. (Eds.), Handbook of High-Resolution Spectroscopy, Vol. 2. Wiley, Chichester, New York, pp. 1321–1344 (Chapter 33).

Gurney, R.W., Condon, E.U., 1928. Wave mechanics and radioactive disintegration. Nature 122, 439.

Gurney, R.W., Condon, E.U., 1929. Wave mechanics and radioactive disintegration. Phys. Rev. 33, 127–140.

Hall, F.H.J., Eberle, P., Hegi, G., Raoult, M., Aymar, M., Dulieu, O., Willitsch, S., 2013. Ion-neutral chemistry at ultralow energies: dynamics of reactive collisions between lasercooled Ca^+ ions and Rb atoms in an ion-atom hybrid trap. Mol. Phys. 111, 2020–2032.

Hamm, P., Stock, G., 2013. Vibrational conical intersections in the water dimer. Mol. Phys. 111, 2046–2056.

Hänninen, V., Horn, M., Halonen, L., 1999. Torsional motion and vibrational overtone spectroscopy of methanol. J. Chem. Phys. 111, 3018–3026.

Hargis, J.C., Evangelista, F.A., Ingels, J.B., Schaefer III, H.F., 2008. Short intramolecular hydrogen bonds: derivatives of malonaldehyde with symmetrical substituents. J. Am. Chem. Soc. 130, 17471–17478.

Hartmann, C., Joyeux, M., Trommsdorff, H.P., Vial, J.C., von Borczyskowski, J., 1992. Optical measurements of methyl group tunneling in molecular crystals: temperature dependence of the nuclear spin conversion rate. J. Chem. Phys. 96, 6335–6343.

Hauge, E.H., Stoevneng, J.A., 1989. Tunneling times: a critical review. Rev. Modern Phys. 61, 917–936.

Haupt, J., 1972. A new effect of dynamic polarization in a solid obtained by rapid change of temperature. Phys. Lett. A 38, 389–390.

Hauser, A.W., Pototschnig, J.V., Ernst, W.E., 2015. A classic case of Jahn–Teller effect theory revisited: ab initio simulation of hyperfine coupling and pseudorotational tunneling in the $1\,^2E'$ state of Na_3. Chem. Phys. 460, 2–13.

Häusler, W., 1990. Theory of spin-conversion in XH_3-systems. Z. Phys. B, Condens. Matter 81, 265–272.

Havenith, M., Birer, O., 2011. High-resolution IR-laser jet spectroscopy of the formic acid dimer. In: Quack, M., Merkt, F. (Eds.), Handbook of High-Resolution Spectroscopy, Vol. 2. Wiley, Chichester, New York, pp. 1119–1128 (Chapter 29).

Hawbaker, N.A., Blackmond, D.G., 2019. Energy threshold for chiral symmetry breaking in molecular self-replication. Nat. Chem. 11, 957–962.

Hawking, S.W., 1975. Particle creation by black holes. Comm. Math. Phys. 43, 199–220.

He, Y., Müller, H.B., Quack, M., Suhm, M.A., 2007. High resolution FTIR and diode laser supersonic jet spectroscopy of the $N = 2$ HF-stretching polyad in $(HF)_2$ and (HFDF): hydrogen bond switching and predissociation dynamics. Z. Phys. Chem. 221, 1581–1645.

Heidemann, A., Magerl, A., Prager, M., Richter, D., Springer, T., 1987. Quantum Aspects of Molecular Motions in Solids. Springer Proceedings in Physics, vol. 17. Springer, Berlin, Heidelberg.

Heilbronner, E., Günthard, H.H., Gerdil, R., 1956. Linearkombination Hermite'scher Orthogonalfunktionen, ein Verfahren zur Behandlung eindimensionaler Molekel-Modellen der Quanten-Chemie. Helv. Chim. Acta 39, 1171–1181.

Helmchen, G., 2016. 50 Jahre Spezifikation der molekularen Chiralität durch Cahn, Ingold und Prelog. Angew. Chem. 128, 6910–6911.

Henkel, S., Sander, W., 2015. Activation of molecular hydrogen by a singlet carbene through quantum mechanical tunneling. Angew. Chem., Int. Ed. 54, 4603–4607.

Hermann, G., Liu, C.H., Manz, J., Paulus, B., Peérez-Torres, J.F., Pohl, V., Tremblay, J.C., 2016. Multidirectional angular electronic flux during adiabatic attosecond charge migration in excited benzene. J. Phys. Chem. A 120, 5360–5369.

Hernandez, R., Miller, W.H., 1993. Semiclassical transition state theory. A new perspective. Chem. Phys. Lett. 214, 129–136.

Herschbach, D.R., 1973. Reactive scattering. Faraday Discuss. Chem. Soc. 55, 233–251.

Herschbach, D.R., 1987. Molecular dynamics of elementary chemical reactions (Nobel lecture). Angew. Chem., Int. Ed. 26, 1221–1243.

Herzberg, G., 1939. Molekülspektren und Molekülstruktur. Steinkopff, Dresden.

Herzberg, G., 1945. Molecular Spectra and Molecular Structure: II. Infrared and Raman Spectra. Van Nostrand, New York.

Herzberg, G., 1966. Molecular Spectra and Molecular Structure: III. Electronic Spectra and Electronic Structure of Polyatomic Molecules. Van Nostrand, New York.

Hippler, M., Miloglyadov, E., Quack, M., Seyfang, G., 2011. Mass and isotope selective infrared spectroscopy. In: Quack, M., Merkt, F. (Eds.), Handbook of High Resolution Spectroscopy, Vol. 2. Wiley, Chichester, New York, pp. 1069–1118 (Chapter 28).

Hippler, M., Oeltjen, L., Quack, M., 2007. High-resolution continuous-wave-diode laser cavity ring-down spectroscopy of the hydrogen fluoride dimer in a pulsed slit jet expansion: two components of the $n = 2$ triad near 1.3 micrometer. J. Phys. Chem. A 111 (49), 12659–12668.

Hofacker, L., 1963. Quantentheorie chemischer Reaktionen. Z. Naturforsch. A 18, 607–619.

Hoffmann, R., 1998. Qualitative thinking in the age of modern computational chemistry – or what Lionel Salem knows. J. Mol. Struct. 424, 1–6.

Hofmann, C., Landsman, A.S., Keller, U., 2019. Attoclock revisited on electron tunnelling time. J. Modern Opt. 66, 1052–1070.

Hollenstein, U., Merkt, F., Meyer, L., Seiler, R., Softley, T.P., Willitsch, S., 2007. Rovibronic photoionization dynamics of ammonia isotopomers. Mol. Phys. 105, 1711–1722.

Hölsch, N., Beyer, M., Salumbides, E.J., Eikema, K.S.E., Ubachs, W., Jungen, C., Merkt, F., 2019. Benchmarking theory with an improved measurement of the ionization and dissociation energies of H_2. Phys. Rev. Lett. 122, 103002.

Homayoon, Z., Bowman, J.M., Evangelista, F.A., 2014. Calculations of mode-specific tunneling of double-hydrogen transfer in porphycene agree with and illuminate experiment. J. Phys. Chem. Lett. 5, 2723–2727.

Horká-Zelenková, V., Seyfang, G., Dietiker, P., Quack, M., 2019. Nuclear spin symmetry conservation studied for symmetric top molecules (CH_3D, CHD_3, CH_3F, and CH_3Cl) in supersonic jet expansions. J. Phys. Chem. A 123, 6160–6174.

Horný, L., Quack, M., 2015. Computation of molecular parity violation using the coupled-cluster linear response approach. Mol. Phys. 113 (13–14), 1768–1779.

Horný, L., Quack, M., Schaefer III, H.F., Willeke, M., 2016. Chlorine peroxide (Cl_2O_2) and its isomers: structures, spectroscopy, formation and thermochemistry. Mol. Phys. 114, 1135–1147.

Horsewill, A.J., 1999. Quantum tunnelling aspects of methyl group rotation studied by NMR. Prog. Nucl. Magn. Reson. Spectrosc. 35, 359–389.

Hoshina, H., Fushitani, M., Momose, T., Shida, T., 2004. Tunneling chemical reactions in solid parahydrogen: direct measurement of the rate constants of $R + H_2 \rightarrow RH + H$ ($R = CD_3$, CD_2H, CDH_2, CH_3, at 5 K. J. Chem. Phys. 120, 3706–3715.

Hougen, J.T., Bunker, P.R., Johns, J.W.C., 1970. Vibration-rotation problem in triatomic molecules allowing for a large-amplitude bending vibration. J. Mol. Spectrosc. 34, 136–172.

Hund, F., 1927a. Symmetriecharaktere von Termen bei Systemen mit gleichen Partikeln in der Quantenmechanik. Z. Phys. 43, 788–804.

Hund, F., 1927b. Zur Deutung der Molekelspektren. III. -Bemerkungen über das Schwingungs- und Rotationsspektrum bei Molekeln mit mehr als zwei Kernen. Z. Phys. 43, 805–826.

Hund, F., 1927c. Zur Deutung der Molekülspektren I. Z. Phys. 40, 742–764.

Icker, M., Berger, S., 2012. Unexpected multiplet patterns induced by the Haupt-effect. J. Magn. Reson. 219, 1–3.

Inui, H., Sawada, K., Oishi, S., Ushida, K., McMahon, R.J., 2013. Aryl nitrene rearrangements: spectroscopic observation of a benzazirine and its ring expansion to a ketenimine by heavy-atom tunneling. J. Am. Chem. Soc. 135, 10246–10249.

Ivanov, S.D., Grant, I.M., Marx, D., 2015. Quantum free energy landscapes from ab initio path integral metadynamics: double proton transfer in the formic acid dimer is concerted but not correlated. J. Chem. Phys. 143, 124304.

Jambrina, P.G., Aldegunde, J., Aoiz, F.J., Sneha, M., Zare, R.N., 2016. Effects of reagent rotation on interferences in the product angular distributions of chemical reactions. Chem. Sci. 7, 642–649.

Jankunas, J., Sneha, M., Zare, R.N., Bouakline, F., Althorpe, S.C., 2013a. Disagreement between theory and experiment grows with increasing rotational excitation of HD(v′,J′) product for the $H + D_2$ reaction. J. Chem. Phys. 138, 094310.

Jankunas, J., Sneha, M., Zare, R.N., Bouakline, F., Althorpe, S.C., 2013b. Hunt for geometric phase effects in $H + HD \rightarrow HD(v',J') + H$. J. Chem. Phys. 139, 144316.

Jankunas, J., Zare, R.N., Bouakline, F., Althorpe, S.C., Diego Herráez-Aguilar, D., Aoiz, F.J., 2012. Seemingly anomalous angular distributions in $H + D_2$ reactive scattering. Science 336, 1687–1691.

Janoschek, R., 1991. Theories on the origin of biomolecular homochirality. In: Janoschek, R. (Ed.), Chirality - From Weak Bosons to the α-Helix. Springer, Berlin.

Jortner, J., 2006. Conditions for the emergence of life on the early Earth: summary and reflections. Philos. Trans. R. Soc. Lond. B, Biol. Sci. 361, 1877–1891.

Karplus, M., 2014. Development of multiscale models for complex chemical systems: from $H+H_2$ to biomolecules (Nobel lecture). Angew. Chem., Int. Ed. 53, 9992–10005.

Kästner, J., 2013. Path length determines the tunneling decay of substituted carbenes. Chem. Eur. J. 13, 8207–8212.

Kästner, J., 2014a. Der Tunneleffekt in chemischen Reaktionen. Bunsen-Magazin 1, 15–19.

Kästner, J., 2014b. Theory and simulation of atom tunneling in chemical reactions. WIREs Comput. Mol. Sci. 4, 158–168.

Kawasaki, T., Matsumura, Y., Tsutsumi, T., Suzuki, K., Ito, M., Soai, K., 2009. Asymmetric autocatalysis triggered by carbon isotope ($^{13}C/^{12}C$) chirality. Science 324, 492–496.

Keutsch, F.N., Fellers, R.S., Brown, M.G., Viant, M.R., Petersen, P.B., Saykally, R.J., 2001. Hydrogen bond breaking dynamics of the water trimer in the translational and librational band region of liquid water. J. Am. Chem. Soc. 123, 5938–5941.

Kilaj, A., Gao, H., Rösch, D., Rivero, U., Küpper, J., Willitsch, S., 2018. Observation of different reactivities of para and ortho-water towards trapped diazenylium ions. Nat. Commun. 9, 2096.

Klopper, W., Quack, M., Suhm, M.A., 1998a. Explicitly correlated coupled cluster calculations of the dissociation energies and barriers to concerted hydrogen exchange of $(HF)_n$ oligomers ($n = 2, 3, 4, 5$). Mol. Phys. 94 (1), 105–119.

Klopper, W., Quack, M., Suhm, M.A., 1998b. HF dimer: empirically refined analytical potential energy and dipole hypersurfaces from ab initio calculations. J. Chem. Phys. 108 (24), 10096–10115 (88 pages supplementary material published as AIP Document No PAPS JCPS 16-108-303 820-88 by American Institute of Physics, Physics Auxiliary Publication Service).

Klopper, W., Samson, C.C.M., Tarczay, G., Császár, A., 2001. Equilibrium inversion barrier of NH_3 from extrapolated coupled-cluster pair energies. J. Comput. Chem. 22, 1306–1314.

Kneba, M., Wolfrum, J., 1980. Bimolecular reaction of vibrationally excited molecules. Annu. Rev. Phys. Chem. 31, 47–79.

Koeppe, B., Guo, J., Tolstoy, P.M., Denisov, G.S., Limbach, H.-H., 2013. Solvent and H/D isotope effects on the proton transfer pathways in heteroconjugated hydrogen-bonded phenol-carboxylic acid anions observed by combined UV-vis and NMR spectroscopy. J. Am. Chem. Soc. 135, 7553–7568.

Kolesnikov, A.I., Reiter, G.F., Choudhury, N., Prisk, T.R., Mamontov, E., Podlesnyak, A., Ehlers, G., Seel, A.G., Wesolowski, D.J., Anovitz, L.H., 2016. Quantum tunneling of water in beryl: a new state of the water molecule. Phys. Rev. Lett. 116, 167802.

Koszinowski, K., Goldberg, N.T., Pomerantz, A.E., Zare, R.N., Juanes-Marcos, J.C., Althorpe, S.C., 2005. Collision-energy dependence of HD($v' = 1$, J') product rotational distributions for the $H + D_2$ reaction. J. Chem. Phys. 123, 054306.

Kozuch, S., 2014a. Heavy atom tunneling in the automerization of pentalene and other antiaromatic systems. RSC Adv. 4, 21650–21656.

Kozuch, S., 2014b. The reactivity game: theoretical predictions for heavy atom tunneling in adamantyl and related carbenes. Phys. Chem. Chem. Phys. 16, 7718–7727.

Kozuch, S., Zhang, X., Hrovat, D.A., Borden, W.T., 2013. Calculations on tunneling in the reactions of noradamantyl carbenes. J. Am. Chem. Soc. 135, 17274–117277.

Kramers, H.A., 1926. Wellenmechanik und halbzahlige Quantisierung. Z. Phys. 39, 828–840.

Kuhn, B., Rizzo, T.R., Luckhaus, D., Quack, M., Suhm, M.A., 1998. A new six-dimensional analytical potential up to chemically significant energies for the electronic ground state of hydrogen peroxide. J. Chem. Phys. 111, 2565–2587.

Kundu, A., Piccini, G.M., Sillar, K., Sauer, J., 2016. Ab initio prediction of adsorption isotherms for small molecules in metal-organic frameworks. J. Am. Chem. Soc. 138, 14047–14056.

Kushnarenko, A., Miloglyadov, E., Quack, M., Seyfang, G., 2018. Intramolecular vibrational energy redistribution in $HCCCH_2X$ (X = Cl, Br, I) measured by femtosecond pump-probe experiments in a hollow waveguide. Phys. Chem. Chem. Phys. 20, 10949–10959.

Laane, J., 1999. Spectroscopic determination of ground and excited state vibrational potential energy surfaces. Int. Rev. Phys. Chem. 18, 301–341.

Ladenthin, J.N., Frederiksen, T., Persson, M., Sharp, J.C., Gawinkowski, S., Waluk, J., Kumagai, T., 2016. Force-induced tautomerization in a single molecule. Nat. Chem. 8, 935–940.

Lalowicz, Z.T., Werner, U., Müller-Warmuth, W., 1988. Rotational tunneling of CD_3 groups in molecular crystals as studied by NMR spectra. Z. Naturforsch. A 43, 219–227.

Lamberts, T., Samanta, P.K., Köhn, A., Kästner, J., 2016. Quantum tunneling during interstellar surface-catalyzed formation of water: the reaction $H + H_2O_2 \rightarrow H_2O + OH$. Phys. Chem. Chem. Phys. 18, 33021–33030.

Landauer, R., Martin, T., 1994. Barrier interaction time in tunneling. Rev. Modern Phys. 66, 217–228.

Landsman, A.S., Keller, U., 2014. Tunnelling time in strong field ionisation. J. Phys. B: At. Mol. Phys. 47, 204024.

Landsman, A.S., Keller, U., 2015. Attosecond science and the tunnelling time problem. Phys. Rep. 547, 1–24.

Landsman, A.S., Weger, M., Maurer, J., Boge, R., Ludwig, A., Heuser, S., Cirelli, C., Gallmann, L., Keller, U., 2014. Ultrafast resolution of tunneling delay time. Optica 1, 343–349.

Lauvergnat, D., Felker, P., Scribano, Y., Benoit, D.M., Bačić, Z., 2019. H_2, HD, and D_2 in the small cage of structure II. Clathrate hydrate: vibrational frequency shifts from fully coupled quantum six-dimensional calculations of the vibration-translation-rotation eigenstates. J. Chem. Phys. 150, 154303.

Lee, Y.T., 1987. Molecular beam studies of elementary chemical processes (Nobel lecture). Angew. Chem., Int. Ed. 26, 939–958.

Lee, T.D., Yang, C.N., 1956. Question of parity conservation in weak interactions. Phys. Rev. 104, 254–258.

Leforestier, C., 2012. Infrared shifts of the water dimer from the fully flexible ab initio HBB2 potential. Philos. Trans. R. Soc. Lond. Ser. A 370, 2675–2690.

Lehn, J.M., 1970. Nitrogen inversion – experiment and theory. In: Davison, A., Dewar, M.J.S., Hafner, K., Heilbronner, E., Hofmann, K., Niedenzu, U., Schäfer, K., Wittig, C. (Eds.), Fortschritte der Chemischen Forschung – Topics in Current Chemistry, Vol. 15. Springer, Berlin, Heidelberg, New York, pp. 311–377.

Lehn, J.M., 2002. Toward complex matter: supramolecular chemistry and self-organization. Proc. Nat. Acad. Sci. 99, 4763–4768.

Lépine, F., Ivanov, M.Y., Vrakking, M.J.J., 2014. Attosecond molecular dynamics: fact or fiction? Nat. Photonics 8, 195–204.

Levine, R.D., 2005. Molecular Reaction Dynamics, first ed. Cambridge Univ. Press, Cambridge.

Levine, R.D., Bernstein, R.B., 1989. Molecular Reaction Dynamics and Chemical Reactivity. Oxford Univ. Press, Oxford.

Levitt, M., 2014. Birth and future of multiscale modeling for macromolecular systems (Nobel lecture). Angew. Chem., Int. Ed. 53, 10006–10018.

Li, L.Y., Seifert, N.A., Xie, F., Heger, M., Xu, Y., Jäger, W., 2018. A spectroscopic and ab initio study of the hydrogen peroxide-formic acid complex: hindering the internal motion of H_2O_2. Phys. Chem. Chem. Phys. 20, 21345–21351.
Light, J.C., Carrington Jr., T., 2001. Discrete-variable representations and their utilization. Adv. Chem. Phys. 114, 263–310.
Limbach, H.H., 2007. Single and multiple hydrogen/deuterium transfer reactions in liquids and solids. In: Hynes, J.T., Klinman, J.P., Limbach, H., Schowen, R.L. (Eds.), Hydrogen-Transfer Reactions. Wiley, Weinheim, pp. 135–221.
Liu, C.M., Manz, J., Yang, Y., 2015. Nuclear fluxes during coherent tunneling in asymmetric double well potentials. J. Phys. B: At. Mol. Phys. 48, 164001.
Longuet-Higgins, H.C., 1963. The symmetry group of non-rigid molecules. Mol. Phys. 6, 445–461.
Low, F.E., 1998. Comments on apparent superluminal propagation. Ann. Phys. (Leipzig) 7, 660–661.
Löwdin, P.O., 1963. Proton tunneling in DNA and its biological implications. Rev. Modern Phys. 35, 724–732.
Lozada-Garcia, R.R., Ceponkus, J., Chevalier, M., Chin, W., Mestdagh, J.M., Crépin, C., 2012. Nuclear spin conversion to probe the methyl rotation effect on hydrogen-bond and vibrational dynamics. Angew. Chem., Int. Ed. 51, 6947–6950.
Lu, C.M., Manz, J., Yang, Y., 2016. Staircase patterns of nuclear fluxes during coherent tunneling in excited doublets of symmetric double well potentials. Phys. Chem. Chem. Phys. 18, 5048–5055.
Luckhaus, D., 2006. Concerted hydrogen exchange tunneling in formic acid dimer. J. Phys. Chem. A 110, 3151–3158.
Luckhaus, D., Quack, M., 1992. Spectrum and dynamics of the CH chromophore in CD_2HF. 1. Vibrational Hamiltonian and analysis of rovibrational spectra. Chem. Phys. Lett. 190 (6), 581–589.
Luckhaus, D., Quack, M., Schmitt, U., Suhm, M.A., 1995. On FTIR spectroscopy in asynchronously pulsed supersonic free jet expansions and on the interpretation of stretching spectra of HF clusters. Ber. Bunsenges. Phys. Chem. 99 (3), 457–468. Also: Abstracts of the Conference on Molecular Spectroscopy and Molecular Dynamics, Theory and Experiment, Grainau 1994, p. 73.
Ludwig, C., Saunders, M., Marin-Montesinos, I., Günther, U.L., 2010. Quantum rotor induced hyperpolarization. Proc. Nat. Acad. Sci. 107, 10799–10803.
Luisi, P.L., 2006. The Emergence of Life – From Chemical Origins to Synthetic Biology. Cambridge University Press, Cambridge.
Luk, L.Y.P., Ruiz-Pernía, J.J., Dawson, W.M., Roca, M., Loveridge, E.J., Glowacki, D.R., Harvey, J.N., Mulholland, A.J., Tunón, I., Moliner, V., Allemann, R.K., 2013. Unraveling the role of protein dynamics in dihydrofolate reductase catalysis. Proc. Nat. Acad. Sci. 110, 16344–16349.
Lüthy, J., Rétey, J., Arigoni, D., 1969. Preparation and detection of chiral methyl groups. Nature 221, 1213–1215.
Lüttschwager, N.O.B., Wassermann, T.N., Coussan, S., Suhm, M.A., 2013. Vibrational tuning of the hydrogen transfer in malonaldehyde – a combined FTIR and Raman jet study. Mol. Phys. 111 (14–15), 2211–2227.
Luzar, A., 2000. Resolving the hydrogen bond dynamics conundrum. J. Chem. Phys. 113, 10663–10675.
Luzar, A., Chandler, D., 1996. Hydrogen-bond kinetics in liquid water. Nature 379, 55–57.
MacColl, L.A., 1932. Note on the transmission and reflection of wave packets by potential barriers. Phys. Rev. 40, 621–626.
Maerker, C., Schleyer, P.V., Liedl, K.R., Ha, T.K., Quack, M., Suhm, M.A., 1997. A critical analysis of electronic density functionals for structural, energetic, dynamic, and magnetic properties of hydrogen fluoride clusters. J. Comput. Chem. 18 (14), 1695–1719. Supp. Material ftp://wiley.com/public/journals/jcc/suppmat/18/1695 or http://journals.wiley.com/jcc.
Mamone, S., Concistrè, M., Carignani, E., Meier, B., Krachmalnicoff, A., Johannessen, O.G., Lei, X., Li, Y., Denning, M., Carravetta, M., Goh, K., Horsewill, A.J., Whitby, R.J., Levitt, M.H., 2014. Nuclear spin conversion of water inside fullerene cages detected by low-temperature nuclear magnetic resonance. J. Chem. Phys. 140, 194306.
Manca Tanner, C., Quack, M., Schmidiger, D., 2013. Nuclear spin symmetry conservation and relaxation in water ($^1H_2\ ^{16}O$) studied by cavity ring-down (CRD) spectroscopy of supersonic jets. J. Phys. Chem. A 117 (39), 10105–10118.
Manca Tanner, C., Quack, M., Schmidiger, D., 2018. Nuclear spin symmetry conservation and relaxation of water (H_2O) seeded in supersonic jets of argon and oxygen: measurements by cavity ring-down laser spectroscopy. Mol. Phys. 116, 3718–3730.
Manca, C., Quack, M., Willeke, M., 2008. Vibrational predissociation in hydrogen bonded dimers: the case of $(HF)_2$ and its isotopomers. Chimia 62 (4), 235–239.
Manning, M.F., 1935. Energy levels of a symmetrical double minima problem with applications to the NH_3 and ND_3 molecules. J. Chem. Phys. 3, 136–138.
Manthe, U., 2015. The multi-configurational time-dependent Hartree approach revisited. J. Chem. Phys. 142, 244109.
Marcus, R.A., 1964. Generalization of the activated-complex theory of reaction rates. I. Quantum mechanical treatment. J. Chem. Phys. 41, 2614–2623.
Marcus, R.A., 1965. Generalization of activated-complex theory. III. Vibrational adiabaticity, separation of variables, and a connection with analytical mechanics. J. Chem. Phys. 43, 1598–1605.
Marcus, R.A., Coltrin, M.E., 1977. A new tunneling path for reactions such as $H + H_2 \rightarrow H_2 + H$. J. Chem. Phys. 67, 2609–2613.
Mardyukov, A., Quanz, H., Schreiner, P.R., 2016. Conformer-specific hydrogen atom tunnelling in trifluoromethylhydroxycarbene. Nat. Chem. 9, 71–76.
Marquardt, R., Quack, M., 1989. Infrared-multiphoton excitation and wave packet motion of the harmonic and anharmonic-oscillators – exact-solutions and quasiresonant approximation. J. Chem. Phys. 90 (11), 6320–6327.
Marquardt, R., Quack, M., 2011. Global analytical potential energy surfaces for high resolution molecular spectroscopy and reaction dynamics. In: Quack, M., Merkt, F. (Eds.), Handbook of High-Resolution Spectroscopy, Vol. 1. Wiley, Chichester, New York, pp. 511–549 (Chapter 12).

Marquardt, R., Quack, M., 2020. Molecular Spectroscopy and Quantum Dynamics. Elsevier, Amsterdam. Chapter 1 (this book).

Marquardt, R., Quack, M., Thanopulos, I., Luckhaus, D., 2003a. A global electric dipole function of ammonia and isotopomers in the electronic ground state. J. Chem. Phys. 119 (20), 10724–10732.

Marquardt, R., Quack, M., Thanopulos, I., Luckhaus, D., 2003b. Tunneling dynamics of the NH chromophore in NHD_2 during and after coherent infrared excitation. J. Chem. Phys. 118 (2), 643–658.

Marquardt, R., Sagui, K., Klopper, W., Quack, M., 2005. Global analytical potential energy surface for large amplitude nuclear motions in ammonia. J. Phys. Chem. B 109 (17), 8439–8451.

Marquardt, R., Sagui, K., Zheng, J., Thiel, W., Luckhaus, D., Yurchenko, S., Mariotti, F., Quack, M., 2013. A global analytical potential energy surface for the electronic ground state of NH_3 from high level ab initio calculations. J. Phys. Chem. A 117 (32), 7502–7522.

Marx, D., 2006. Advanced Car-Parrinello techniques: path integrals and nonadiabaticity in condensed matter simulations. Lecture Notes in Phys. 704, 508–539.

Matsumoto, A., Ozaki, H., Harada, S., Tada, K., Ayugase, T., Ozawa, H., Kawasaki, T., Soai, K., 2016. Asymmetric induction by a nitrogen $^{14}N/^{15}N$ isotopomer in conjunction with asymmetric autocatalysis. Angew. Chem., Int. Ed. 55, 15472–15475.

Mátyus, E., Wales, D.J., Althorpe, S.C., 2016. Quantum tunneling splittings from path-integral molecular dynamics. J. Chem. Phys. 144, 114108.

Meier, K., Choutko, A., Dolenc, J., Eichenberger, A.P., Riniker, S., van Gunsteren, W.F., 2013b. Multi-resolution simulation of biomolecular systems: a review of methodological issues. Angew. Chem., Int. Ed. 52, 2820–2834.

Meier, B., Dumez, J.N., Stevanato, G., Hill-Cousins, J.T., Roy, S.S., Hakansson, P., Mamone, S., Brown, R.C.D., Pileio, G., Levitt, M.H., 2013a. Long-lived nuclear spin states in methyl groups and quantum-rotor-induced polarization. J. Am. Chem. Soc. 135, 18746–18749.

Meierhenrich, U., 2008. Aminoacids and Asymmetry of Life. Springer, Berlin.

Meisner, J., Kästner, J., 2016. Reaction rates and kinetic isotope effects of $H_2 + OH \rightarrow H_2O + H$. J. Chem. Phys. 144, 174303.

Meisner, J., Kästner, J., 2018. Dual-level approach to instanton theory. J. Chem. Theory Comput. 14, 1865–1872.

Mengesha, E.T., Zehnacker-Rentien, A., Sepio, J., Kijak, M., Waluk, J., 2015. Spectroscopic study of jet-cooled deuterated porphycenes: unusual isotopic effects on proton tunneling. J. Phys. Chem. B 119, 2193–2203.

Merkel, A., Zülicke, L., 1987. Nonempirical parameter estimate for the statistical adiabatic theory of unimolecular fragmentation. Mol. Phys. 60 (6), 1379–1393.

Merkt, F., Quack, M., 2011. Molecular quantum mechanics and molecular spectra, molecular symmetry, and interaction of matter with radiation. In: Quack, M., Merkt, F. (Eds.), Handbook of High-Resolution Spectroscopy, Vol. 1. Wiley, Chichester, New York, pp. 1–55 (Chapter 1). See also preface to this Handbook.

Merkt, F., Willitsch, S., Hollenstein, U., 2011. High-resolution photoelectron spectroscopy. In: Quack, M., Merkt, F. (Eds.), Handbook of High-Resolution Spectroscopy, Vol. 3. Wiley, Chichester, New York, pp. 1617–1654 (Chapter 44).

Merzbacher, E., 2002. The early history of quantum tunneling. Phys. Today 59, 44–49.

Meyer, R., 1970. Trigonometric interpolation method for one dimensional quantum mechanical problems. J. Chem. Phys. 52 (4), 2053–2059.

Meyer, H.-D., Gatti, F., Worth, G.A., 2009. Multidimensional Quantum Dynamics: MCTDH Theory and Applications. John Wiley-VCH, Weinheim.

Meyer, H.-D., Manthe, U., Cederbaum, L.S., 1990. The multiconfigurational time-dependent Hartree approach. Chem. Phys. Lett. 165 (1), 73–78.

Mielke, S.L., Garrett, B.C., Fleming, D.G., Truhlar, D.G., 2015. Zero-point energy, tunnelling, and vibrational adiabaticity in the Mu + H_2 reaction. Mol. Phys. 113, 160–175.

Miller, W.H., 1974. Classical-limit quantum mechanics and the theory of molecular collisions. Adv. Chem. Phys. 25, 69–177.

Miller, W.H., 1975a. The classical S-matrix in molecular collisions. Adv. Chem. Phys. 30, 77–136.

Miller, W.H., 1975b. Semiclassical limit of quantum mechanical transition state theory for nonseparable systems. J. Chem. Phys. 62 (1), 1899–1906.

Miller, W.H., 2014. A journey through chemical dynamics. Annu. Rev. Phys. Chem. 65, 1–19.

Miller, W.H., Handy, N.C., Adams, J.E., 1980. Reaction path Hamiltonian for polyatomic molecules. J. Chem. Phys. 72 (1), 99–112.

Mills, I., Quack, M., 2002. The symmetry groups of non-rigid molecules – introductory comment. Mol. Phys. 100 (1), 9–10.

Minissale, M., Congiu, E., Baouche, S., Chaabouni, H., Moudens, A., Dulieu, F., Accolla, M., Cazaux, S., Manicó, G., Pirronello, V., 2013. Quantum tunneling of oxygen atoms on very cold surfaces. Phys. Rev. Lett. 111, 053201.

Minissale, M., Congiu, E., Dulieu, F., 2014. Oxygen diffusion and reactivity at low temperature on bare amorphous olivine-type silicate. J. Chem. Phys. 140, 074705.

Miyamoto, Y., Tsubouchi, M., Momose, T., 2013. Infrared spectroscopy of chloromethyl radical in solid parahydrogen and its nuclear spin conversion. J. Phys. Chem. A 117, 9510–9517.

Morse, P.M., Stückelberg, E.C.G., 1931. Lösung des Eigenwertproblems eines Potentialfeldes mit zwei Minima. Helv. Phys. Acta 4, 337–354.

Moruzzi, G., Winnewisser, B.P., Winnewisser, M., Mukhopadhyay, I., Strumia, F., 2018. Microwave, Infrared and Laser Transitions in Methanol – Atlas of Assigned Lines from 0 to 1258 cm^{-1}, second ed., reprint after first (1995) ed. CRC Press, Boca Raton, FL.

Mukherjee, N., Perreault, W.E., Zare, R.N., 2017. Stark-induced adiabatic Raman ladder for preparing highly vibrationally excited quantum states of molecular hydrogen. J. Phys. B: At. Mol. Phys. 50, 144005.

Mukhopadhyay, A., Xantheas, S.S., Saykally, R.J., 2018. The water dimer II: theoretical investigations. Chem. Phys. Lett. 700, 163–175.

Müller-Dethlefs, K., Riese, M., 2011. Molecular clusters and noncovalent bonds probed by photoionization and photoelectron spectroscopy. In: Quack, M., Merkt, F. (Eds.), Handbook of High-Resolution Spectroscopy, Vol. 3. Wiley, Chichester, New York, pp. 1713–1740 (Chapter 56).

Nesbitt, D.J., 1994. High-resolution, direct laser absorption spectroscopy in slit supersonic jets: intermolecular forces and unimolecular vibrational dynamics in clusters. Annu. Rev. Phys. Chem. 45, 367–399.

Newton, R.R., Thomas, L.H., 1948. Internal molecular motions of large amplitude illustrated by the symmetrical vibration of ammonia. J. Chem. Phys. 16, 310–323.

Nguyen, N.T.T., Furukawa, H., Gándara, F., Nguyen, H.T., Cordova, K.E., Yaghi, O.M., 2014. Selective capture of carbon dioxide under humid conditions by hydrophobic chabazite-type zeolitic imidazolate frameworks. Angew. Chem., Int. Ed. 53, 10645–10648.

Nikitin, E.E., 1965. Statistical theory of endothermic reactions – Part 2. Monomolecular reactions. Teor. Eksp. Khim. 1, 90–94.

Nikitin, E.E., Troe, J., 2010a. Dynamics of ion-molecule complex formation at very low energies and temperatures. Phys. Chem. Chem. Phys. 7, 1540–1551.

Nikitin, E.E., Troe, J., 2010b. Mutual capture of dipolar molecules at low and very low energies. I. Approximate analytical treatment. J. Phys. Chem. A 114, 9762–9767.

Nimtz, G., 2011. Tunneling confronts special relativity. Found. Phys. 41, 1193–1199.

Nimtz, G., Haibel, A., 2004. Tunneleffekt – Räume ohne Zeit: Vom Urknall zum Wurmloch. John Wiley-VCH, Weinheim.

Nunes, C.M., Knezz, S.N., Reva, I., Fausto, R., McMahon, R.J., 2016. Evidence of a nitrene tunneling reaction: spontaneous rearrangement of 2-formyl phenylnitrene to an imino ketene in low-temperature matrixes. J. Am. Chem. Soc. 138, 15287–15290.

Oka, T., 2011. Orders of magnitude and symmetry in molecular spectroscopy. In: Quack, M., Merkt, F. (Eds.), Handbook of High-Resolution Spectroscopy, Vol. 1. Wiley, Chichester, New York, pp. 633–658 (Chapter 17).

Oppenheimer, J.R., 1928. Three notes on the quantum theory of aperiodic effects. Phys. Rev. 13, 66–81.

Ortlieb, M., Havenith, M., 2007. Proton transfer in $(HCOOH)_2$: an IR high-resolution spectroscopic study of the antisymmetric C-O stretch. J. Phys. Chem. A 111, 7355–7363.

Ospelkaus, S., Ni, K.K., Wang, D., de Miranda, M.H.G., Neyenhuis, B., Quéméner, G., Julienne, P.S., Bohn, J.L., Jin, D.S., Ye, J., 2010. Quantum-state controlled chemical reactions of ultracold potassium-rubidium molecules. Science 327, 853–857.

Ottinger, P., Leutwyler, S., 2012. Excitonic splitting and coherent electronic energy transfer in the gas-phase benzoic acid dimer. J. Chem. Phys. 137, 204303.

Ottinger, P., Leutwyler, S., Köppel, H., 2012. Vibrational quenching of excitonic splittings in H-bonded molecular dimers: the electronic Davydov splittings cannot match experiment. J. Chem. Phys. 136, 174308.

Paesani, F., 2016. Getting the right answers for the right reasons: toward predictive molecular simulations of water with many-body potential energy functions. Acc. Chem. Res. 49, 1844–1851.

Pechukas, P., Light, J.C., 1965. On detailed balancing and statistical theories of chemical kinetics. J. Chem. Phys. 42, 3281–3291.

Perreault, W.E., Mukherjee, N., Zare, R.N., 2017. Quantum control of molecular collisions at 1 Kelvin. Science 358, 356–359.

Perry, D.S., 2008. Torsion-vibration coupling in methanol: diabatic behavior in the CH overtone region. J. Phys. Chem. A 112, 215–223.

Perry, D.S., 2009. The adiabatic approximation as a diagnostic tool for torsion-vibration dynamics. J. Mol. Spectrosc. 257, 1–10.

Petersen, J., Pollak, E., 2017. Tunneling flight time, chemistry, and special relativity. J. Phys. Chem. Lett. 8, 4017–4022.

Petersen, J., Pollak, E., 2018. Quantum coherence in the reflection of above barrier wavepackets. J. Chem. Phys. 148, 074111.

Pfeiffer, P., 1983. Molecular structure derived from first-principles quantum mechanics: two examples. In: Hinze, J. (Ed.), Energy Storage and Redistribution in Molecules, Proc. of Two Workshops. Bielefeld, June 1980. Plenum Press, New York, pp. 315–326.

Pham, T., Forrest, K.A., Falcao, E.H.L., Eckert, J., Space, B., 2016a. Exceptional H_2 sorption characteristics in a Mg^{2+}-based metal-organic framework with small pores: insights from experimental and theoretical studies. Phys. Chem. Chem. Phys. 18, 1786–1796.

Pham, T., Forrest, K.A., Space, B., Eckert, J., 2016b. Dynamics of H_2 adsorbed in porous materials as revealed by computational analysis of inelastic neutron scattering spectra. Phys. Chem. Chem. Phys. 18, 17141–17158.

Piccini, G.M., Alessio, M., Sauer, J., 2018. Ab initio study of methanol and ethanol adsorption on Brœnsted sites in zeolite H-MFI. Phys. Chem. Chem. Phys. 20, 19964–19970.

Piecha-Bisiorek, A., Bator, G., Sawka-Dobrowolska, W., Sobczyk, L., Rok, M., Medycki, W., Schneider, G.J., 2014. Structure and tunneling splitting spectra of methyl groups of tetramethylpyrazine in complexes with chloranilic and bromanilic acids. J. Phys. Chem. A 118, 7159–7166.

Pine, A.S., Howard, B.J., 1986. Hydrogen bond energies of the HF and HCl dimers from absolute infrared intensities. J. Chem. Phys. 84, 590–596.

Pine, A.S., Lafferty, W.J., 1983. Rotational structure and vibrational predissociation in the HF stretching bands of the HF dimer. J. Chem. Phys. 78, 2154–2162.

Pine, A.S., Lafferty, W.J., Howard, B.J., 1984. Vibrational predissociation, tunneling, and rotational saturation in the HF and DF dimers. J. Chem. Phys. 81, 2939–2950.

Pittico, L., Schäfer, M., Merkt, F., 2012. Structure and dynamics of the electronically excited C_1 and D_0^+ states of ArXe from high-resolution vacuum ultraviolet spectra. J. Chem. Phys. 136, 074304.

Plazanet, M., Neumann, M.A., Trommsdorff, H.P., 2000. Methyl group rotational tunneling in vibrational spectra of crystals at low temperatures. Chem. Phys. Lett. 320, 651–657.

Polanyi, J.C., 1987. Some concepts in reaction dynamics (Nobel lecture). Angew. Chem., Int. Ed. 26, 952–971.

Pollak, E., 2017. Transition path time distribution, tunneling times, friction, and uncertainty. Phys. Rev. Lett. 116, 070401.

Pomerantz, A.E., Ausfelder, F., Zare, R.N., Althorpe, S.C., Aoiz, F.J., Banares, L., Castillo, J.F., 2004. Disagreement between theory and experiment in the simplest chemical reaction: collision energy dependent rotational distributions for $H + D_2 \rightarrow HD(v' = 3,J') + D$. J. Chem. Phys. 120, 3244–3255.

Poms, J., Hauser, A.W., Ernst, W.E., 2012. Helium nanodroplets doped with xenon and rubidium atoms: a case study of Van der Waals interactions between heliophilic and heliophobic dopants. Phys. Chem. Chem. Phys. 14, 15158–15165.

Potapov, A., Asselin, P., 2014. High-resolution jet spectroscopy of weakly bound binary complexes involving water. Int. Rev. Phys. Chem. 33, 275–300.

Powers, A., Marsalek, O., Xu, M., Ulivi, L., Colognesi, D., Tuckerman, M.E., Bačić, Z., 2016. Impact of the condensed-phase environment on the translation-rotation eigenstates and spectra of a hydrogen molecule in clathrate hydrates. J. Phys. Chem. Lett. 7, 308–313.

Prager, M., Heidemann, A., 1997. Rotational tunneling and neutron spectroscopy: a compilation. Chem. Rev. 97, 2933–2966.

Pratt, D.W., 2011. Electronic spectroscopy in the gas phase. In: Quack, M., Merkt, F. (Eds.), Handbook of High-Resolution Spectroscopy, Vol. 2. Wiley, Chichester, New York, pp. 1291–1320 (Chapter 34).

Prelog, V., Wieland, P., 1944. Über die Spaltung der Trögerschen Base in optisehe Antipoden, ein Beitrag zur Stereochemie des dreiwertigen Stickstoffs. Helv. Chim. Acta 27, 1127–1134.

Prentner, R., Quack, M., Stohner, J., Willeke, M., 2015. Wavepacket dynamics of the axially chiral molecule Cl-O-O-Cl under coherent radiative excitation and including electroweak parity violation. J. Phys. Chem. A 119 (51), 12805–12822.

Press, W., 1981. Single-Particle Rotations in Molecular Crystals. Springer Tracts in Modern Physics, vol. 92. Springer, Berlin, Heidelberg.

Primas, H., 1981. Chemistry, Quantum Mechanics and Reductionism: Perspectives in Theoretical Chemistry. Springer, Berlin.

Pylaeva, S., Allolio, S., Koeppe, B., Gleb, S., Denisov, G.S., Limbach, H.-H., Sebastianid, D., Tolstoy, P.M., 2015. Proton transfer in a short hydrogen bond caused by solvation shell fluctuations: an ab initio MD and NMR/UV study of an $(OHO)^-$ bonded system. Mol. Phys. 114, 2251–2262.

Qu, C., Bowman, J.M., 2013. Full-dimensional, ab initio potential energy surface for $CH_3OH \rightarrow CH_3$+OH. Mol. Phys. 111, 1964–1971.

Qu, C., Bowman, J.M., 2016. An ab initio potential energy surface for the formic acid dimer: zero-point energy, selected anharmonic fundamental energies, and ground-state tunneling splitting calculated in relaxed 1-4-mode subspaces. Phys. Chem. Chem. Phys. 18, 24835–24840.

Quack, M., 1977. Detailed symmetry selection-rules for reactive collisions. Mol. Phys. 34 (2), 477–504.

Quack, M., 1978. Theory of unimolecular reactions induced by monochromatic infrared radiation. J. Chem. Phys. 69 (3), 1282–1307.

Quack, M., 1979. Quantitative comparison between detailed (state selected) relative rate data and averaged (thermal) absolute rate data for complex-forming reactions. J. Phys. Chem. 83 (1), 150–158.

Quack, M., 1980. Statistical models for product energy distributions in bimolecular reactions with metastable intermediates. Chem. Phys. 51, 353–367.

Quack, M., 1981. Statistical-mechanics and dynamics of molecular fragmentation. Nuovo Cimento Soc. Ital. Fis. B 63 (1), 358–377.

Quack, M., 1985. On the densities and numbers of rovibronic states of a given symmetry species: rigid and nonrigid molecules, transition states, and scattering channels. J. Chem. Phys. 82 (7), 3277–3283.

Quack, M., 1986. On the measurement of the parity violating energy difference between enantiomers. Chem. Phys. Lett. 132, 147–153.

Quack, M., 1989. Structure and dynamics of chiral molecules. Angew. Chem., Int. Ed. 28 (5), 571–586. Angew. Chem. 101, 1989 588–604.

Quack, M., 1990. The role of quantum intramolecular dynamics in unimolecular reactions. Philos. Trans. R. Soc. Lond. A 332 (1625), 203–220.

Quack, M., 1999. Intramolekulare Dynamik: Irreversibilität, Zeitumkehrsymmetrie und eine absolute Moleküluhr. Nova Acta Leopoldina 81 (Neue Folge 314), 137–173.

Quack, M., 2001. Molecules in motion. Chimia 55, 753–758.

Quack, M., 2002. How important is parity violation for molecular and biomolecular chirality? Angew. Chem., Int. Ed. 41, 4618–4630. Angew. Chem. 114, 2002 4812–4825.

Quack, M., 2003. Molecular spectra, reaction dynamics, symmetries and life. Chimia 57 (4), 147–160.

Quack, M., 2004. Time and time reversal symmetry in quantum chemical kinetics. In: Brändas, E.J., Kryachko, E.S. (Eds.), Fundamental World of Quantum Chemistry. A Tribute to the Memory of Per-Olov Löwdin, Vol. 3. Kluwer Academic Publishers, Dordrecht, pp. 423–474.

Quack, M., 2006. Electroweak quantum chemistry and the dynamics of parity violation. In: Naidoo, K.J., Brady, J., Field, M.J., Gao, J., Hann, M. (Eds.), Modelling Molecular Structure and Reactivity. Royal Society of Chemistry, Cambridge.

Quack, M., 2011a. Frontiers in spectroscopy (concluding paper to Faraday discussion 150. Faraday Discuss. Chem. Soc. 150, 533–565.

Quack, M., 2011b. Fundamental symmetries and symmetry violations from high resolution spectroscopy. In: Quack, M., Merkt, F. (Eds.), Handbook of High Resolution Spectroscopy, Vol. 1. Wiley, Chichester, New York, pp. 659–722 (Chapter 18).

Quack, M., 2014. The concept of law and models in chemistry. Eur. Rev. 22, S50–S86.

Quack, M., 2015a. Die Spiegelsymmetrie des Raumes und die Chiralität in Chemie, Physik, und in der biologischen Evolution. Nova Acta Leopoldina NF 127 (412), 19 and pp. 119–166 (English summary p. 33).

Quack, M., 2015b. On biomolecular homochirality as a quasi-fossil of the evolution of life. Adv. Chem. Phys. 157, 249–290 (Chapter 18).

Quack, M., Jans-Bürli, S., 1986. Molekulare Thermodynamik und Kinetik, Vol. 1. Vd F Publishers, Zürich, pp. A61–A71.

Quack, M., Merkt, F. (Eds.), 2011. Handbook of High-Resolution Spectroscopy. John Wiley, New York (3 volumes).

Quack, M., Schmitt, U., Suhm, M.A., 1993a. Evidence for the $(HF)_5$ complex in the HF stretching FTIR absorption-spectra of pulsed and continuous supersonic jet expansions of hydrogen-fluoride. Chem. Phys. Lett. 208 (5–6), 446–452.

Quack, M., Schmitt, U., Suhm, M.A., 1997. FTIR spectroscopy of hydrogen fluoride clusters in synchronously pulsed supersonic jets. Isotopic isolation, substitution and 3-d condensation. Chem. Phys. Lett. 269 (1–2), 29–38. Also: J. Aerosol Sci. 28 (Supplement) (1997) 363–364.

Quack, M., Stockburger, M., 1972. Resonance fluorescence of aniline vapor. J. Mol. Spectrosc. 43 (1), 87–116.

Quack, M., Stohner, J., 2000. Influence of parity violating weak nuclear potentials on vibrational and rotational frequencies in chiral molecules. Phys. Rev. Lett. 84 (17), 3807–3810.

Quack, M., Stohner, J., Suhm, M.A., 1993b. Vibrational dynamics of $(HF)_n$ aggregates from an ab initio based analytical $(1+2+3)$-body potential. J. Mol. Struct. 294, 33–36.

Quack, M., Stohner, J., Suhm, M.A., 2001. Analytical three-body interaction potentials and hydrogen bond dynamics of hydrogen fluoride aggregates, $(HF)_n$, $n \geq 3$. J. Mol. Struct. 599 (1–3), 381–425.

Quack, M., Stohner, J., Willeke, M., 2008. High-resolution spectroscopic studies and theory of parity violation in chiral molecules. Annu. Rev. Phys. Chem. 59, 741–769.

Quack, M., Suhm, M.A., 1991a. Potential energy surfaces, quasi-adiabatic channels, rovibrational spectra, and intramolecular dynamics of $(HF)_2$ and its isotopomers from quantum Monte Carlo calculations. J. Chem. Phys. 95 (1), 28–59.

Quack, M., Suhm, M.A., 1991b. Quasi-adiabatic channels and effective transition-state barriers for the disrotatory in-plane hydrogen-bond exchange motion in $(HF)_2$. Chem. Phys. Lett. 183 (3–4), 187–194.

Quack, M., Suhm, M.A., 1995. Accurate quantum Monte-Carlo calculations of the tunneling splitting in $(HF)_2$ on a 6-dimensional potential hypersurface. Chem. Phys. Lett. 234 (1–3), 71–76.

Quack, M., Suhm, M.A., 1997. Potential energy hypersurfaces for hydrogen bonded clusters $(HF)_n$. In: Kryachko, E.S., Calais, J.L. (Eds.), Conceptual Perspectives in Quantum Chemistry. Kluwer, Dordrecht, pp. 415–463.

Quack, M., Suhm, M.A., 1998. Spectroscopy and quantum dynamics of hydrogen fluoride clusters. In: Bačić, Z., Bowman, J. (Eds.), Advances in Molecular Vibrations and Collision Dynamics, Vol. 3, Molecular Clusters. JAI Press Inc., Stamford, Conn. and London, England, pp. 205–248.

Quack, M., Sutcliffe, E., 1985. On the validity of the quasiresonant approximation for molecular infrared-multiphoton excitation. J. Chem. Phys. 83 (8), 3805–3812.

Quack, M., Sutcliffe, B.T., 1986. URIMIR: programs for the calculation of the quantum dynamics of IR multiphoton excitation and dissociation (unimolecular reactions induced by monochromatic infrared radiation), quantum chemistry program exchange, program 515. QCPE Bull. 6, 98. Extended and updated in: Marquardt, R., Quack, M., Stohner, J., Thanopulos, I., Quantum dynamics of the iodine atom in a strong laser field as calculated with the URIMIR package, Mol. Phys. 117 (2019) 3132–3147.

Quack, M., Troe, J., 1974. Specific rate constants of unimolecular processes: statistical adiabatic channel model. Ber. Bunsenges. Phys. Chem. 78, 240–252.

Quack, M., Troe, J., 1975a. Complex formation in reactive and inelastic scattering. Ber. Bunsenges. Phys. Chem. 79, 170–183.

Quack, M., Troe, J., 1975b. Product state distributions after dissociation. Ber. Bunsenges. Phys. Chem. 79, 469–475.

Quack, M., Troe, J., 1976. Information, memory and statistical theories of elementary chemical reactions. Ber. Bunsenges. Phys. Chem. 80, 1140–1149.

Quack, M., Troe, J., 1977a. Maximum free energy criterion for the high pressure limit of dissociation reactions. Ber. Bunsenges. Phys. Chem. 81, 329–337.

Quack, M., Troe, J., 1977b. Unimolecular Reactions and Energy Transfer of Highly Excited Molecules, Vol. 2. The Chemical Society, London, pp. 175–238.

Quack, M., Troe, J., 1977c. Vibrational-relaxation of diatomic-molecules in complex-forming collisions with reactive atoms. Ber. Bunsenges. Phys. Chem. 81 (2), 160–162.

Quack, M., Troe, J., 1981. Statistical methods in scattering. In: Henderson, D. (Ed.), Theoretical Chemistry: Advances and Perspectives (Theory of Scattering, Papers in Honor of Henry Eyring), Vol. 6B. Academic Press, New York, pp. 199–276.

Quack, M., Troe, J., 1998. Statistical adiabatic channel model. In: von Ragué Schleyer, P., Allinger, N., Clark, T., Gasteiger, J., Kollman, P.A., Schaefer III, H.F., Schreiner, P.R. (Eds.), Encyclopedia of Computational Chemistry, Vol. 4. John Wiley and Sons, pp. 2708–2726.

Quack, M., Willeke, M., 1999. Ab initio calculations for the anharmonic vibrational resonance dynamics in the overtone spectra of the coupled OH and CH chromophores in CD_2H-OH. J. Chem. Phys. 110 (24), 11958–11970.

Quack, M., Willeke, M., 2006. Stereomutation tunneling switching dynamics and parity violation in chlorineperoxide Cl–O–O–Cl. J. Phys. Chem. A 110 (9), 3338–3348.

Reiher, M., Wolf, A., 2009. Relativistic Quantum Chemistry: The Fundamental Theory of Molecular Science, first ed. Wiley-VCH, Weinheim.

Reiss, H.R., 2014. The tunnelling model of laser-induced ionization and its failure at low frequencies. J. Phys. B: At. Mol. Phys. 47, 204006.

Reva, I., Nunes, C.M., Biczysko, M., Fausto, R., 2015. Conformational switching in pyruvic acid isolated in Ar and N_2 matrixes: spectroscopic analysis, anharmonic simulation, and tunneling. J. Phys. Chem. A 119, 2614–2627.

Rice, S.A., 1975. Some comments on the dynamics of primary photochemical processes. In: Lim, E.C. (Ed.), Excited States, Vol. 2. Elsevier Inc., Amsterdam, pp. 111–320.

Richard, R.M., Lao, K.U., Herbert, J.M., 2014. Aiming for benchmark accuracy with the many-body expansion. Acc. Chem. Res. 47, 2828–2836.

Richardson, J.O., 2016. Derivation of instanton rate theory from first principles. J. Chem. Phys. 144, 114106.

Richardson, J.O., 2018. Ring-polymer instanton theory. Int. Rev. Phys. Chem. 37, 171–216.

Richardson, J.O., Althorpe, S.C., 2009. Ring-polymer molecular dynamics rate-theory in the deep-tunneling regime: connection with semiclassical instanton theory. J. Chem. Phys. 131, 214106.

Richardson, J.O., Althorpe, S.C., 2011. Ring-polymer instanton method for calculating tunneling splittings. J. Chem. Phys. 134, 054109.

Richardson, J.O., Althorpe, S.C., Wales, D.J., 2011. Instanton calculations of tunneling splittings for water dimer and trimer. J. Chem. Phys. 135, 124109.

Richardson, J.O., Bauer, R., Thoss, T., 2015. Semiclassical Green's functions and an instanton formulation of electron-transfer rates in the nonadiabatic limit. J. Chem. Phys. 143, 134115.

Richardson, J.O., Pérez, C., Lobsinger, S., Reid, A.A., Temelso, B., Shields, G.C., Kisiel, Z., Wales, D.J., Pate, B.H., Althorpe, S.C., 2016. Concerted hydrogen-bond breaking by quantum tunneling in the water hexamer prism. Science 351, 1310–1314.

Richardson, J.O., Wales, D.J., Althorpe, S.C., McLaughlin, R.P., Viant, M.R., Shih, O., Saykally, R.J., 2013. Investigation of terahertz vibration-rotation tunneling spectra for the water octamer. J. Phys. Chem. A 117, 6960–6966.

Riniker, S., Allison, J.A., van Gunsteren, W.F., 2012. On developing coarse-grained models for biomolecular simulation: a review. Phys. Chem. Chem. Phys. 14, 12423–12430.

Rommel, J.P., Goumans, T.M., Kästner, J., 2011. Locating instantons in many degrees of freedom. J. Chem. Theory Comput. 7, 690–698.

Roston, D., Islam, Z., Kohen, A., 2014. Kinetic isotope effects as a probe of hydrogen transfers to and from common enzymatic cofactors. Arch. Biochem. Biophys. 544, 96–104.

Roston, D., Kohen, A., 2013. A critical test of the "tunneling and coupled motion" concept in enzymatic alcohol oxidation. J. Am. Chem. Soc. 135, 13624–13627.

Ruiz-Pernía, J.J., Luk, L.Y.P., Garcia-Meseguer, R., Marti, S., Loveridge, E.J., Tunón, I., Moliner, V., Allemann, R.K., 2013. Increased dynamic effects in a catalytically compromised variant of escherichia coli dihydrofolate reductase. J. Am. Chem. Soc. 135, 18689–18696.

Rungtaweevoranit, B., Baek, J., Araujo, J.R., Archanjo, B.S., Choi, K.M., Yaghi, O.M., Somorjai, G.A., 2016. Asymmetric autocatalysis triggered by carbon isotope ($^{13}C/^{12}C$) chirality. Nano Lett. 16, 7645–7649.

Rutherford, E., 1900. Radioactive substance emitted from thorium compounds. Philos. Mag. 49 (1).

Sala, M., Guérin, S., Gatti, F., Marquardt, R., Meyer, H.-D., 2012. Laser-induced enhancement of tunneling in NHD_2. J. Chem. Phys. 113, 194308.

Sarka, J., Császár, A.G., 2016. Interpretation of the vibrational energy level structure of the astructural molecular ion H_5^+ and all of its deuterated isotopomers. J. Chem. Phys. 18, 154309.

Sarka, J., Császár, A.G., Althorpe, S.A., Wales, D.J., Mátyus, E., 2016a. Rovibrational transitions of the methane–water dimer from intermolecular quantum dynamical computations. Phys. Chem. Chem. Phys. 18, 22816–22826.

Sarka, J., Lauvergnat, D., Brites, V., Császár, A.G., Léonard, C., 2016b. Rovibrational energy levels of the $F^-(H_2O)$ and $F^-(D_2O)$ complexes. Phys. Chem. Chem. Phys. 18, 17678–17690.

Sato, I., Urabe, H., Saori, I., Ishiguro, S., Shibata, T., Soai, K., 2003. Amplification of chirality from extremely low to greater than 99.5% ee by asymmetric autocatalysis. Angew. Chem., Int. Ed. 42, 315–317.

Sauer, J., 2016. Broensted activity of two-dimensional zeolites compared to bulk materials. Faraday Discuss. Chem. Soc. 188, 227–234.

Sauer, J., Freund, H.J., 2015. Models in catalysis. Catal. Lett. 145, 109–125.

Schmitt, M., Meerts, W.L., 2011. Rotationally resolved electronic spectroscopy and automatic assignment techniques using evolutionary algorithms. In: Quack, M., Merkt, F. (Eds.), Handbook of High-Resolution Spectroscopy, Vol. 2. Wiley, Chichester, New York, pp. 1345–1372 (Chapter 36).

Schnell, M., 2011. Group theory for high-resolution spectroscopy of nonrigid molecules. In: Quack, M., Merkt, F. (Eds.), Handbook of High-Resolution Spectroscopy, Vol. 1. Wiley, Chichester, New York, pp. 607–623 (Chapter 16).

Schnitzler, E.G., Jäger, W., 2014. The benzoic acid–water complex: a potential atmospheric nucleation precursor studied using microwave spectroscopy and ab initio calculations. Phys. Chem. Chem. Phys. 16, 2305–2314.

Schoedel, A., Ji, Z., Yaghi, O.M., 2016. The role of metal-organic frameworks in a carbon-neutral energy cycle. Nat. Energy 1, 16034–16046.

Schopper, H., 1957. Circular polarization of gamma rays – further proof for parity-failure in beta decay. Philos. Mag. 2, 710–713.

Schottky, W., 1931. Leitungs- und Photoeffekte an Sperrschichten. Z. Phys. 32, 833–842.

Schreiner, P.R., 2017. Tunneling control of chemical reactions: the third reactivity paradigm. J. Am. Chem. Soc. 139, 15276–15283.

Schreiner, P.R., Reisenauer, H.P., Ley, D., Gerbig, D., Wu, C.H., Allen, W.D., 2011. Methylhydroxycarbene: tunneling control of a chemical reaction. Science 332, 1300–1303.

Schreiner, P.R., Wagner, J.P., Reisenauer, H.P., Gerbig, D., Ley, D., Sarka, J., Császár, A.G., Vaughn, A., Allen, W.D., 2015. Domino tunneling. J. Am. Chem. Soc. 137, 7828–7834.

Schulenburg, A.M., Merkt, F., 2010. Internal rotation in Jahn–Teller coupled systems: the ethene and allene cations. Chem. Phys. 377, 66–77.

Schultz, A., Cruse, H.W., Zare, R.N., 1972. Laser-induced fluorescence: a method to measure the internal state distribution of reaction products. J. Chem. Phys. 57, 1354–1355.

Seyfang, G., Quack, M., 2018. Atomare und molekulare Tunnelprozesse. Nachr. Chem. 66, 307–315.

Shan, X., Burd, T.A.H., Clary, D.C., 2019. New developments in semiclassical transition-state theory. J. Phys. Chem. A 123, 4639–4657.

Shenderovich, I.G., Lesnichin, S.B., Tu, C., Silverman, D.N., Tolstoy, P.M., Denisov, G.S., Limbach, H.-H., 2015. NMR studies of active-site properties of human carbonic anhydrase II by using ^{15}N-labeled 4-methylimidazole as a local probe and histidine hydrogen-bond correlations. Chem. Eur. J. 21, 2915–2929.

Shipman, S.T., Pate, B.H., 2011. New techniques in microwave spectroscopy. In: Quack, M., Merkt, F. (Eds.), Handbook of High-Resolution Spectroscopy, Vol. 2. Wiley, Chichester, New York, pp. 801–827 (Chapter 20).

Shubert, V.A., Schmitz, D., Schnell, M., 2013. Communication through the phenyl ring: internal rotation and nuclear quadrupole splitting in p-halotoluenes. Mol. Phys. 111, 2189–2197.

Signorell, R., Merkt, F., 2000. PFI-ZEKE photoelectron spectra of the methane cation and the dynamic Jahn-Teller effect. Faraday Discuss. Chem. Soc. 115, 205–228.

Signorell, R., Sommavilla, M., Merkt, F., 1999. Jahn–Teller distortion in $CD_2H_2^+$ from a rotationally resolved photoelectron spectrum. Chem. Phys. Lett. 312, 139–148.

Simmen, B., Mátyus, E., Reiher, M., 2013. Elimination of the translational kinetic energy contamination in pre-Born–Oppenheimer calculations. Mol. Phys. 111, 2086–2092.

Smith, I.W.M., 2006. Reactions at very low temperatures: gas kinetics at a new frontier. Angew. Chem., Int. Ed. 45, 2842–2861.

Snels, M., Fusina, L., Hollenstein, H., Quack, M., 2000. The ν_1 and ν_3 bands of ND_3. Mol. Phys. 98 (13), 837–854.

Snels, M., Hollenstein, H., Quack, M., 2003. The NH and ND stretching fundamentals of $^{14}ND_2H$. J. Chem. Phys. 119 (15), 7893–7902.

Snels, M., Hollenstein, H., Quack, M., 2006a. Mode selective tunneling dynamics observed by high resolution spectroscopy of the bending fundamentals of $^{14}NH_2D$ and $^{14}ND_2H$. J. Chem. Phys. 125, 194319.

Snels, M., Hollenstein, H., Quack, M., 2006b. The NH and ND stretching fundamentals of $^{14}NH_2D$. J. Mol. Spectros. 237 (2), 143–148.

Snels, M., Horká-Zelenková, V., Hollenstein, H., Quack, M., 2011. High resolution FTIR and diode laser spectroscopy of supersonic jets. In: Quack, M., Merkt, F. (Eds.), Handbook of High Resolution Spectroscopy; High Resolution FTIR and Diode Laser Spectroscopy of Supersonic Jets, Vol. 2. Wiley, Chichester, New York, pp. 1021–1067 (Chapter 27).

Soai, K., Shibata, T., Morioka, H., Choji, K., 1995. Asymmetric autocatalysis and amplification of enantiomeric excess of a chiral molecule. Nature 373, 767–768.

Song, L., Kästner, J., 2016. Formation of the prebiotic molecule NH_2CHO on astronomical amorphous solid water surfaces: accurate tunneling rate calculations. Phys. Chem. Chem. Phys. 18, 29278–29285.

Sprecher, D., Beyer, M., Merkt, F., 2013. Precision measurement of the ionisation energy of the $3d\sigma$ GK state of H_2. Mol. Phys. 111, 2100–2107.

Stocker, T.F., Johnson, E.R., 1991. The trapping and scattering of topographic waves by estuaries and headlands. J. Fluid Mech. 222, 501–524.

Stohner, J., Quack, M., 2011. Conventions, symbols, quantities, units and constants for high resolution molecular spectroscopy. In: Quack, M., Merkt, F. (Eds.), Handbook of High-Resolution Spectroscopy, Vol. 1. Wiley, Chichester, New York, pp. 263–324 (Chapter 5).

Stratt, R.M., Handy, N.C., Miller, W.H., 1979. On the quantum mechanical implications of classical ergodicity. J. Chem. Phys. 71, 3311–3322.

Swalen, J.D., Ibers, J.A., 1962. Potential function for the inversion of ammonia. J. Chem. Phys. 36, 1914–1918.

Tan, X.Q., Majewski, W.A., Plusquellic, D.F., Pratt, D.W., 1989. Methyl torsional barriers in different electronic states. Simultaneous determination from the rotationally resolved fluorescence excitation spectrum of a large molecule. J. Chem. Phys. 90, 2521–2522.

Tan, X.Q., Majewski, W.A., Plusquellic, D.F., Pratt, D.W., 1991. Methyl group torsional dynamics from rotationally resolved electronic spectra. 1- and 2-methylnaphthalene. J. Chem. Phys. 94, 7721–7733.

Tanaka, K., Harada, K., Endo, Y., 2019. FTMW Spectroscopy of ^{13}C-Tropolone. In: Proc. HRMS. Dijon.

Tanaka, K., Harada, K., Yamada, K.M.T., 2011. THz and submillimeter-wave spectroscopy of molecular complexes. In: Quack, M., Merkt, F. (Eds.), Handbook of High-Resolution Spectroscopy, Vol. 2. Wiley, Chichester, New York, pp. 853–896 (Chapter 22).

Tanaka, K., Honjo, H., Tanaka, T., Kohguchi, H., Ohshima, Y., Endo, Y., 1999. Determination of the proton tunneling splitting of tropolone in the ground state by microwave spectroscopy. J. Chem. Phys. 110, 1969–1978.

Tautermann, C.S., Voegele, A.F., Loerting, T., Liedl, K.R., 2002. The optimal tunneling path for the proton transfer in malonaldehyde. J. Chem. Phys. 117, 1962–1966.

Telle, H.R., Steinmeyer, G., Dunlop, A.E., Stenger, J., Sutter, D.H., Keller, U., 1999. Carrier-envelope offset phase control: a novel concept for absolute optical frequency measurement and ultrashort pulse generation. Appl. Phys. B 69, 327–332.

Tennyson, J., 2011. High accuracy rotation-vibration calculations on small molecules. In: Quack, M., Merkt, F. (Eds.), Handbook of High-Resolution Spectroscopy, Vol. 1. Wiley, Chichester, New York, pp. 551–572 (Chapter 13).

Thomas, J., Liu, X., Jäger, W., Xu, Y., 2015. Unusual H-bond topology and bifurcated H-bonds in the 2-fluoroethanol trimer. Angew. Chem., Int. Ed. 54, 11711–11715.

Toh, S.Y., Djuricanin, P., Momose, T., Miyazaki, J., 2015. UV photochemistry of benzene and cyclohexadienyl radical in solid parahydrogen. J. Phys. Chem. A 119, 2683–2691.

Tomaselli, M., Degen, C., Meier, B.H., 2003. Haupt magnetic double resonance. J. Chem. Phys. 118, 8559–8562.

Tomaselli, M., Meier, U., Meier, B.H., 2004. Tunneling-induced spin alignment at low and zero field. J. Chem. Phys. 120, 4051–4054.

Townes, C.H., 1964. Production of coherent radiation by atoms and molecules. The Noble Foundation, Stockholm.

Townes, C.H., 1965. Production of coherent radiation by atoms and molecules. Science 149, 831–841.

Townes, C.H., Schawlow, A.L., 1975. Microwave Spectroscopy. Dover Books, New York. Corrected republication of the first edition, McGraw-Hill, 1955.

Troe, J., 1987. Statistical adiabatic channel model for ion-molecule capture processes. J. Chem. Phys. 87, 2773–2780.

Troe, J., 1992. Statistical aspects of ion-molecule reactions. Adv. Chem. Phys. 82, 485–529.

Troe, J., 1996. Statistical adiabatic channel model for ion-molecule capture processes II. Analytical treatment of ion-dipole capture. J. Chem. Phys. 105, 6249–6262.

Truhlar, D.G., Garrett, B.C., 1984. Variational transition-state theory. Annu. Rev. Phys. Chem. 35, 159–189.

Truhlar, D.G., Garrett, B.C., Klippenstein, S.J., 1996. Current status of transition-state theory. J. Phys. Chem. 100, 12771–12800.

Tuma, C., Sauer, J., 2015. Quantum chemical ab initio prediction of proton exchange barriers between CH_4 and different H-zeolites. J. Chem. Phys. 143, 102810.

Uy, D., Cordonnier, M., Oka, T., 1997. Observation of ortho-para H_3^+ selection rules in plasma chemistry. Phys. Rev. Lett. 78, 3844–3847.

Vaillant, C.L., Wales, D.J., Althorpe, S.C., 2018. Tunneling splittings from path-integral molecular dynamics using a Langevin thermostat. J. Chem. Phys. 148, 234102.

van Gunsteren, W.F., Bakowies, D., Baron, R., Chandrasekhar, I., Christen, M., Daura, X., Gee, P., Geerke, D.P., Glättli, A., Hünenberger, P.H., Kastenholz, M.A., Oostenbrink, C., Schenk, M., Trzesniak, D., an der Vegt, N.F.A., Yu, H.B., 2006. Biomolecular modeling: goals, problems, perspectives. Angew. Chem., Int. Ed. 45, 4064–4092.

Vandemaele, G., Coppens, P., Van Gerven, L., 1986. New method to study spin conversion of a nuclear-spin rotor with low tunnei splitting. Phys. Rev. Lett. 56, 1202–1205.

Vasilatou, K., Schäfer, M., Merkt, F., 2010. The rotational structure of the origin band of the pulsed-field-ionization, zero-kinetic-energy photoelectron spectra of propene-H_6 and propene-D_6. J. Phys. Chem. A 114, 11085–11090.

Veillard, A., Lehn, J.M., Munsch, B., 1968. An ab initio SCF-LCAO-MO study of the nitrogen inversion barriers in ammonia and in ethylenimine. Theor. Chim. Acta 9, 275–277.

Vilenkin, A., 1988. Quantum cosmology and the initial state of the Universe. Phys. Rev. D 37, 888–897.

Vissers, G.W.M., Groenenboom, G.C., van der Avoird, A., 2003. Spectrum and vibrational predissociation of the HF dimer. I. Bound and quasibound states. J. Chem. Phys. 119, 277–285.

von Puttkamer, K., Quack, M., 1985. High-resolution FTIR overtone spectra and hydrogen-bond dissociation dynamics in $(HF)_2$. Chimia 39 (11), 358–360.

von Puttkamer, K., Quack, M., 1987. High-resolution interferometric FTIR spectroscopy of $(HF)_2$ - analysis of a low-frequency fundamental near 400 cm^{-1}. Mol. Phys. 62 (5), 1047–1064.

von Puttkamer, K., Quack, M., 1989. Vibrational-spectra of $(HF)_2$, $(HF)_n$ and their D-isotopomers – mode selective rearrangements and nonstatistical unimolecular decay. Chem. Phys. 139 (1), 31–53.

von Puttkamer, K., Quack, M., Suhm, M.A., 1988. Observation and assignment of tunnelling rotational transitions in the far infrared-spectrum of $(HF)_2$. Mol. Phys. 65 (5), 1025–1045.

Wagner, J.P., Reisenauer, H.P., Hirvonen, V., Wu, C.-H., Tyberg, J.L., Allen, W.D., Schreiner, P.R., 2016. Tunnelling in carbonic acid. Chem. Commun. 52, 7858–7861.

Wall, F.T., Glockler, G., 1937. The double minimum problem applied to the ammonia molecules. J. Chem. Phys. 5, 314–315.

Waluk, J., 2017. Spectroscopy and tautomerization studies of porphycenes. Chem. Rev. 117, 2447–2480.

Wang, Y., Bowman, J.M., 2013. Mode-specific tunneling using the Q_{im} path: theory and an application to full-dimensional malonaldehyde. J. Chem. Phys. 139, 154303.

Wang, X., Perry, D.S., 1998. An internal coordinate model of coupling between the torsion and C-H vibrations in methanol. J. Chem. Phys. 109, 10795–10805.

Warshel, A., 2014. Multiscale modeling of biological functions: from enzymes to molecular machines (Nobel lecture). Angew. Chem., Int. Ed. 53, 10020–10031.

Weber, B., Nagata, Y., Ketzetzi, S., Tang, F., Smit, W.J., Bakker, H.J., Backus, E.H.G., Bonn, M., Bonn, D., 2018. Molecular insight into the slipperiness of ice. J. Phys. Chem. Lett. 9, 2838–2842.

Wentzel, G., 1926. Eine Verallgemeinerung der Quantenbedingungen für die Zwecke der Wellenmechanik. Z. Phys. 38, 518–529.

Wichmann, G., Miloglyadov, E., Seyfang, G., Quack, M., 2020. Nuclear spin symmetry conservation studied by cavity ring-down spectroscopy of ammonia in a seeded supersonic jet from a pulsed slit nozzle. Mol. Phys., e1752946. https://doi.org/10.1080/00268976.2020.1752946.

Wigner, E., 1932. Über das Überschreiten der Potentialschwelle bei chemischen Reaktionen. Z. Phys. Chem. B 19, 203–216.

Wigner, E., 1938. The transition state method. Trans. Faraday Soc. 34, 29–41.

Willitsch, S., 2011. Experimental methods in cation spectroscopy. In: Quack, M., Merkt, F. (Eds.), Handbook of High-Resolution Spectroscopy, Vol. 3. Wiley, Chichester, New York, pp. 1691–1712 (Chapter 46).

Wolfrum, J., 2001. Advanced laser spectroscopy in combustion chemistry: from elementary steps to practical devices. Faraday Discuss. Chem. Soc. 119, 1–26.

Wong, Y.T.A., Toh, S.Y., Djuricanin, P., Momose, T., 2015. Conformational composition and population analysis of β-alanine isolated in solid parahydrogen. J. Mol. Spectrosc. 310, 23–31.

Wörner, H.J., Corkum, P.B., 2011. Attosecond spectroscopy. In: Quack, M., Merkt, F. (Eds.), Handbook of High-Resolution Spectroscopy, Vol. 3. Wiley, Chichester, New York, pp. 1781–1804 (Chapter 49).

Wörner, H.J., Merkt, F., 2009. Jahn–Teller effects in molecular cations studied by photoelectron spectroscopy and group theory. Angew. Chem., Int. Ed. 48, 6404–6424.

Wörner, H.J., Merkt, F., 2011. Fundamentals of electronic spectroscopy. In: Quack, M., Merkt, F. (Eds.), Handbook of High-Resolution Spectroscopy, Vol. 1. Wiley, Chichester, New York, pp. 175–262 (Chapter 4).

Wörner, H.J., Qian, X., Merkt, F., 2007. Jahn-Teller effect in tetrahedral symmetry: large-amplitude tunneling motion and rovibronic structure of CH_4^+ and CD_4^+. J. Chem. Phys. 126, 144305.

Wu, C.S., Ambler, E., Hayward, R.W., Hoppes, D.D., Hudson, R.P., 1957. Experimental test of parity conservation in beta decay. Phys. Rev. 105, 1413–1415.

Wu, Q., Zhang, D.H., Zhang, J.Z.H., 1995. 6D quantum calculation of energy levels for HF stretching excited $(HF)_2$. J. Chem. Phys. 103, 2548–2554.

Würger, A., 1990. Nuclear spin conversion of methyl groups. Z. Phys. B, Condens. Matter 81, 273–279.

Xantheas, S.S., 1996. Significance of higher-order many-body interaction energy terms in water clusters and bulk water. Philos. Mag. B 76, 107–115.

Xu, M., Felker, P.M., Mamone, S., Horsewill, A.J., Rols, S., Whitby, R.J., Bačić, Z., 2019. The endofullerene HF@C_{60}: inelastic neutron scattering spectra from quantum simulations and experiment, validity of the selection rule, and symmetry breaking. J. Phys. Chem. Lett. 10, 5365–5371.

Xu, L.H., Hougen, J.T., Fisher, J.M., Lees, R.M., 2010. Symmetry and Fourier analysis of the ab initio-determined torsional variation of structural and Hessian-related quantities for application to vibration-torsion-rotation interactions in CH_3OH. J. Mol. Spectrosc. 260, 88–104.

Xu, L.H., Hougen, J.T., Lees, R.M., 2011. Comparison of independently calculated ab initio normal-mode displacements for the three C-H stretching vibrations of methanol along the internal rotation path. J. Mol. Spectrosc. 293, 38–59.

Xu, L.H., Hougen, J.T., Lees, R.M., Hougen, J.T., Bowman, J.M., Huang, X., Carter, S., 2014. On the physical interpretation of ab initio normal-mode coordinates for the three C–H stretching vibrations of methanol along the internal-rotation path. J. Mol. Spectrosc. 299, 11–16.

Xu, L.H., Wang, X., Cronin, T.J., Perry, D.S., Fraser, G.T., Pine, A.S., 1997. Sub-Doppler infrared spectra and torsion–rotation energy manifold of methanol in the CH-stretch fundamental region. J. Mol. Spectrosc. 185, 158–172.

Xu, M., Ye, S., Powers, A., Lawler, R., Turro, N.J., Bačić, Z., 2013. Inelastic neutron scattering spectrum of H_2@C_{60} and its temperature dependence decoded using rigorous quantum calculations and a new selection rule. J. Chem. Phys. 139, 064309.

Xue, Z., Suhm, M.A., 2009. Probing the stiffness of the simplest double hydrogen bond: the symmetric hydrogen bond modes of jet-cooled formic acid dimer. J. Chem. Phys. 131 (5), 054301.

Yaghi, O.M., 2016. Reticular chemistry - construction, properties, and precision reactions of frameworks. J. Am. Chem. Soc. 138, 15507–15509.

Yaghi, O.M., 2019. Reticular chemistry in all dimensions. ACS Central Sci. 5, 1295–1300.

Yaghi, O.M., Kalmutzki, M.J., Diercks, C.S., 2019. Introduction to Reticular Chemistry Metal - Organic Frameworks and Covalent Organic Frameworks, first ed. Wiley-VCH, Weinheim.

Yamaguchi, Y., Schaefer III, H.F., 2011. Analytic derivative methods in molecular electronic structure theory: a new dimension to quantum chemistry and its applications to spectroscopy. In: Quack, M., Merkt, F. (Eds.), Handbook of High-Resolution Spectroscopy, Vol. 1. Wiley, Chichester, New York, pp. 325–362 (Chapter 6).

Yang, Y., Brorsen, K.R., Culpitt, T., Pak, M.V., Hammes-Schiffer, S., 2017. Development of a practical multicomponent density functional for electron–proton correlation to produce accurate proton densities. J. Chem. Phys. 147, 114113.

Yarkony, D.R., 1996. Diabolical conical intersections. Rev. Modern Phys. 68, 985–1013.

Yoder, B.L., Bravaya, K.B., Bodi, A., West, A.H.C., Sztáray, B., Signorell, R., 2015. Barrierless proton transfer across weak CH$\cdots$O hydrogen bonds in dimethyl ether dimer. J. Chem. Phys. 142, 114303.

Yu, Z., Hammam, E., Klemperer, W., 2005. The (4, 0) mode of HF dimer at 14700 cm^{-1}. J. Chem. Phys. 122, 194318.

Zare, R.N., 1988. Angular Momentum, first ed. John Wiley, New York.

Zeller, S., Kunitski, M., Voigtsberger, J., Kalinin, A., Schottelius, A., Schober, C., Waitz, M., Sann, H., Hartung, A., Bauer, T., Pitzer, M., Trinter, F., Goihl, C., Janke, C., Richter, M., Kastirke, G., Weller, M., Czasch, A., Kitzler, M., Braune, M., Grisenti, R.E., Schöllkopf, W., Schmidt, L.P.H., Schöffler, M.S., Williams, J.B., Jahnke, T., Dörner, R., 2016. Imaging the He_2 quantum halo state using a free electron laser. Proc. Nat. Acad. Sci. 113, 14651–14655.

Zhang, X., Hrovat, D.A., Borden, W.T., 2010. Calculations predict that carbon tunneling allows the degenerate Cope rearrangement of semibullvalene to occur rapidly at cryogenic temperatures. Org. Lett. 12, 2798–2801.

Zhou, H.C., Long, J.R., Yaghi, O.M., 2016. Introduction to metal–organic frameworks. Chem. Rev. 112, 673–674.

Zielke, P., Suhm, M.A., 2007. Raman jet spectroscopy of formic acid dimers: low frequency vibrational dynamics and beyond. Phys. Chem. Chem. Phys. 9, 4528–4534.

Zimmermann, H., 1964. Protonic states in chemistry. Angew. Chem., Int. Ed. 3, 157–164.

Zimmermann, T., Vaníček, J., 2010. Three applications of path integrals: equilibrium and kinetic isotope effects, and the temperature dependence of the rate constant of the [1, 5] sigmatropic hydrogen shift in (z)-1, 3-Pentadiene. J. Mol. Mod. 16, 1779–1787.